INFORMATION TO USERS

This dissertation was produced from a microfilm copy of the original document. While the most advanced technological means to photograph and reproduce this document have been used, the quality is heavily dependent upon the quality of the original submitted.

The following explanation of techniques is provided to help you understand markings or patterns which may appear on this reproduction.

1. The sign or "target" for pages apparently lacking from the document photographed is "Missing Page(s)". If it was possible to obtain the missing page(s) or section, they are spliced into the film along with adjacent pages. This may have necessitated cutting thru an image and duplicating adjacent pages to insure you complete continuity.

2. When an image on the film is obliterated with a large round black mark, it is an indication that the photographer suspected that the copy may have moved during exposure and thus cause a blurred image. You will find a good image of the page in the adjacent frame.

3. When a map, drawing or chart, etc., was part of the material being photographed the photographer followed a definite method in "sectioning" the material. It is customary to begin photoing at the upper left hand corner of a large sheet and to continue photoing from left to right in equal sections with a small overlap. If necessary, sectioning is continued again — beginning below the first row and continuing on until complete.

4. The majority of users indicate that the textual content is of greatest value, however, a somewhat higher quality reproduction could be made from "photographs" if essential to the understanding of the dissertation. Silver prints of "photographs" may be ordered at additional charge by writing the Order Department, giving the catalog number, title, author and specific pages you wish reproduced.

University Microfilms

300 North Zeeb Road
Ann Arbor, Michigan 48106

A Xerox Education Company

CONTRIBUTIONS TO THE THEORY OF MECHANISM BALANCING

by

FREDERICK R. TEPPER

A dissertation submitted to the Graduate Faculty in Engineering in partial fulfillment of the requirements for the degree of Doctor of Philosophy, The City University of New York.

1972

This manuscript has been read and accepted for the Graduate Faculty in Engineering in satisfaction of the dissertation requirement for the degree of Doctor of Philosophy.

5/11/72
date

Gerard G. Lowen
Chairman of Examining Committee

5/11/72
date

Jacques E. Bemeniste
Executive Officer

Prof. G. G. Lowen (Chairman)

Prof. A. F. Baldo

Prof. S. B. Menkes

Prof. M. L. Pei

Supervisory Committee

The City University of New York

ACKNOWLEDGEMENTS

First and foremost, I wish to express my sincerest appreciation to my advisor, Professor Gerard G. Lowen. I am indebted to him for his continued guidance, assistance, encouragement and counsel during the course of my work and the preparation of this dissertation. His enthusiasm and tireless energy have been significant factors in making this research possible.

I am also grateful for the interest shown by the other members of my guidance committee, Professors Antonio F. Baldo, Sherwood B. Menkes, and Ming L. Pei, and by the members of my examining committee, Professors Ferdinand F. Freudenstein and Kenneth H. Hunt.

The financial support received from the National Science Foundation under Grant Nos. GK-3703 and GK-31274 and the Faculty Research Award of the City University of New York under Grant No. RF-1264 is gratefully acknowledged. In addition, I am indebted to the City College Computation Center for their cooperation. I would also like to thank Mrs. Susan Hall for her typing assistance.

Finally, I owe a special debt of gratitude to my wife, Linda, and son, Alan, whose considerable love, patience and understanding have made this work possible.

TABLE OF CONTENTS

NOMENCLATURE

a_j = pivot-to-pivot dimension of link j

a_{j_x}, a_{j_y} = x and y positions of j^{th} ground connection

$a'_j(t)$ = j^{th} time dependent link to link length arising from presence of prismatic pairs

$a'_{rj}(t)$ = j^{th} time dependent link to link length arising from presence of prismatic pairs appearing in the r^{th} loop equation

b_j = pivot-to-pivot dimension of link j (used in Section II and Appendices B and C)

b_j, c_j = body-fixed coordinates of the position of the center of mass of link j (used in Section IV and Appendix A)

B_j, B_j^o, B_j^* = dimensionless masses of total link, existing link and counterweight, respectively

C_j, C_j^o, C_j^* = dimensionless moments of inertia taken with respect to center of mass of total link, existing link and counterweight, respectively

$\bar{d}$ = constant vector

D_j^* = thickness-density ratio of counterweight attached to link j

E = Lagrange function

f_{jg_x}, f_{jg_y} = dimensionless x and y force components transmitted by mechanism to ground

f_{rs_x}, f_{rs_y} = dimensionless x and y force components exerted by link r on link s

$f_{rs_{RMS}}$, $f_{rs_{RMS_b}}$, $f_{rs_{RMS_u}}$ = RMS values of dimensionless force exerted by link r on link s of partially balanced, fully force balanced and unbalanced mechanism, respectively

f_{S_x}, f_{S_y} = dimensionless x and y components of shaking force

$f_{S_{RMS}}$ = RMS value of dimensionless shaking force

f_{wj} = dimensionless constant

F_{jg_x}, F_{jg_y} = x and y force components transmitted by link j to ground

F_{rs_x}, F_{rs_y} = x and y force components exerted by link r on link s

$F_{rs_{RMS}}$, $F_{rs_{RMS_u}}$ = RMS values of force exerted by link r on link s of partially balanced and unbalanced mechanism, respectively

F_{S_x}, F_{S_y} = x and y components of shaking force

$F_{S_{RMS}}$ = RMS value of shaking force

$\bar{F}^{f(j)}_{rs}$, $\bar{F}^{m(j)}_{rs}$ = forces exerted by link r on link s due to D'Alembert force and moment, respectively, on link j

$\bar{F}_{D_j}$ = D'Alembert force acting on link j

h_j, h_j^* = thickness of link j and its attached counterweight, respectively

$\bar{i}$, $\bar{j}$, $\bar{k}$ = space-fixed unit vectors

I_j, J_j, K_j = dimensionless constants

L_j = j^{th} expression involving parameters of links 1 and 2 and constant input angular velocity

m_j, m_j^o, m_j^* = masses of total link, existing link and counterweight, respectively

M_{g1} = required input moment to run at prescribed angular velocity

$\bar{M}_{D_j}$ = D'Alembert moment acting on link j

$M_{M/G}$ = shaking moment (total moment transmitted by mechanism to ground)

$M'_{M/G}$ = RMS value of shaking moment

M_{41} = input torque of four-bar linkage

$M_{41}^{f(j)}$, $M_{41}^{m(j)}$ = input torques of four-bar linkage due to D'Alembert force and moment, respectively, on link j

n = number of links

N_{ar} = "apparent" minimum number of counterweights necessary to force balance pinned linkages

N_{as} = "apparent" minimum number of counterweights necessary to force balance mechanisms containing both revolutes and sliders

N_j = j^{th} expression involving parameters of link 2 and constant input angular velocity

p = total number of ground connections

p_g = number of "surrounding" prismatic pairs of the g^{th} "surrounded" group

P_j = j^{th} coefficient of 16^{th} degree solution polynomial

q_j = constraint factor indicating allowable increase of the RMS ground bearing forces at the j^{th} ground pivot (used in Section IV and Appendices E, F, H and I)

q_j, Q_j = coefficients of m_1 and m_2, respectively, in j^{th} force balancing equation (used in Section II)

r_j = body-fixed link dimension locating center of mass S_j of link j (scalar)

$\bar{r}_S$ = position vector of total center of mass taken with respect to reference origin O_1

$\bar{r}_{S_j}$ = position vector of total center of mass S_j of link j taken with respect to reference origin O_1

r_j^* = radius of counterweight attached to link j

R_j^* = dimensionless radius of counterweight attached to link j

s = number of sliders

u_j, t_j = dimensionless components of mass-distance product of total center of mass of link j

U_j, T_j = dimensionless body-fixed coordinates of position of total center of mass of link j

U_j^o, T_j^o = dimensionless body-fixed coordinates of position of center of mass of existing link j

U_j^*, T_j^* = dimensionless body-fixed coordinates of position of center of mass of counterweight attached to link j

v_j = dimensionless total moment of inertia of link j taken with respect to pivot

W_j, W_j^o, W_j^* = dimensionless radius of gyration of total link, existing link and counterweight, respectively

x_C, y_C = coordinates of point of minimum RMS shaking moment in original coordinate system

$\ddot{x}_j$, $\ddot{y}_j$ = x and y components of the acceleration of the center of mass of link j

z_w = dimensionless constant

α_j, β_j, γ_w, σ_{wj} = angular dimensions (used in Section II and Appendices B and C)

α_j = link length ratio (used in Section IV and Appendices A, G and J)

β_j = link width ratio (used in Section IV and Appendices A, G and J)

γ_j = link thickness ratio (used in Section IV and Appendices A, G and J)

Γ_j = dimensionless constant

δ_j = ratio of thickness of counterweight attached to link j to thickness of link j

θ_j, θ_j^o, θ_j^* = angular dimensions locating center of mass of total link, existing link and counterweight, respectively

Θ = angle between positive x/a_1-axis and positive ξ/a_1-axis

κ_j = radius of gyration of link j

λ_j = j^{th} Lagrange Multiplier

μ_{g1} = dimensionless moment exerted by ground and motor stator on rotor

$\mu_{M/G}$ = dimensionless shaking moment

$\mu'_{M/G}$ = dimensionless RMS shaking moment of unbalanced mechanism

$\mu'_{M/G|m}$ = minimum dimensionless RMS shaking moment of unbalanced mechanism

$\bar{\mu}_{RMS}$ = dimensionless RMS shaking moment of balanced mechanism

ξ_C, η_C = coordinates of point of minimum RMS shaking moment in rotated coordinate system

$\tilde{\xi}$, $\tilde{\eta}$ = axes of rotated and translated coordinate system (point of minimum RMS shaking moment given by $\tilde{\xi}_C = 0$, $\tilde{\eta}_C = 0$)

ρ = common link mass density (lb-sec^2/in.^{4})

ρ_j^o, ρ_j^* = mass densities of existing link and counterweight, respectively (lb-sec^2/in.^{4})

σ_j = ratio expressing position of center of mass of link j

φ_j = angular position of link j taken with respect to x-axis

$\mathscr{D}$ = value of determinant

$\mathscr{I}_j$ = moment of inertia of link j taken with respect to its center of mass

$\mathscr{M}$ = total mass of moving links of mechanism

ν_f = ratio of RMS shaking force of partially balanced mechanism to that of unbalanced mechanism

$(mhe^{i\alpha})_{kj}$ = mass-distance product involving fixed pivot-to-pivot distance

$(ma'(t)e^{i\beta})_{\mu j}$ = mass-distance products involving time dependent link to link distance

ABSTRACT

Certain contributions to the theory of mechanism balancing have been made:

A criterion which indicates whether a planar mechanism is amenable to full force balancing has been devised together with a simple means of determining the minimum number of counterweights necessary to achieve this balance. Further, a method for comparing the RMS shaking moment of balanced and unbalanced planar mechanisms has been found. Finally, a trade-off procedure has been developed which minimizes the shaking force of a four-bar linkage while constraining the ground bearing forces to predictable values.

LIST OF TABLES

LIST OF FIGURES

I. INTRODUCTION

Better control of the dynamic behavior of machines and mechanisms is frequently a necessary condition for increasing productivity.

In the present work an attempt has been made to contribute towards this goal by resolving some of the hitherto unanswered questions in the theory of mechanism balancing: First, a criterion has been established which determines whether a given planar linkage may be fully force balanced by internal mass redistribution alone. Then, a simple formula has been derived which gives the minimum number of counterweights necessary to achieve this full force balance. In addition, it has been proven that the root-mean-square shaking moment of an unbalanced planar mechanism is constant with respect to reference points located on certain concentric and proportional ellipses in the mechanism plane, and that the center of this family of ellipses represents a unique reference point with respect to which the RMS shaking moment is a minimum. This theory of isomomental ellipses allows the determination of the influence of full force balancing on the RMS shaking moment of a given planar mechanism. Finally, a trade-off procedure which employs Lagrange Multipliers has been shown to be capable of minimizing the RMS shaking force of a four-bar linkage while constraining the RMS ground bearing forces to certain predetermined values.

A. Background

The state of the art of linkage balancing as of 1968 was reviewed by G. G. Lowen and R. S. Berkof [13].* In this review it was shown that the technical literature abounded in publications concerning the balancing of aggregates of slider-crank mechanisms as found in prime movers and pumps, and that there was considerably less work available pertaining to balancing of other types of planar and spatial mechanisms.

Since that time, the above authors have developed the novel Method of Linearly Independent Vectors for completely force balancing four-bar and six-bar linkages [2]. In addition, they formalized a shaking moment optimization theory for force balanced four-bar linkages [3], and subsequently, applied it to a standard linkage configuration [14].

Other recent contributions in the area of full force balancing were made by the following researchers:

P. Jacobi [9] has completely force balanced n-bar linkages derivable from the four-bar linkage by the addition of dyads. R. E. Kaufman and G. N. Sandor [12] have used stretch-rotation operator notation to obtain full force balance of RSSR and RSSP spatial linkages with symmetrical coupler links.

---

*Numbers in brackets designate References at end of dissertation.

In the field of partial balancing, W. L. Carson and J. Tinsley [5] determined for a given slider-crank mechanism that theoretical variation in input velocity which leads to the greatest reduction of shaking forces and input moments. A. A. Sherwood and B. A. Hockey [18] generalized an analytic technique for the determination of general point mass systems which are dynamically similar to the actual links of a mechanism. This method is used to minimize the cyclic fluctuations of the kinetic energy of a mechanism, and thus, is helpful in the control of the input torque. Hockey [8] applied the above work to spatial mechanisms. D. Tesar and C. E. Benedict [20] worked along somewhat similar lines and improved the operating speed fluctuations of a highly complex mechanism. This was accomplished by a suitable choice of mass redistributions, springs and cam programs. Ye. A. Shorokh [19] extended the work of Ya. L. Geronimus [7] by minimizing not only the shaking forces, but also the resultant moment of the centrifugal forces of the counterweights. Both least square and best uniform optimizations were shown.

B. Results of Investigation

The present section reports briefly on the results of the investigation, which consists of the following parts:

1. General Theorems Concerning Full Force Balancing of Planar Linkages by Internal Mass Redistribution.

2. Distribution of the RMS Shaking Moment of Unbalanced Planar Mechanisms: Theory of Isomomental Ellipses.

3. Shaking Force Optimization of the Four-Bar Linkage in the Presence of Adjustable Constraint Conditions on the Ground Bearing Forces.

1. General Theorems Concerning Full Force Balancing of Planar Linkages by Internal Mass Redistribution

The question whether a planar mechanism can or cannot be fully force balanced by internal mass redistribution alone is answered by the following theorem: A planar mechanism without axisymmetric link groupings can be fully force balanced by internal mass redistribution if, and only if, from each link there is at least one contour to the ground by way of revolutes only. Unless such a contour exists, the terms containing time dependent coefficients in the center of mass trajectory equation of the total mechanism cannot be replaced with the help of the loop equations by terms with constant coefficients. Therefore, the total center of mass cannot be made stationary.

Associated with the question of the balanceability of a mechanism is that concerned with the minimum number of counterweights which can effect such a force balance. By generalizing the Method of Linearly Independent Vectors, it

is shown that the "apparent" minimum number of counterweights for all balanceable planar mechanisms equals n/2, where n represents the total number of links. The term "apparent" minimum number of counterweights is used since, from a purely mathematical point of view, the resulting equations offer no obstacle to a further reduction in the number of counterweights. In spite of all effort, it was not possible to make the number of counterweights smaller than n/2 for any of the mechanisms considered.

2. Distribution of the RMS Shaking Moment of Unbalanced Planar Mechanisms: Theory of Isomomental Ellipses

While the shaking moment of a fully force balanced mechanism has been known to be invariant with respect to reference point, there was no knowledge concerning the distribution of the shaking moment of an unbalanced mechanism. The resulting absence of a meaningful reference point has made it difficult up till now to judge the effect of full force balancing on the magnitude of the shaking moment.

The present work proves that when unbalanced planar linkages run at constant or periodically varying input speed, the RMS shaking moment is constant with respect to all points in the mechanism plane located along certain concentric and proportional ellipses. It is further demonstrated that the center of this family of ellipses represents that point in the mechanism plane with respect

to which the RMS shaking moment is a minimum. This new and unique reference point furnishes a means of comparing the effect of full force balancing on the RMS shaking moment of a planar mechanism. For the sake of generality, the analysis and results are presented in dimensionless form.

A suitable example, using a four-bar linkage of standard configuration, serves to demonstrate the results.

3. Shaking Force Optimization of the Four-Bar Linkage in the Presence of Adjustable Constraint Conditions on the Ground Bearing Forces

The full force balancing of a mechanism generally causes a considerable increase in its bearing forces, input moment, as well as shaking moment. These increases may become untenable to the design engineer, and the necessity for a compromise becomes apparent.

The present work shows such a trade-off wherein the Lagrange Multiplier Method is applied to the minimization of the RMS shaking force of a four-bar linkage running at constant input angular velocity. The RMS ground bearing forces are constrained to a given percentage increase over those of the unbalanced mechanism while being kept well below those of the fully force balanced mechanism. (No effort is made to control either the input moment or RMS shaking moment.)

This is accomplished in two different ways. In the first, a counterweight is attached to the output link, while in the second, counterweights are attached to both

the input and output links.

While the solution for the single counterweight method may be completely attained by analytical means, the two counterweight approach necessitates the numerical solution of a 16^{th} degree polynomial in one of the counterweight parameters. Once this problem variable has been determined, the other variables are found by substitution into analytical expressions.

Both cases are shown to represent conditions of minimum RMS shaking force for the given constraint conditions.

The identical four-bar linkage of standard configuration is used for numerical examples for both methods. Solutions are obtained for many different constraint conditions, and the results are given in dimensionless form by way of suitable design graphs. As expected, the two counterweight approach allows considerably greater reductions in RMS shaking force while the RMS ground bearing forces are restricted to minimal increases.

II. GENERAL THEOREMS CONCERNING FULL FORCE BALANCING OF PLANAR LINKAGES BY INTERNAL MASS REDISTRIBUTION

In this section two basic questions concerning the full force balancing of n-linked planar mechanisms with pinned and sliding joints are resolved. A contour theorem is shown to differentiate between mechanisms which can be fully force balanced and those which cannot. (Mechanisms with axi-symmetric link groupings are excluded.) In addition, a generalization of the Method of Linearly Independent Vectors for single degree of freedom mechanisms is given, and it is proven that the "apparent" minimum number of counterweights producing full force balancing by internal mass redistribution alone equals n/2.

A. Introduction

The present section attempts to state certain general principles concerning full force balancing of planar mechanisms. It represents an extension and generalization of the work of R. S. Berkof and G. G. Lowen [2], as well as T. H. Davies [6], P. Jacobi [9] and V. A. Kamenskii [10].

A contour theorem which examines the nature of the paths from the individual links to the ground is developed. It shows whether a planar mechanism is amenable to full force balancing. Throughout it is assumed that this balance is attained by internal mass redistribution, i.e. the addition of counterweights, rather than by the addition of axially symmetrical duplicate mechanisms. Further, it is assumed that the mechanisms under consideration do not contain such duplicate groups of links to start with. The previously developed Method of Linearly Independent Vectors [2] is generalized and used to show that single degree of freedom mechanisms require an "apparent" minimum number of counterweights for full force balancing.

For listing of nomenclature, refer to page x.

B. Balancing Criterion (Contour Theorem)

1. Trajectory of the Center of Mass of a Planar Mechanism

The center of mass trajectory of an arbitrary n-linked planar mechanism, as shown in Fig. 1, may be written in the following form:

$$\bar{r}_S = \frac{1}{\mathcal{M}} \sum_{j=1}^{n-1} m_j \bar{r}_{S_j} \quad \text{(the ground represents the } n^{th} \text{ link).} \tag{2.1}$$

Let the position vectors of the individual link centers of mass be expressed with the help of the unit vectors $e^{i\varphi_j}$; further, let the resulting terms be separated into those with constant coefficients, which originate from fixed link to link distances, and others with time dependent coefficients, which are due to time dependent link to link distances. Equation (2.1) then becomes:

$$\bar{r}_S = \frac{1}{\mathcal{M}} \left\{ \sum_{j=1}^{n-1} \left[\left(m_j r_j e^{i\theta_j} + \sum_{k=1}^{k^*} (mhe^{i\alpha})_{kj} \right) e^{i\varphi_j} + \sum_{\mu=1}^{\mu^*} (ma'(t)e^{i\beta})_{\mu j} e^{i\varphi_j} \right] + \bar{d} \right\} . \tag{2.2}$$

In the above, there will always be n-1 terms of the type $m_j r_j e^{i\theta_j}$, which refer to the mass-distance products of the individual link centers of mass with respect to their body-fixed origins. The k^* terms containing the constant coefficients $(mhe^{i\alpha})_{kj}$ represent the k^* mass-distance products

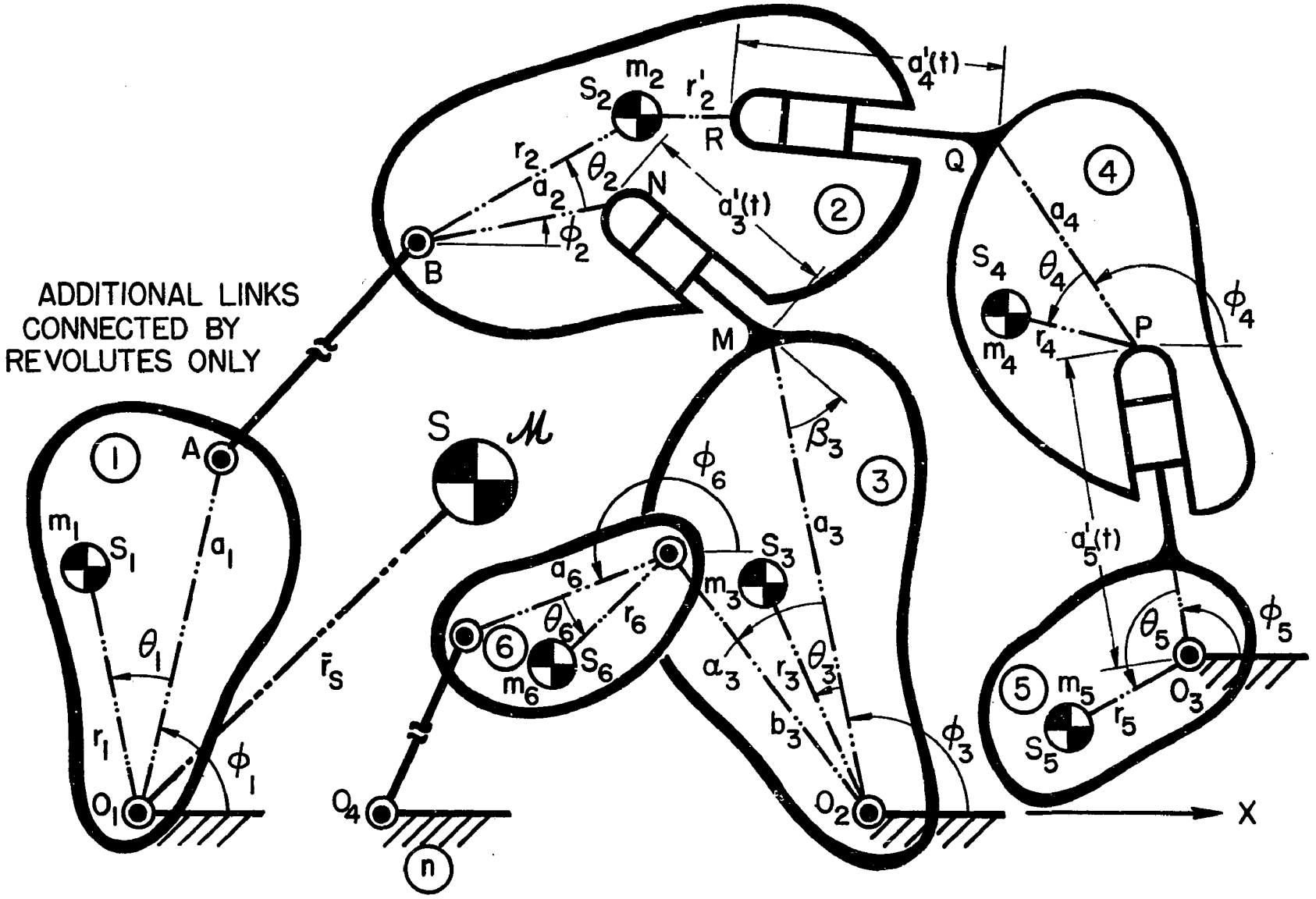

Fig. 1 Arbitrary chain of links

which involve the fixed pivot-to-pivot vectors $he^{i\alpha}$ (such as $b_3e^{i\alpha_3}$ in Fig. 1). They occur only when the description of the center of mass trajectory of a specific link includes the fixed pivot-to-pivot distances of another link (for example, when the center of mass trajectory $\bar{r}_{S_2}$ is defined by way of the contour O_1ABS_2). The μ^* terms containing the coefficients $(ma'(t)e^{i\beta})_{\mu j}$ represent mass-distance products which involve the time dependent link to link vectors $a'(t)e^{i\beta}$ (such as $a'(t)e^{i\beta_3}$ in Fig. 1). Such a term occurs, for example, if $\bar{r}_{S_2}$ in Fig. 1 is described by way of the contour $O_1O_2MNS_2$. Finally, $\bar{d}/M$ is a constant vector, and represents the stationary position of the center of mass of a mechanism which has been completely force balanced by an elementary method. (See below, and for an example, see equation (4) in [2].)

2. Definition of Balancing Criterion (Elementary Balancing Method)

a. Required Form of Center of Mass Trajectory Equation for Full Force Balance

Any plane mechanism may always be fully force balanced if it is possible to make its total center of mass stationary. (This condition is necessary as well as sufficient since the center of mass of a mechanism cannot be made to move with constant rectilinear velocity. This occurs because the center of mass trajectory of practical mechanisms is a closed curve.) In order to achieve this goal by internal mass

redistribution only, the coefficients of all time dependent unit vectors $e^{i\varphi_j}$ in equation (2.2) must be constants. This can occur whenever equation (2.2) does not contain coefficients of the type $(ma'(t)e^{i\beta})$, or when it is possible to transform terms containing these coefficients with the help of loop equations into a sum of terms with constant coefficients. (See Section IIB-2b.*) Under these circumstances, the center of mass trajectory equation becomes:

$$\bar{r}_S = \frac{1}{\mathcal{M}} \sum_{j=1}^{n-1} \left[\left(m_j r_j e^{i\theta_j} + \sum_{k=1}^{k^*} (mhe^{i\alpha})_{kj} \right) e^{i\varphi_j} \right] + \frac{\bar{d}}{\mathcal{M}} , \qquad (2.3)$$

and the center of mass can now be made stationary at the position $\bar{d}/\mathcal{M}$ by setting the individual coefficients of the unit vectors $e^{i\varphi_j}$ equal to zero. The resulting system of equations is then solved for the $m_j r_j e^{i\theta_j}$ terms, i.e. those mass-distance vectors of the centers of mass of the individual links, which will cause the mechanism to be fully force balanced. For this result to be achieved physically, the necessary mass rearrangements are obtained with the help of the counterweights. The above is another mathematical formulation of the elementary balancing methods shown by T. H. Davies [6] and V. A. Kamenskii [10]. Since pinned planar linkages never contain time dependent coefficients in their center of mass trajectory equation, they can always be

*Note that in mechanisms with axi-symmetric link groupings, pairs of terms with time dependent coefficients appear with opposite signs.

force balanced.

b. Elimination of Time Dependent Terms

The elimination of time dependent coefficients from the center of mass trajectory equation is related to the existence of independent loop equations which contain only one time dependent coefficient. The r^{th} independent loop equation of a mechanism containing n links is of the form:

$$\sum_{j=1}^{\nu} a'_{rj}(t)e^{i\beta_{rj}}e^{i\varphi_j} + \sum_{j=\nu+1}^{n} h_{rj}e^{i\alpha_{rj}}e^{i\varphi_j} = 0 \ , \quad (\varphi_n = 0) \ . \tag{2.4}$$

In the above, ν stands for the number of sliders which produce terms with time dependent coefficients of the type $a'_{rj}(t)$ within a specific loop, and h_{rj} represents the constant length of the j^{th} link, which appears in the r^{th} loop equation. Whenever $\nu = 1$ (such is the case for the slider-crank mechanism), terms containing time dependent coefficients in equation (2.2), such as $(ma'(t)e^{i\beta})_{\mu j}e^{i\varphi_j}$, can be replaced by a sum of terms with constant coefficients obtained from equation (2.4), and thus the total center of mass can be made stationary at a position $\bar{d}/\mathcal{M}$. Appendix B demonstrates that whenever there are two or more terms with time dependent coefficients in a loop equation, and one or more of the identical terms appear in the center of mass trajectory equation, the loop equations cannot be solved simultaneously for these terms in order to replace them in the trajectory equation with terms containing constant coefficients. This proof shows that

these terms with time dependent coefficients are not linearly independent.

c. Contour Theorem

The dependence of the ability to obtain full force balance on the number of terms with time dependent coefficients in the loop equations may be expressed by the following contour* theorem: A planar mechanism without axi-symmetric link groupings can be fully force balanced by internal mass redistribution if, and only if, from each link there is at least one contour to the ground by way of revolutes only.

The above is equivalent to stating that each equation within a set of independent loop equations cannot contain more than one term with a time dependent coefficient. As an example, consider the loop $O_1ABNMO_2O_1$ in Fig. 1. The center of mass trajectory of link 2 with respect to the ground can be expressed by two paths. The contour S_2NMO_2 contains a term with a time dependent coefficient, while the second contour S_2BAO_1 consists of revolutes only. The alternate description does not exist when a link is surrounded by sliders, such as link 4 of the figure. Whatever contour to the ground is chosen, it will contain prismatic pairs, and therefore, there will be a minimum of two terms with time dependent coefficients in the loop $O_3PQRNMO_2O_3$.

---

*A contour is to be defined as an open path from a link to the ground.

C. Generalization of the Method of Linearly Independent Vectors, Minimum Number of Counterweights

As has already been stated in Section IIB-2, an elementary force balance may be obtained for pinned linkages when each of the n - 1 constant coefficients of the type

$$m_j r_j e^{i\vartheta_j} + \sum_{k=1}^{k^*} (mhe^{i\alpha})_{kj} \tag{2.5}$$

of equation (2.3) is set equal to zero. This may be accomplished with the help of n - 1 counterweights, which make the necessary mass adjustments of the n - 1 links. When the mechanism contains s sliders, and it is possible to remove the time dependent coefficients due to the sliders by means of the loop equations, equation (2.3) will have n - 1 - s terms with constant coefficients of the above type. In this case, n - 1 - s mass adjustments must be undertaken on the same number of links.

The number of counterweights may be reduced by applying a generalization of the Method of Linearly Independent Vectors, a technique which was first used by R. S. Berkof and G. G. Lowen [2] in connection with the total force balancing of arbitrary four and six-bar linkages. The procedure consists of using the mechanism loop equations to eliminate some of the time dependent exponential terms from the center of mass trajectory equation (2.3). This results in fewer coefficients which must be equated to zero in order to make the total center of mass stationary. This will now

be demonstrated both for mechanisms containing revolutes only, as well as mechanisms containing both revolutes and sliders.

1. Mechanisms Containing Revolutes Only

Since a planar mechanism containing revolutes only has no time dependent link to link lengths, the center of mass trajectory can always be written in the form of equation (2.3). To reduce the number of time dependent exponentials in equation (2.3), one considers that according to B. Paul [16], one may write n/2 - 1 independent loop equations for a single degree of freedom mechanism. The minimum number of coefficients N_{ar} then becomes:

$$N_{ar} = (n - 1) - (n/2 - 1) = n/2 \ . \qquad (2.6)$$

It will now be shown that N_{ar} also represents the "apparent" minimum number of counterweights necessary to force balance pinned linkages. The term "apparent" minimum number of counterweights is used because it can be demonstrated that it is theoretically possible to balance such mechanisms with less than n/2 counterweights. (See below.)

The mechanism loop equations (see equation (2.4)) may be reduced to the following form when the linkage contains only revolutes:

$$\sum_{j=1}^{n} h_{rj} e^{i\alpha_{rj}} e^{i\varphi_j} = 0 \quad (r=1,2,\ldots,n/2 - 1 \text{ and } \varphi_n = 0). \qquad (2.7)$$

In the above, the links are numbered such that this system

of equations may be solved for the last $n/2 - 1$ $e^{i\varphi_j}$'s, excluding $e^{i\varphi_n}$, in terms of the remaining $e^{i\varphi_j}$'s. Solving equations (2.7) in this manner yields the following:

$$e^{i\varphi_w} = \sum_{j=1}^{n/2} f_{wj} e^{i\sigma_{wj}} e^{i\varphi_j} + z_w e^{i\gamma_w} \quad (w=n/2+1, n/2+2, \ldots, n-1), \tag{2.8}$$

where f_{wj}, z_w, σ_{wj} and γ_w are constants resulting from certain arithmetic manipulations. Equations (2.8) are now substituted into equation (2.3), and one obtains the new expression for the center of mass trajectory:

$$\begin{aligned}\bar{r}_S = \frac{1}{\mathcal{M}} \Bigg\{ \sum_{j=1}^{n/2} \Bigg[\Bigg(m_j r_j e^{i\theta_j} + \sum_{w=n/2+1}^{n-1} f_{wj} e^{i\sigma_{wj}} m_w r_w e^{i\theta_w} \\ + \sum_{k=1}^{k^*} \Bigg((mhe^{i\alpha})_{kj} + \sum_{w=n/2+1}^{n-1} f_{wj} e^{i\sigma_{wj}} (mhe^{i\alpha})_{kw} \Bigg) \Bigg) e^{i\varphi_j} \Bigg] \\ + \bar{d} + \sum_{w=n/2+1}^{n-1} z_w e^{i\gamma_w} \Bigg(m_w r_w e^{i\theta_w} + \sum_{k=1}^{k^*} (mhe^{i\alpha})_{kw} \Bigg) \Bigg\} \, . \end{aligned} \tag{2.9a}$$

The time dependent exponentials in equation (2.9a) represent a combination of $n/2$ linearly independent vectors. To make the center of mass of the mechanism stationary at the position*

---

*For an example, see equations (6) and (30) of [2].

$$\frac{1}{\mathcal{M}}\left\{\bar{d} + \sum_{w=n/2+1}^{n-1} z_w e^{i\gamma_w}\left(m_w r_w e^{i\theta_w} + \sum_{k=1}^{k^*}(mhe^{i\alpha})_{kw}\right)\right\}, \qquad (2.9b)$$

the coefficients of these vectors must be made to vanish, and the following set of n/2 vector equations results:

$$m_j r_j e^{i\theta_j} + \sum_{w=n/2+1}^{n-1} f_{wj} e^{i\sigma_{wj}} m_w r_w e^{i\theta_w}$$

$$+ \sum_{k=1}^{k^*}\left((mhe^{i\alpha})_{kj} + \sum_{w=n/2+1}^{n-1} f_{wj} e^{i\sigma_{wj}}(mhe^{i\alpha})_{kw}\right) = 0 \quad (j=1,2,\ldots,n/2). \qquad (2.10)$$

It will now be shown that the above represents a system which can be solved for n/2 unknown vectors $m_j r_j e^{i\theta_j}$. After rewriting equations (2.10) in x-y component form, and then transforming the resulting expressions into a matrix, where the terms $m_j r_j \cos\theta_j$, $m_j r_j \sin\theta_j$ $(j=1,2,\ldots,n/2)$ are designated as the unknowns, one obtains:

$$\begin{bmatrix} 1 & 0 & \dots & 0 & 0 \\ 0 & 1 & \dots & 0 & 0 \\ \vdots & \vdots & & \vdots & \vdots \\ 0 & 0 & \dots & 1 & 0 \\ 0 & 0 & \dots & 0 & 1 \end{bmatrix} \begin{bmatrix} m_1 r_1 \cos\theta_1 \\ m_1 r_1 \sin\theta_1 \\ \vdots \\ m_{n/2} r_{n/2} \cos\theta_{n/2} \\ m_{n/2} r_{n/2} \sin\theta_{n/2} \end{bmatrix} \qquad (2.11)$$

$$= -\begin{bmatrix} \sum_{w=n/2+1}^{n-1} f_{w1} m_w r_w \cos(\theta_w+\sigma_{w1}) + \sum_{k=1}^{k^*}\left[(mh\cos\alpha)_{k1} + \sum_{w=n/2+1}^{n-1} f_{w1}(mh\cos(\alpha+\sigma_{w1}))_{k1}\right] \\ \sum_{w=n/2+1}^{n-1} f_{w1} m_w r_w \sin(\theta_w+\sigma_{w1}) + \sum_{k=1}^{k^*}\left[(mh\sin\alpha)_{k1} + \sum_{w=n/2+1}^{n-1} f_{w1}(mh\sin(\alpha+\sigma_{w1}))_{k1}\right] \\ \vdots \\ \sum_{w=n/2+1}^{n-1} f_{w,n/2} m_w r_w \cos(\theta_w+\sigma_{w,n/2}) + \sum_{k=1}^{k^*}\left[(mh\cos\alpha)_{k,n/2} + \sum_{w=n/2+1}^{n-1} f_{w,n/2}(mh\cos(\alpha+\sigma_{w,n/2}))_{k,n/2}\right] \\ \sum_{w=n/2+1}^{n-1} f_{w,n/2} m_w r_w \sin(\theta_w+\sigma_{w,n/2}) + \sum_{k=1}^{k^*}\left[(mh\sin\alpha)_{k,n/2} + \sum_{w=n/2+1}^{n-1} f_{w,n/2}(mh\sin(\alpha+\sigma_{w,n/2}))_{k,n/2}\right] \end{bmatrix}$$

This system of equations can be solved for the $m_j r_j \cos\theta_j$ and $m_j r_j \sin\theta_j$ terms since the coefficient matrix of these vectors is a unit matrix, and hence nonsingular. The above terms indicate those n/2 mass-distance vectors of the individual link centers of mass which make the total center of mass of the mechanism stationary, and thus guarantee full force balance. To effect this solution physically, n/2 counterweights need be introduced, (see equations (14a)-(15b) in [2]), and it therefore appears that n/2 represents the minimum number of counterweights for full force balance of an n-linked mechanism containing only revolutes.

Section IIC-3 shows that under certain circumstances, equations (2.10) may theoretically be solved for other unknowns. This would seem to make it possible to obtain full force balance with less than n/2 counterweights. The author has found it impossible to obtain physically realizable solutions in this manner, however, and has come to the conclusion that n/2 therefore represents the "apparent" minimum number of counterweights.

2. Mechanisms Containing Both Revolutes and Sliders

According to Section IIB-2, whenever a mechanism contains s sliders, and for each link there is a contour to the ground by way of revolutes only, the mechanism can be fully force balanced. The trajectory of the center of mass will then be of the form of equation (2.3), and, as has been discussed in the introduction to Section IIC, will consist of n - 1 - s time dependent terms with constant coefficients

involving the unit vectors $e^{i\varphi_j}$. When applying the Method of Linearly Independent Vectors, one may eliminate as many counterweights as there are loop equations which do not contain time dependent coefficients. Since there can only be as many such loop equations with single and uniquely appearing time dependent terms as there are sliders in this type of mechanism, their number will equal n/2 - 1 - s. Therefore, the "apparent" minimum number of counterweights N_{as} for mechanisms containing both revolutes and sliders again becomes

$$N_{as} = (n - 1 - s) - (n/2 - 1 - s) = n/2 \quad . \qquad (2.12)$$

(Note that whenever the number of independent loop equations equals the number of sliders, the Method of Linearly Independent Vectors is identical to the elementary method.)

3. Theoretical Minimum Number of Counterweights

The following explores the theoretical possibility of force balancing mechanisms with less than n/2 mass adjustments, i.e. counterweights. It is based upon the ability to solve the n/2 vector force balancing equations (2.10) for a set of variables which represents less than n/2 links.

The center of mass trajectory of a link not attached to the ground always contains a term of the form $(mhe^{i\alpha})$, where m represents the mass of such a link. This offers the opportunity for solving the force balancing equations

for $n/2 - 1$ pairs of terms involving $m_j r_j \cos\theta_j$ and $m_j r_j \sin\theta_j$ $(j=1,2,\ldots,n/2 - 1)$ and two terms of the form $(mhe^{i\alpha})_{kj}$ which refer to the masses of two of these $n/2 - 1$ links. The total set of variables will then represent only $n/2 - 1$ links, and only $n/2 - 1$ counterweights will be required. A criterion will now be developed to determine under what circumstances one may use links which are not attached to the ground to this end.

Suppose that links 1 and 2 of a mechanism which can be balanced are not attached to the ground, and that it is desired to counterweight links 1, 2,..., $n/2 - 1$. The force balancing equations (2.10) can then be solved for the following:

(a) For links 1 and 2, one finds $m_j r_j \cos\theta_j$, $m_j r_j \sin\theta_j$, as well as m_j $(j = 1, 2)$.

(b) For the remaining links, one finds only $m_j r_j \cos\theta_j$, $m_j r_j \sin\theta_j$ $(j = 3, 4,\ldots, n/2 - 1)$.

If one now designates the coefficients of m_1 and m_2 in the balancing equations as q_r and Q_r $(r = 1, 2,\ldots, n)$, the force balancing equations (2.10) can be written in the following modified form (compare equation (2.11)):

$$\begin{bmatrix} 1 & 0 & \dots & 0 & 0 & q_1 & Q_1 \\ 0 & 1 & \dots & 0 & 0 & q_2 & Q_2 \\ \vdots & \vdots & & \vdots & \vdots & \vdots & \vdots \\ 0 & 0 & \dots & 1 & 0 & q_{n-3} & Q_{n-3} \\ 0 & 0 & \dots & 0 & 1 & q_{n-2} & Q_{n-2} \\ 0 & 0 & \dots & 0 & 0 & q_{n-1} & Q_{n-1} \\ 0 & 0 & \dots & 0 & 0 & q_n & Q_n \end{bmatrix} \begin{bmatrix} m_1 r_1 \cos\theta_1 \\ m_1 r_1 \sin\theta_1 \\ \vdots \\ m_{n/2-1} r_{n/2-1} \cos\theta_{n/2-1} \\ m_{n/2-1} r_{n/2-1} \sin\theta_{n/2-1} \\ m_1 \\ m_2 \end{bmatrix} \qquad (2.13)$$

$$= -\begin{bmatrix} \sum_{w=n/2+1}^{n-1} f_{w1} m_w r_w \cos(\theta_w+\sigma_{w1}) + \sum_{k=3}^{k^*} \left[(mh\cos\alpha)_{k1} + \sum_{w=n/2+1}^{n-1} f_{w1} (mh\cos(\alpha+\sigma_{w1}))_{k1} \right] \\ \sum_{w=n/2+1}^{n-1} f_{w1} m_w r_w \sin(\theta_w+\sigma_{w1}) + \sum_{k=3}^{k^*} \left[(mh\sin\alpha)_{k1} + \sum_{w=n/2+1}^{n-1} f_{w1} (mh\sin(\alpha+\sigma_{w1}))_{k1} \right] \\ \vdots \\ \sum_{w=n/2}^{n-1} f_{w,n/2} m_w r_w \cos(\theta_w+\sigma_{w,n/2}) + \sum_{k=3}^{k^*} \left[(mh\cos\alpha)_{k,n/2} + \sum_{w=n/2+1}^{n-1} f_{w,n/2} (mh\cos(\alpha+\sigma_{w,n/2})) \right] \\ \sum_{w=n/2}^{n-1} f_{w,n/2} m_w r_w \sin(\theta_w+\sigma_{w,n/2}) + \sum_{k=3}^{k^*} \left[(mh\sin\alpha)_{k,n/2} + \sum_{w=n/2+1}^{n-1} f_{w,n/2} (mh\sin(\alpha+\sigma_{w,n/2})) \right] \end{bmatrix}$$

The determinant of the above coefficient matrix may be evaluated by expanding the matrix along the columns. Following this procedure, one obtains for the determinant:

$$\mathscr{D} = q_{n-1}Q_n - q_nQ_{n-1} \quad . \tag{2.14}$$

If $\mathscr{D} \neq 0$, the system can be solved for the designated unknowns, and the mechanism can theoretically be force balanced with $n/2 - 1$ counterweights. In case this is not possible, other combinations of unknowns which correspond to $n/2 - 1$ links, two of which are not connected to the ground, can be tried. If all such possibilities fail, it can be concluded that the mechanism cannot be force balanced with less than $n/2$ counterweights. Appendix C presents an example of a mechanism which under certain circumstances can be theoretically force balanced with $n/2 - 1$ counterweights.

Notwithstanding the theoretical possibilities, the author was unable to find a practical case where such balancing could be realized without requiring some of the link masses to be negative.

D. Conclusions

Certain general conclusions concerning full force balancing of planar linkages by internal mass redistribution may be drawn:

(a) Planar mechanisms can be fully force balanced by internal mass redistribution if, and only if, from each link there is a contour to the ground by way of revolutes only. This means that all pinned linkages can be fully force balanced. Further, all linkages containing sliders can be force balanced as long as none of the loop equations of the mechanism contain more than one time dependent link to link dimension. (Mechanisms with axi-symmetric link groupings are excluded.)

(b) The generalization of the Method of Linearly Independent Vectors for single degree of freedom mechanisms has shown that all balanceable n-linked mechanisms can be fully force balanced with n/2 counterweights, i.e., internal mass rearrangements. In addition, it has been shown that n/2 represents the "apparent" minimum number of counterweights.

III. DISTRIBUTION OF THE RMS SHAKING MOMENT OF UNBALANCED PLANAR MECHANISMS: THEORY OF ISOMOMENTAL ELLIPSES

In this part it is shown that the RMS shaking moment of unbalanced planar mechanisms is constant with respect to all points along certain concentric ellipses (isomomental ellipses) in the mechanism plane. The RMS shaking moment decreases for reference points located on ellipses of decreasing size, and the center of this family of ellipses represents the point about which the RMS shaking moment of the mechanism is a minimum. This theory provides a useful tool for evaluating the effect of full force balancing on the RMS shaking moment of a given planar mechanism.

A. Introduction

The shaking moment* of a planar mechanism with respect to an arbitrary point in the mechanism plane is a vector perpendicular to this plane (all link centers of mass are assumed to move in the above plane), and is generally composed of a pure couple due to the reaction of the motor stator, as well as the sum of the moments of the ground bearing forces with respect to that point [3].

For the special case of a fully force balanced planar mechanism, where the vector sum of the ground pivot forces equals zero, the total shaking moment becomes a pure couple, and its magnitude is independent of reference point.

This section examines the distribution of the RMS shaking moment of unbalanced planar mechanisms with respect to arbitrary points in the mechanism plane. It is shown that this moment of a given mechanism is constant with respect to all points along certain concentric and proportional ellipses. It is further demonstrated that the RMS shaking moment decreases for reference points located on ellipses of decreasing size, and that the center of these isomomental ellipses represents that point in the mechanism plane with respect to which the RMS shaking moment is a minimum. Once the minimum RMS shaking moment, together with its associated reference point and certain mechanism constants have been found, it is possible to determine the

---

*The shaking moment is defined as the vector sum of all moments on the frame due to mass effects only. The effects of friction are disregarded.

RMS shaking moment with respect to an arbitrary point in the mechanism plane with the help of a simple algebraic equation.

More importantly, the above results make it possible to determine the influence of full force balancing on the RMS shaking moment of a planar linkage, and offers aid in the design of baseplates or frames which will avoid the rocking of machinery due to the effects of the shaking moment:

(a) If the RMS shaking moment after full force balancing is smaller than, or equal to, that of the unbalanced mechanism with respect to its point of minimum RMS shaking moment, then force balancing will be shown to lower the RMS shaking moment with respect to all points in the mechanism plane.

(b) If the RMS shaking moment of the fully force balanced linkage is larger than that of the unbalanced linkage with respect to its point of minimum RMS shaking moment, one may obtain the limiting elliptical region in the mechanism plane beyond which the RMS shaking moment in the balanced mechanism is smaller than that of the unbalanced mechanism.

Even though the derivation assumes constant input angular velocity and identical density for all links, the results may be extended to planar mechanisms which run with a known periodically varying input velocity and/or consist of links of different densities.

After the theoretical basis is established in dimension-

less form for arbitrary planar mechanisms, an example is given which determines the point of minimum RMS shaking moment, as well as some associated isomomental ellipses, for an unbalanced four-bar linkage. In addition, the limiting elliptical region is determined beyond which the RMS shaking moment of this mechanism becomes smaller after full force balancing.

For listing of nomenclature, refer to page x.

B. Shaking Moment of Unbalanced Planar Mechanism With Respect to Arbitrary Reference Point

The shaking moment of a general n-linked, one degree of freedom planar mechanism with respect to the arbitrary point R(x,y) of Fig. 2 may be written in the following manner (see also equation (40) of [3]):

$$M_{M/G} = M_{1g} + \sum_{j=1}^{p} \left[(-x + a_{j_x}) F_{jg_y} + (y - a_{j_y}) F_{jg_x} \right] . \qquad (3.1)$$

In the above, F_{jg_x} and F_{jg_y} denote the respective x and y force components transmitted to the ground by the p ground connections. The moment M_{1g} is exerted by the motor stator on the ground and is equal in magnitude, but opposite in direction, to the required input moment M_{g1}. The distances a_{j_x} and a_{j_y} represent the x and y positions of the respective ground pivots.

In order to make the results of this paper independent of mechanism magnification, all moments, forces and distances are expressed in dimensionless form as functions of the input length a_1, the link mass density ρ, which is assumed common to all links, and the constant input angular velocity $\dot{\varphi}_1$. Equation (3.1) then becomes:

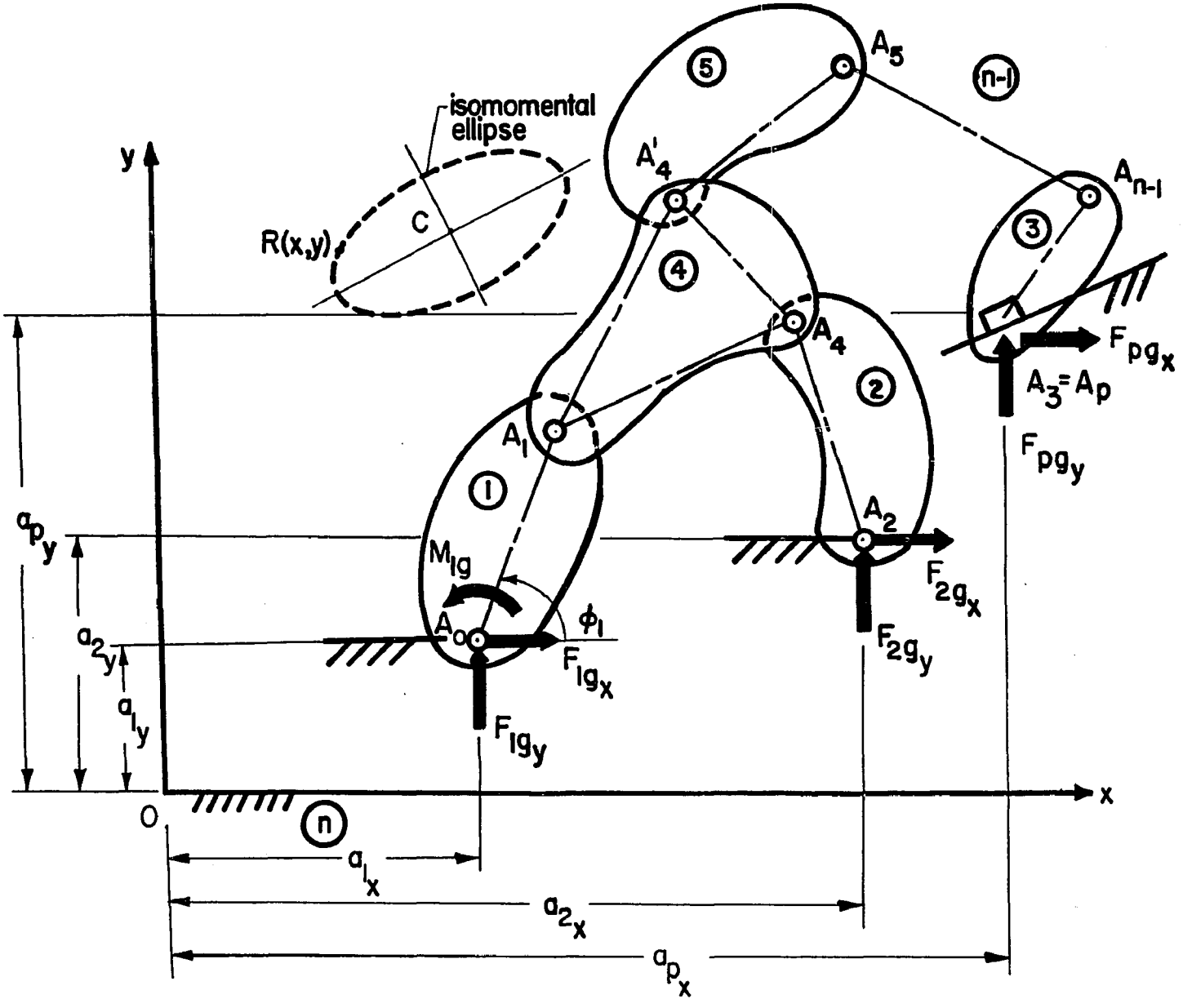

Fig. 2 Arbitrary n-linked mechanism showing reference point R(x,y) and ground bearing forces

$$\mu_{M/G} = \mu_{1g} - \left(\frac{x}{a_1}\right) \sum_{j=1}^{p} f_{jg_y} + \sum_{j=1}^{p} \frac{a_{j_x}}{a_1} f_{jg_y} + \left(\frac{y}{a_1}\right) \sum_{j=1}^{p} f_{jg_x}$$

$$- \sum_{j=1}^{p} \frac{a_{j_y}}{a_1} f_{jg_x} \quad , \tag{3.2}$$

where

$$\mu_{M/G} = \frac{M_{M/G}}{\rho a_1^5 \dot{\varphi}_1^2} \quad , \text{ the dimensionless shaking moment} \tag{3.3a}$$

$$\mu_{1g} = \frac{M_{1g}}{\rho a_1^5 \dot{\varphi}_1^2} \quad , \text{ the dimensionless rotor torque on the ground by way of the stator} \tag{3.3b}$$

$$f_{jg_x} = \frac{F_{jg_x}}{\rho a_1^4 \dot{\varphi}_1^2} \quad , \text{ the dimensionless x component of the } j^{th} \text{ bearing force on the ground} \tag{3.3c}$$

$$f_{jg_y} = \frac{F_{jg_y}}{\rho a_1^4 \dot{\varphi}_1^2} \quad , \text{ the dimensionless y component of the } j^{th} \text{ bearing force on the ground.} \tag{3.3d}$$

The quantities (x/a_1) and (y/a_1), which express the position of the reference point, can be interpreted to refer to a dimensionless coordinate system. (See Fig. 3.)

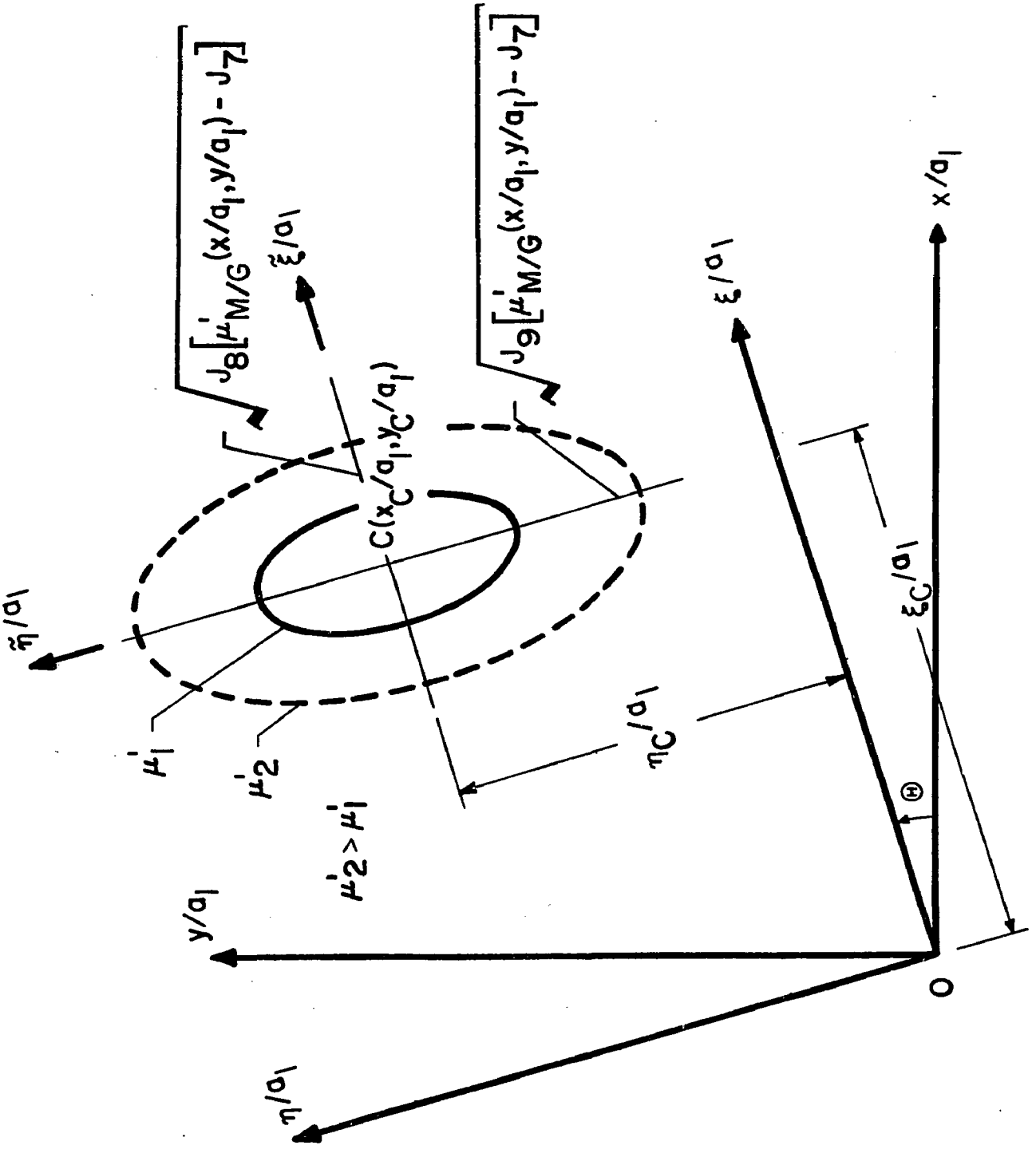
$\sqrt{J_8[\mu'_{M/G}(x/a_1, y/a_1) - J_7]}$
$\sqrt{J_9[\mu'_{M/G}(x/a_1, y/a_1) - J_7]}$
$\tilde{\xi}/a_1$
$\tilde{\eta}/a_1$
$C(x_C/a_1, y_C/a_1)$
μ'_1
μ'_2
$\mu'_2 > \mu'_1$
ξ/a_1
x/a_1
y/a_1
η/a_1
ξ_C/a_1
η_C/a_1
θ
O

C. Locus of Points of Constant RMS Shaking Moment (Isomomental Ellipses)

The root-mean-square of the dimensionless shaking moment with respect to point $R(\frac{x}{a_1},\frac{y}{a_1})$ is given by

$$\mu'_{M/G}(\frac{x}{a_1},\frac{y}{a_1}) = \sqrt{\frac{1}{2\pi}\int_0^{2\pi} \mu^2_{M/G}(\frac{x}{a_1},\frac{y}{a_1})d\varphi_1} \quad . \tag{3.4}$$

Squaring this expression and substituting equation (3.2) leads to:

$$J_1\left(\frac{x}{a_1}\right)^2 + J_2\left(\frac{y}{a_1}\right)^2 + 2J_3\left(\frac{x}{a_1}\right)\left(\frac{y}{a_1}\right) + 2J_4\left(\frac{x}{a_1}\right) + 2J_5\left(\frac{y}{a_1}\right)$$

$$+ (J_6 - \mu'^2_{M/G}(\frac{x}{a_1},\frac{y}{a_1})) = 0 \quad , \tag{3.5}$$

where the J's represent the following dimensionless mechanism constants, which are functions of the link lengths and the link geometry only (see equations (A.120) - (A.124) of Appendix A for definition of forces and moments as functions of overall geometry):

$$J_1 = \frac{1}{2\pi}\int_0^{2\pi} \left(\sum_{j=1}^{p} f_{jg_y}\right)^2 d\varphi_1 \tag{3.6a}$$

$$J_2 = \frac{1}{2\pi}\int_0^{2\pi} \left(\sum_{j=1}^{p} f_{jg_x}\right)^2 d\varphi_1 \tag{3.6b}$$

$$J_3 = -\frac{1}{2\pi}\int_0^{2\pi}\left[\left(\sum_{j=1}^{p} f_{jg_x}\right)\left(\sum_{j=1}^{p} f_{jg_y}\right)\right]d\varphi_1 \qquad (3.6c)$$

$$J_4 = -\frac{1}{2\pi}\int_0^{2\pi}\left\{\left[\mu_{1g} + \sum_{j=1}^{p}\left(\frac{a_{j_x}}{a_1} f_{jg_y} - \frac{a_{j_y}}{a_1} f_{jg_x}\right)\right]\sum_{j=1}^{p} f_{jg_y}\right\}d\varphi_1 \qquad (3.6d)$$

$$J_5 = \frac{1}{2\pi}\int_0^{2\pi}\left\{\left[\mu_{1g} + \sum_{j=1}^{p}\left(\frac{a_{j_x}}{a_1} f_{jg_y} - \frac{a_{j_y}}{a_1} f_{jg_x}\right)\right]\sum_{j=1}^{p} f_{jg_x}\right\}d\varphi_1 \qquad (3.6e)$$

$$J_6 = \frac{1}{2\pi}\int_0^{2\pi}\left[\mu_{1g} + \sum_{j=1}^{p}\left(\frac{a_{j_x}}{a_1} f_{jg_y} - \frac{a_{j_y}}{a_1} f_{jg_x}\right)\right]^2 d\varphi_1 \; . \qquad (3.6f)$$

Equation (3.5) will now be shown to represent the dimensionless expressions of families of ellipses describing all those reference points with respect to which the square of the RMS moments, and with that the RMS moments, are constant (isomomental ellipses).

The general equation of a conic [17], i.e.

$$Ax^2 + By^2 + 2Hxy + 2Gx + 2Fy + C = 0 \qquad (3.7)$$

is that of an ellipse if

$$H^2 - AB < 0 \; . \qquad (3.8)$$

Equation (3.5) corresponds to equation (3.7) and inequality (3.8) becomes for the present case

$$J_3^2 - J_1 J_2 < 0 \ , \tag{3.9}$$

or with the help of equations (3.6a) - (3.6c):

$$\left[\int_0^{2\pi}\left(\sum_{j=1}^{p} f_{jg_x}\right)\left(\sum_{j=1}^{p} f_{jg_y}\right)d\varphi_1\right]^2$$

$$-\int_0^{2\pi}\left(\sum_{j=1}^{p} f_{jg_x}\right)^2 d\varphi_1 \int_0^{2\pi}\left(\sum_{j=1}^{p} f_{jg_y}\right)^2 d\varphi_1 < 0 \ . \tag{3.10}$$

The latter expression is satisfied according to the integral form of Schwarz's inequality [11] as long as $\sum_{j=1}^{p} f_{jg_x}$ and $\sum_{j=1}^{p} f_{jg_y}$ are linearly independent.

The above summations are linearly independent since they stand for the Cartesian components of the rotating vector $-\mathcal{M}\ddot{\bar{r}}_S$, which represents the negative of the total force of the ground on the mechanism. While $\mathcal{M}$ denotes the sum of the individual link masses, $\ddot{\bar{r}}_S$ represents the acceleration of the total center of mass of the mechanism. Therefore, inequalities (3.9) and (3.10) hold, and equation (3.5) is proven to represent a family of ellipses.

D. Point of Minimum Dimensionless RMS Shaking Moment

The following demonstrates that the center $C(x_C/a_1, y_C/a_1)$ of the family of isomomental ellipses of equation (3.5) represents the point of minimum dimensionless RMS shaking moment, and its location depends only on mechanism and link geometry, i.e. it is invariant with respect to both input angular velocity and the common link density. (See Fig. 3.) This is accomplished by first transforming equation (3.5) into the standard equation of an ellipse in the $\frac{\xi}{a_1}, \frac{\eta}{a_1}$ system, which corresponds to the semi-axes, and then showing that the length of these axes increases as $\mu'_{M/G}(\xi/a_1, \eta/a_1)$ increases for a given mechanism configuration.

The transformation of variables is accomplished with the help of:

$$\frac{x}{a_1} = \frac{\xi}{a_1}\cos\Theta - \frac{\eta}{a_1}\sin\Theta \qquad (3.11a)$$

$$\frac{y}{a_1} = \frac{\xi}{a_1}\sin\Theta + \frac{\eta}{a_1}\cos\Theta \,, \qquad (3.11b)$$

where, according to [17], the angle between the positive x/a_1-axis and the positive ξ/a_1-axis is given by:

$$\Theta = \frac{1}{2}\tan^{-1}\left(\frac{2H}{A - B}\right) = \frac{1}{2}\tan^{-1}\left(\frac{2J_3}{J_1 - J_2}\right) . \qquad (3.12)$$

(See equation (3.7).)

Substitution of the above into equation (3.5) leads to the standard form of an ellipse in the $\frac{\xi}{a_1}, \frac{\eta}{a_1}$ system:

$$\frac{\left(\frac{\xi}{a_1} - \frac{\xi_C}{a_1}\right)^2}{K_\xi^2} + \frac{\left(\frac{\eta}{a_1} - \frac{\eta_C}{a_1}\right)^2}{K_\eta^2} = 1 \quad . \tag{3.13a}$$

The coordinates of the center C of the ellipses are expressed in terms of the dimensionless constants of equations (3.6), i.e.

$$\frac{\xi_C}{a_1} = \frac{-(J_5\sin\Theta + J_4\cos\Theta)}{J_1\cos^2\Theta + J_2\sin^2\Theta + 2J_3\sin\Theta\cos\Theta} \tag{3.13b}$$

$$\frac{\eta_C}{a_1} = \frac{-(J_5\cos\Theta - J_4\sin\Theta)}{J_1\sin^2\Theta + J_2\cos^2\Theta - 2J_3\sin\Theta\cos\Theta} \quad . \tag{3.13c}$$

Since the J's are dimensionless, the coordinates of C are invariant with respect to both input angular velocity and link density.

The semi-axes are given by

$$K_\xi = \sqrt{J_8\left[\mu'^2_{M/G}\left(\frac{\xi}{a_1}, \frac{\eta}{a_1}\right) - J_7\right]} \tag{3.14a}$$

$$K_\eta = \sqrt{J_9\left[\mu'^2_{M/G}\left(\frac{\xi}{a_1}, \frac{\eta}{a_1}\right) - J_7\right]} \quad , \tag{3.14b}$$

where

$$J_7 = J_6 - (J_5\sin\Theta + J_4\cos\Theta)^2 J_8 - (J_5\cos\Theta - J_4\sin\Theta)^2 J_9 \tag{3.14c}$$

$$J_8 = \frac{1}{J_1\cos^2\Theta + J_2\sin^2\Theta + 2J_3\sin\Theta\cos\Theta} \tag{3.14d}$$

$$J_9 = \frac{1}{J_1\sin^2\Theta + J_2\cos^2\Theta - 2J_3\sin\Theta\cos\Theta} \quad . \tag{3.14e}$$

Appendix D shows that J_9 is larger than J_8. Therefore, the major axes of the ellipses are parallel to the η/a_1-axis. Furthermore, it is to be noted that the ratio of the semi-axes, K_ξ/K_η, is constant, and that for this reason the isomomental ellipses are not only concentric, but also proportional.

When $\xi/a_1 = \xi_C/a_1$ and $\eta/a_1 = \eta_C/a_1$, the ellipses degenerate to the point C, and both numerators and denominators of the left-hand side of equation (3.13a) must be zero since the major and minor semi-axes in the limit become equal to zero. Therefore, $J_8\left[\mu'^2_{M/G}(\frac{\xi}{a_1},\frac{\eta}{a_1}) - J_7\right]$ and $J_9\left[\mu'^2_{M/G}(\frac{\xi}{a_1},\frac{\eta}{a_1}) - J_7\right]$, which generally are positive quantities because of their association with ellipses, must vanish. Since both J_8 and J_9 are mechanism constants which are shown in Appendix D to be positive at all times, the term in brackets in the above expressions vanishes for the case under consideration, and the moment with respect to point C becomes:

$$\mu'_{M/G}|_m = \mu'_{M/G}(\frac{\xi_C}{a_1},\frac{\eta_C}{a_1}) = \sqrt{J_7} \quad . \tag{3.15}$$

In order to show that the above represents the minimum

RMS shaking moment, one considers that all other points $R(\xi/a_1, \eta/a_1)$ must lie on ellipses with major and minor semi-axes larger than zero, and that since J_7 is a mechanism constant, the following must hold for them:

$$\mu'^2_{M/G}\left(\frac{\xi}{a_1}, \frac{\eta}{a_1}\right) - J_7 > 0 \ . \tag{3.16}$$

This means that the RMS shaking moments associated with these points must be larger than that associated with point $C(\xi_C/a_1, \eta_C/a_1)$, and the latter represents the point of minimum RMS shaking moment.

This unique reference point, which may serve for the comparison of the RMS shaking moment under various circumstances, may be found in the $\frac{x}{a_1}, \frac{y}{a_1}$ system with the help of the following expressions, which are due to the transformation equations (3.11a), (3.11b) and (3.12):

$$\frac{x_C}{a_1} = \frac{J_3J_5 - J_2J_4}{J_1J_2 - J_3^2} \tag{3.17a}$$

$$\frac{y_C}{a_1} = \frac{J_3J_4 - J_1J_5}{J_1J_2 - J_3^2} \ . \tag{3.17b}$$

E. Determination of the RMS Shaking Moment With Respect to an Arbitrary Point With the Help of the Point of Minimum RMS Shaking Moment

It will now be shown how to obtain the RMS shaking moment with respect to an arbitrary point in the mechanism plane with the help of a simple computation once the point of minimum RMS shaking moment, the associated minimum RMS shaking moment, $\mu'_{M/G|_m}$, J_8 and J_9 are known for a given mechanism.

Let the arbitrary point be given in the $\frac{\xi}{a_1},\frac{\eta}{a_1}$ coordinate system of Fig. 3, and define

$$\frac{\tilde{\xi}}{a_1} = \frac{\xi}{a_1} - \frac{\xi_C}{a_1} , \tag{3.18a}$$

as well as

$$\frac{\tilde{\eta}}{a_1} = \frac{\eta}{a_1} - \frac{\eta_C}{a_1} . \tag{3.18b}$$

The isomomental ellipse equation (3.13a) then becomes together with equations (3.14a) and (3.14b):

$$\frac{\left(\frac{\tilde{\xi}}{a_1}\right)^2}{J_8\left[\mu'^2_{M/G}(\frac{\tilde{\xi}}{a_1},\frac{\tilde{\eta}}{a_1}) - J_7\right]} + \frac{\left(\frac{\tilde{\eta}}{a_1}\right)^2}{J_9\left[\mu'^2_{M/G}(\frac{\tilde{\xi}}{a_1},\frac{\tilde{\eta}}{a_1}) - J_7\right]} = 1 . \tag{3.19}$$

The above expression may be solved for the desired RMS shaking moment with respect to an arbitrary point $\frac{\tilde{\xi}}{a_1},\frac{\tilde{\eta}}{a_1}$ by using equation (3.15):

$$\mu'_{M/G}\left(\frac{\tilde{\xi}}{a_1},\frac{\tilde{\eta}}{a_1}\right) = \sqrt{\mu'^{,2}_{M/G|_m} + \frac{\left(\frac{\tilde{\xi}}{a_1}\right)^2}{J_8} + \frac{\left(\frac{\tilde{\eta}}{a_1}\right)^2}{J_9}} \quad . \tag{3.20}$$

F. Application to Four-Bar Linkage

The four-bar linkage of Fig. 4, with dimensions listed in Table 1, will now be used as an example for the determination of the point of minimum RMS shaking moment, the magnitude of the corresponding minimum RMS shaking moment, as well as some of the associated isomomental ellipses. This mechanism is designed according to the standard linkage configuration given in [14], and shown again for convenience in Appendix A.

For this mechanism, that region will be determined beyond which the RMS shaking moment of the fully force balanced mechanism* will be smaller than that of the unbalanced mechanism. Finally, the shaking moment with respect to an arbitrary point will be obtained according to the formulation of Section IIIE.

Fig. 4 shows that the origin of the coordinate system is chosen to coincide with the pivot of the input crank, A_0. Thus:

$$\frac{a_{1_x}}{a_1} = \frac{a_{1_y}}{a_1} = \frac{a_{2_y}}{a_1} = 0, \quad \frac{a_{2_x}}{a_1} = \frac{a_4}{a_1} . \tag{3.21}$$

The magnitudes of the J's were determined according to equations (3.6a)-(3.6f) and (3.14c)-(3.14e), and are listed in Table 2.† This was accomplished with the help of the expressions for the dimensionless ground bearing forces and stator moment of the standard linkage configuration as given in Section 6 of Appendix A.

---

*Full force balance is accomplished according to [2,14].

†All computations were performed on the City College IBM 360/50 Computer, with programs written in Fortran IV.

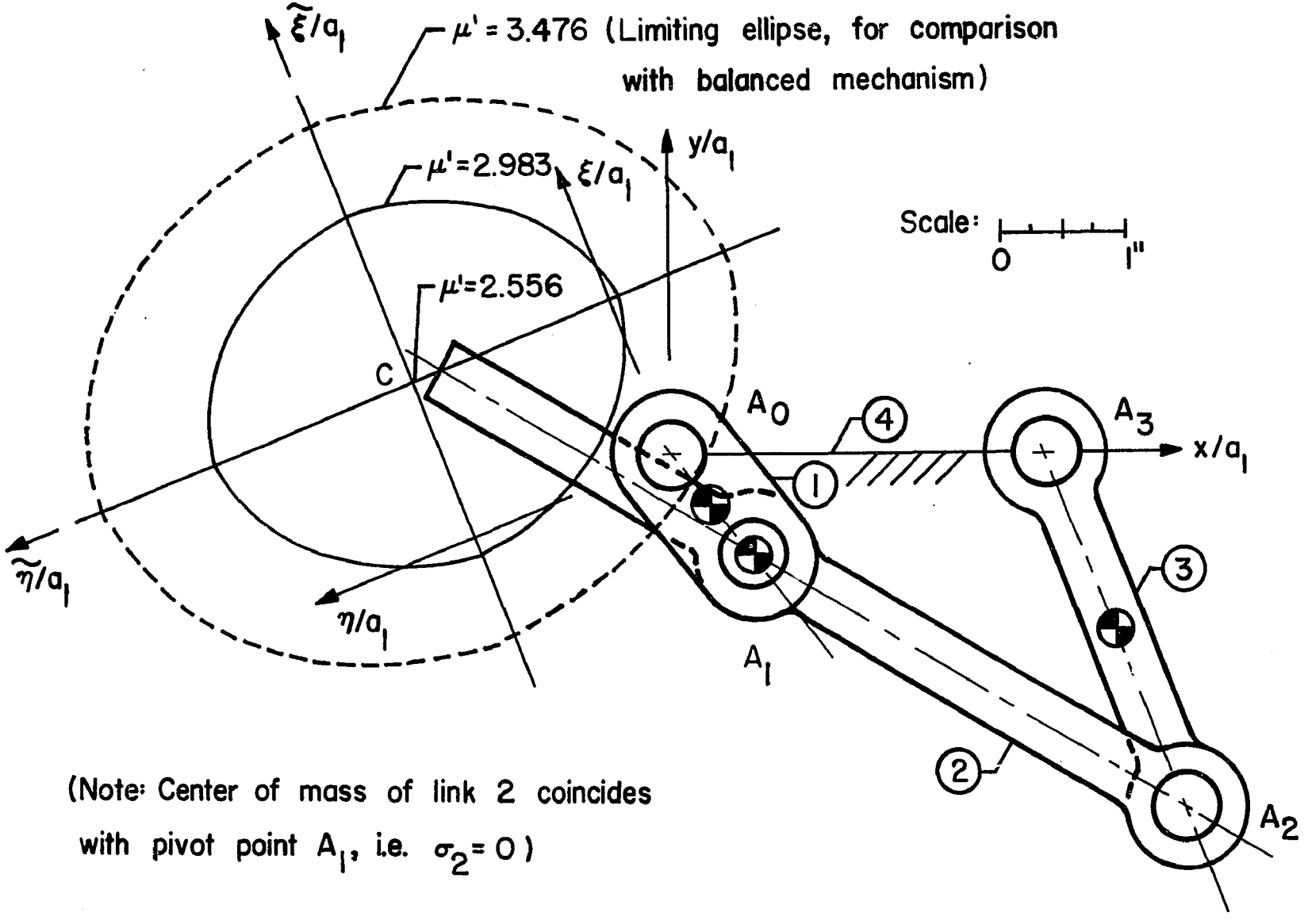

Fig. 4 Point of minimum RMS shaking moment and isomomental ellipses for four-bar linkage of standard configuration (for parameters, see Table 1)

Table 1 Dimensionless Parameters of Four-Bar Linkage

Link i	1	2	3	4
Dimensionless link length $\alpha_i = a_i/a_1$	1.000	4.000	3.000	3.000
Dimensionless position of link center of mass $\sigma_i = r_i/a_i$	0.500	0.000	0.500	—
Dimensionless link width and end radius $\beta_i = d_i/a_i$	0.500	0.500	0.500	—
Dimensionless link thickness $\gamma_i = h_i/d_i$	0.400	0.400	0.400	—
Dimensionless link mass B_i	0.357	1.062	0.514	—
Dimensionless link moment of inertia C_i	not needed	8.110	0.817	—

Table 2 Values of J's

$J_1 = 0.822$	$J_2 = 1.146$	$J_3 = -0.154$
$J_4 = 1.824$	$J_5 = -1.060$	$J_6 = 11.045$
$J_7 = 6.534$	$J_8 = 0.828$	$J_9 = 1.314$

The dimensionless location of the point of minimum RMS shaking moment is obtained with the help of equations (3.17a) and (3.17b), while the angle of the ξ/a_1-axis with respect to the x/a_1-axis is calculated according to equation (3.12). Thus

$$\frac{x_C}{a_1} = -2.098, \quad \frac{y_C}{a_1} = 0.644, \quad \Theta = 111.7^\circ \text{ (angle between } x/a_1 \text{ and } \xi/a_1\text{-axis)}. \tag{3.22}$$

The associated minimum dimensionless RMS shaking moment is computed with the help of equation (3.15):

$$\mu'_{M/G|m} = 2.556 \ . \tag{3.23}$$

For a steel linkage (0.283 lb/in.^{3}) which is run at 1,000 RPM, and where

$$a_1 = 1.000 \text{ in.} \quad \text{and} \quad \rho = 7.33 \times 10^{-4} \text{ lb-sec}^2/\text{in.}^4, \tag{3.24a}$$

one obtains for the point of minimum RMS shaking moment according to equations (3.22):

$$x_C = -2.098 \text{ in.}, \quad y_C = 0.644 \text{ in.} \tag{3.24b}$$

The associated minimum RMS shaking moment becomes with the help of equations (3.3a) and (3.23):

$$M'_{M/G} = 20.545 \text{ in-lb.} \qquad (3.24c)$$

Fig. 4 shows the isomomental ellipse which is associated with a dimensionless RMS shaking moment of 2.983 units. (This corresponds to 25 in-lbs. for the dimensions of Table 1.) The axes of this ellipse are obtained with the help of equations (3.14), noting that the ξ/a_1-axis represents the minor axis.

When this mechanism is fully force balanced according to the criteria set in [3,14], one finds from the data associated with Fig. 7 of [14] that the magnitude of the dimensionless RMS shaking moment with respect to all points in the mechanism plane is given by:

$$\bar{\mu}_{RMS} = 3.476 \ . \qquad (3.25)$$

Fig. 4 shows the isomomental ellipse associated with the above value. Since the RMS shaking moment of the unbalanced mechanism is larger for all points located outside this ellipse, force balancing decreases the RMS shaking moment with respect to all points beyond this limiting region.

Let it now be required to find the dimensionless shaking moment associated with point A_3 of Fig. 4. The coordinates of this point are

$$\frac{x}{a_1} = 3.000, \quad \frac{y}{a_1} = 0.000 \ . \qquad (3.26a)$$

On transformation according to equations (3.11), this becomes:

$$\frac{\xi}{a_1} = -1.110, \quad \frac{\eta}{a_1} = -2.787 \ , \tag{3.26b}$$

and with the help of equations (3.18):

$$\frac{\tilde{\xi}}{a_1} = -2.485, \quad \frac{\tilde{\eta}}{a_1} = -4.498 \ . \tag{3.26c}$$

With the above, as well as the value for $\mu'_{M/G|_m}$ according to equation (3.23), and J_8 and J_9 from Table 2, equation (3.20) gives the following value for the dimensionless RMS shaking moment with respect to point A_3:

$$\mu'_{M/G} = 5.573 \ . \tag{3.27}$$

G. Conclusions

Certain conclusions concerning the theory of isomomental ellipses may be drawn:

(a) The RMS shaking moments of unbalanced planar mechanisms running at constant or periodically varying input angular velocities are constant with respect to all points which lie on certain ellipses.

(b) The center of all families of such isomomental ellipses represents the point of minimum RMS shaking moment of an unbalanced planar mechanism. The location of this minimum point depends only on the link lengths and the link geometry of a particular mechanism.

(c) The theory provides a useful tool for the evaluation of the effect of full force balancing on the RMS shaking moment of a given planar mechanism: It shows that the RMS shaking moment of the balanced linkage is lower throughout the mechanism plane if it is lower than that of the unbalanced mechanism with respect to the minimum point. If the RMS shaking moment of the fully force balanced mechanism is larger than that of the unbalanced mechanism with respect to the minimum point, one may obtain the limiting elliptical region beyond which the RMS shaking moment of the balanced mechanism is smaller than that of the unbalanced mechanism.

IV. SHAKING FORCE OPTIMIZATION OF THE FOUR-BAR LINKAGE IN THE PRESENCE OF ADJUSTABLE CONSTRAINT CONDITIONS ON THE GROUND BEARING FORCES

The present section shows how the Lagrange Multiplier Method may be adapted to minimize the RMS shaking force of a four-bar linkage while constraining the RMS ground bearing forces of the mechanism to certain predetermined values. Solutions are expressed in terms of certain properties of the centers of mass of individual links. These solutions find their practical realization by way of a single counterweight and a two counterweight method.

A. Introduction

1. Background

The field of mechanism balancing is not different from other fields of engineering: For each advantage, a certain penalty must be paid. While it is obviously highly desirable to make the shaking force of a mechanism vanish by fully force balancing it by the method described in Section II and [2], doing so may introduce new design difficulties. In most cases there will be a considerable increase in the bearing forces, the input moment, as well as the shaking moment* [15].

When such a situation arises, the engineer looks for a compromise, i.e. he attempts to trade-off some of the gains of the new method for a reduction of the associated disadvantages. The following work represents such a trade-off method wherein the RMS shaking force of a four-bar linkage is reduced as much as possible with the help of counterweights, while the RMS ground bearing forces are kept from increasing beyond a certain predetermined value above that of the unbalanced mechanism. (No effort is made to control either the RMS input moment or the RMS shaking moment.) The Lagrange Multiplier Method has proven itself as a suitable vehicle to this end.

For listing of nomenclature, refer to page x.

---

*Section III presents examples where the RMS shaking moment increases in certain cases.

2. Application of Lagrange Multiplier Method to Shaking Force Optimization of the Four-Bar Linkage

Sections B and C of the present part of this dissertation show a Lagrange Multiplier formulation for the reduction of the RMS shaking force of a four-bar linkage which has a general mass distribution, as shown in Fig. 5, and which runs runs with a constant input angular velocity. The RMS ground bearing forces at A_0 and A_3 are constrained to a range of values limited, on the one hand, by those of the unbalanced mechanism, and on the other, by those of the mechanism fully force balanced by the Method of Linearly Independent Vectors. This aim is attained in two different ways:

1. A single counterweight attached to the output link 3 is used to realize those total mass-distance products m_3b_3 and m_3c_3 (see Fig. 5), as well as that total moment of inertia $m_3\kappa^2_{3_{A_3}}$, of the link which correspond to the minimum attainable RMS value of the shaking force $F_{S_{RMS}}$ when the individual RMS ground bearing forces are prescribed as stated above.

2. Two counterweights, one attached each to the input and output links, are used to realize the total mass-distance products m_1b_1, m_1c_1, m_3b_3 and m_3c_3 of the respective links which correspond again to the minimum attainable RMS shaking force and preserve the constraints on the RMS ground bearing forces. In this method it is additionally necessary to pre-assign the moment of inertia of link 3. This value is chosen in such a manner that it is larger than that of the original

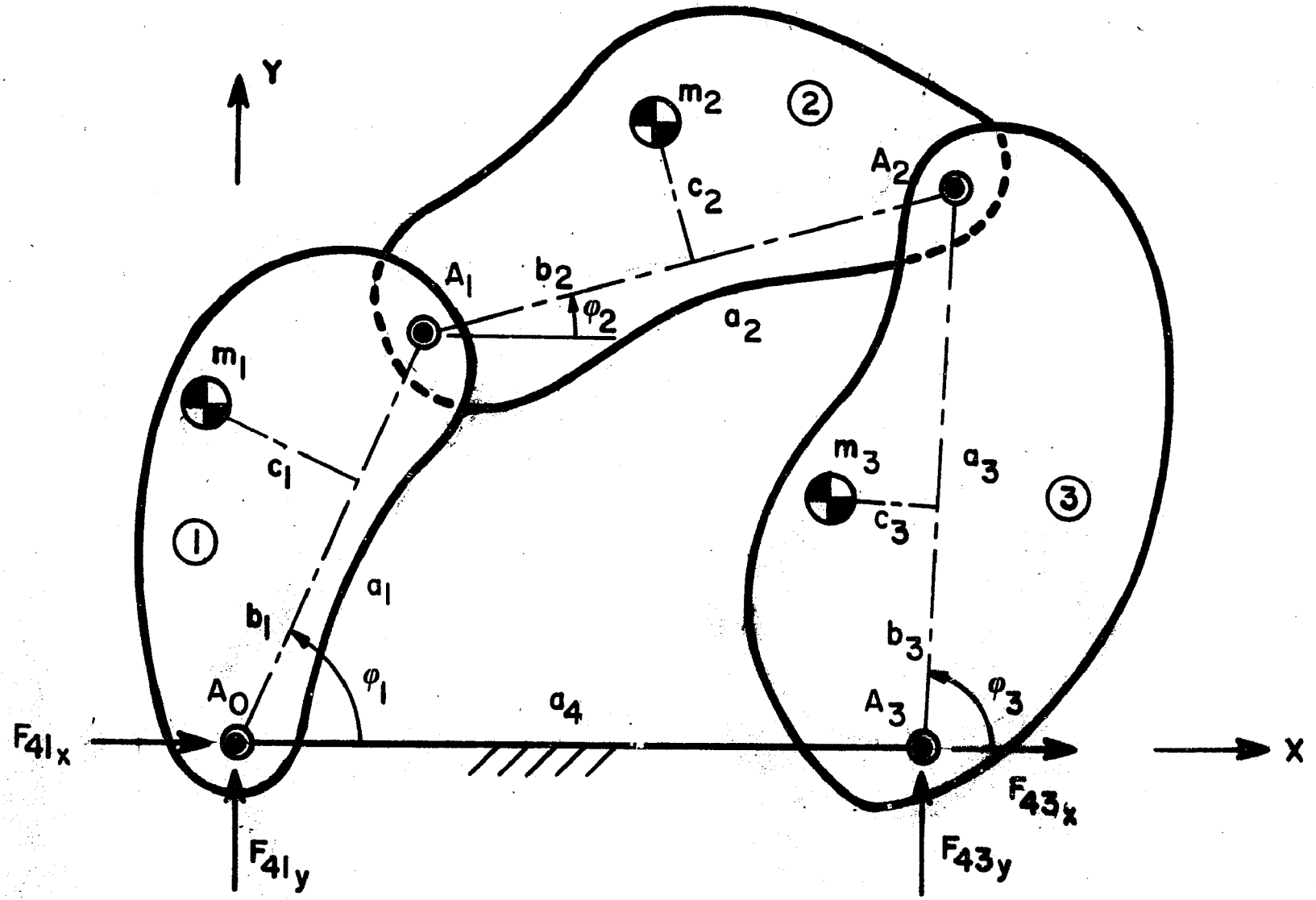

Fig. 5 General four-bar linkage to be optimized

link and smaller than some predetermined value which still permits a reasonable counterweight. It was found mathematically impossible to formulate this method in any other fashion.

Both of the above paths of shaking force optimization may be formulated in the identical manner:

Optimize the RMS shaking force,

$$F_{S_{RMS}} = \sqrt{\frac{1}{2\pi}\int_0^{2\pi} \left[(F_{14_x} + F_{34_x})^2 + (F_{14_y} + F_{34_y})^2 \right] d\varphi_1} \quad , \quad (4.1)$$

subject to the equality constraints

$$F_{41_{RMS}} = q_1 \, F_{41_{RMS_u}}, \quad \text{the RMS ground bearing force at pivot } A_0 \qquad (4.2a)$$

$$F_{43_{RMS}} = q_2 \, F_{43_{RMS_u}}, \quad \text{the RMS ground bearing force at pivot } A_3. \qquad (4.2b)$$

In the above, $F_{41_{RMS_u}}$ and $F_{43_{RMS_u}}$ are the RMS ground bearing reactions before balancing, and q_1 and q_2 are constraint factors which indicate the allowable increase of the RMS ground bearing forces at pivots A_0 and A_3, respectively, over those of the unbalanced mechanism. The parameters q_1 and q_2 are chosen such that

$$1 < q_i < \frac{i^{th} \text{ RMS ground bearing force of fully balanced mechanism}}{i^{th} \text{ RMS ground bearing force of unbalanced mechanism}} \quad . \qquad (4.3)$$

The conventional Lagrange formulation of this problem is given as follows:

$$E' = F_{S_{RMS}} + \lambda_1'(F_{41_{RMS}} - q_1 F_{41_{RMS_u}}) + \lambda_2'(F_{43_{RMS}} - q_2 F_{43_{RMS_u}}), \tag{4.4}$$

where λ_1' and λ_2' are the Lagrange Multipliers.

In order to eliminate the necessity of dealing with square roots in the RMS ground bearing and shaking force expressions, a slightly different approach, which will yield all the solutions inherent in the formulation (4.4), is used:

$$E = F^2_{S_{RMS}} + \lambda_1(F^2_{41_{RMS}} - q_1^2 F^2_{41_{RMS_u}}) + \lambda_2(F^2_{43_{RMS}} - q_2^2 F^2_{43_{RMS_u}}). \tag{4.5}$$

Here, the RMS shaking force expression and both sides of the constraint equations (4.2) have been squared. The desired solution set of equation (4.5) is identical to that of equation (4.4) for the following reasons:

1. Since the RMS expression of the shaking force represents a non-negative value, the minimum of its square occurs at the same argument as the minimum of the function itself.

2. The squaring of both sides of the constraint equations leads to

$$F^2_{41_{RMS}} - q_1^2 F^2_{41_{RMS_u}} = (F_{41_{RMS}} - q_1 F_{41_{RMS_u}})(F_{41_{RMS}} + q_1 F_{41_{RMS_u}}) = 0 \tag{4.6a}$$

$$F^2_{43_{RMS}} - q_2^2 F^2_{43_{RMS_u}} = (F_{43_{RMS}} - q_2 F_{43_{RMS_u}})(F_{43_{RMS}} + q_2 F_{43_{RMS_u}})$$
$$= 0 . \qquad (4.6b)$$

The factors $(F_{41_{RMS}} + q_1 F_{41_{RMS_u}})$ and $(F_{43_{RMS}} + q_2 F_{43_{RMS_u}})$ must always be positive, and therefore, the new constraint equations can only be satisfied if

$$(F_{41_{RMS}} - q_1 F_{41_{RMS_u}}) = 0 \qquad (4.7a)$$

$$(F_{43_{RMS}} - q_2 F_{43_{RMS_u}}) = 0 . \qquad (4.7b)$$

This, of course, corresponds to the original constraint equations (4.2).

In order to make the results independent of proportional linkage magnification, the RMS shaking force and the RMS ground bearing forces will be expressed in dimensionless form. This allows the solution for the following sets of variables for the two cases discussed above:

1. For the single counterweight problem, the dimensionless mass-distance products u_3 and t_3 of the total center of mass of link 3, as well as the dimensionless moment of inertia v_3 with respect to the pivot A_3, are obtained.

2. For the two counterweight problem, the dimensionless mass-distance products u_1, t_1, u_3 and t_3 of the total center of mass of the respective links are obtained for various predetermined values of v_3.

Using the force expressions given by equations (A.62) - (A.67) of Appendix A, and factoring $(\rho a_1^4 \dot{\varphi}_1^2)^2$, equation (4.5) may be rewritten as follows:

$$E = (\rho a_1^4 \dot{\varphi}_1^2)^2 \left[\frac{1}{2\pi} \int_0^{2\pi} (f_{S_x}^2 + f_{S_y}^2) d\varphi_1 + \lambda_1 \left(\frac{1}{2\pi} \int_0^{2\pi} (f_{41_x}^2 + f_{41_y}^2) d\varphi_1 \right.\right.$$

$$\left.\left. - q_1^2 f_{41_{RMS_u}}^2 \right) + \lambda_2 \left(\frac{1}{2\pi} \int_0^{2\pi} (f_{43_x}^2 + f_{43_y}^2) d\varphi_1 - q_2^2 f_{43_{RMS_u}}^2 \right) \right] . \tag{4.8}$$

The f's are dimensionless forces, and are given by equations (A.69) - (A.74).

The above formulation is now applied in the following sections to the single counterweight as well as the two counterweight method.

B. Shaking Force Optimization With Single Counterweight Attached to Output Link

1. Formulation of Lagrange Function

In order to apply the general formulation of equations (4.6) and (4.8) to the single counterweight optimization, the dimensionless forces of equation (4.8) must be written as explicit functions of the mass parameters u_3, t_3 and v_3 (see equations (A.76) - (A.78)). The Lagrange function (4.8) then becomes with the help of equations (A.79) - (A.84):

$$E = (\rho a_1^4 \dot{\varphi}_1^2)^2 \left\{ \frac{1}{2\pi} \int_0^{2\pi} \left[(L_9 + L_6 u_3 + L_7 t_3)^2 + (L_{10} - L_7 u_3 + L_6 t_3)^2 \right] d\varphi_1 \right.$$

$$+ \lambda_1 \left(\frac{1}{2\pi} \int_0^{2\pi} \left[(L_1 + L_2 v_3)^2 + (L_3 + L_4 v_3)^2 \right] d\varphi_1 - q_1^2 f_{41_{RMS_u}}^2 \right)$$

$$\left. + \lambda_2 \left(\frac{1}{2\pi} \int_0^{2\pi} \left[(L_5 + L_6 u_3 + L_7 t_3 - L_2 v_3)^2 + (L_8 - L_7 u_3 + L_6 t_3 - L_4 v_3)^2 \right] d\varphi_1 - q_2^2 f_{43_{RMS_u}}^2 \right) \right\} . \tag{4.9}$$

The L's are functions of the parameters of links 1 and 2, as well as the constant input angular velocity $\dot{\varphi}_1$, and are given by equations (A.85) - (A.94).

2. Derivation of Optimization Equations

To obtain the set of five optimization expressions, which permits the solution for u_3, t_3, v_3, λ_1 and λ_2, the following path will be taken:

a. The two ground bearing constraint equations (4.6) are written in dimensionless form.

b. The Lagrange function (4.9) is differentiated in turn with respect to t_3, u_3 and v_3, and the results are set equal to zero.

a. Constraint Equations

The dimensionless form of the constraint equations (4.6) is obtained with the help of equations (A.79) - (A.82):

$$f_{41_{RMS}}^2 - q_1^2 f_{41_{RMS_u}}^2 = \frac{1}{2\pi}\int_0^{2\pi} \left[(L_1 + L_2 v_3)^2 + (L_3 + L_4 v_3)^2\right] d\varphi_1 - q_1^2 f_{41_{RMS_u}}^2 = 0 \qquad (4.10)$$

$$f_{43_{RMS}}^2 - q_2^2 f_{43_{RMS_u}}^2 = \frac{1}{2\pi}\int_0^{2\pi} \left[(L_5 + L_6 u_3 + L_7 t_3 - L_2 v_3)^2 + (L_8 - L_7 u_3 + L_6 t_3 - L_4 v_3)^2\right] d\varphi_1 - q_2^2 f_{43_{RMS_u}}^2 = 0 . \qquad (4.11)$$

b. Differentiation of Lagrange Function With Respect to t_3, u_3 and v_3

$$\frac{\partial E}{\partial t_3} = 0 = (\rho a_1^{4.2}\varphi_1^2)^2\left\{\frac{1}{\pi}\int_0^{2\pi}\left[(L_9 + L_6u_3 + L_7t_3)L_7 + (L_{10} - L_7u_3 + L_6t_3)L_6\right]d\varphi_1 + \frac{\lambda_2}{\pi}\int_0^{2\pi}\left[(L_5 + L_6u_3 + L_7t_3 - L_2v_3)L_7 + (L_8 - L_7u_3 + L_6t_3 - L_4v_3)L_6\right]d\varphi_1\right\} \tag{4.12}$$

$$\frac{\partial E}{\partial u_3} = 0 = (\rho a_1^{4.2}\varphi_1^2)^2\left\{\frac{1}{\pi}\int_0^{2\pi}\left[(L_9 + L_6u_3 + L_7t_3)L_6 - (L_{10} - L_7u_3 + L_6t_3)L_7\right]d\varphi_1 + \frac{\lambda_2}{\pi}\int_0^{2\pi}\left[(L_5 + L_6u_3 + L_7t_3 - L_2v_3)L_6 - (L_8 - L_7u_3 + L_6t_3 - L_4v_3)L_7\right]d\varphi_1\right\} \tag{4.13}$$

$$\frac{\partial E}{\partial v_3} = 0 = (\rho a_1^{4.2}\varphi_1)^2\left\{\frac{\lambda_1}{\pi}\int_0^{2\pi}\left[(L_1 + L_2v_3)L_2 + (L_3 + L_4v_3)L_4\right]d\varphi_1\right.$$

$$+ \frac{\lambda_2}{\pi}\int_0^{2\pi}\left[-(L_5 + L_6u_3 + L_7t_3 - L_2v_3)L_2\right.$$

$$\left.\left. - (L_8 - L_7u_3 + L_6t_3 - L_4v_3)L_4\right]d\varphi_1\right\} . \qquad (4.14)$$

c. Simplification of Expressions

To facilitate the solution of the optimization equations (4.10) - (4.14), the following terms are defined:

$$K_1 = \int_0^{2\pi}(L_7L_9 + L_6L_{10})d\varphi_1 \qquad (4.15a)$$

$$K_2 = \int_0^{2\pi}(L_6^2 + L_7^2)d\varphi_1 \qquad (4.15b)$$

$$K_3 = \int_0^{2\pi}(L_5L_7 + L_6L_8)d\varphi_1 \qquad (4.15c)$$

$$K_4 = \int_0^{2\pi}(L_2L_7 + L_4L_6)d\varphi_1 \qquad (4.15d)$$

$$K_5 = \int_0^{2\pi}(L_6L_9 - L_7L_{10})d\varphi_1 \qquad (4.15e)$$

$$K_6 = \int_0^{2\pi}(L_5L_6 - L_7L_8)d\varphi_1 \qquad (4.15f)$$

$$K_7 = \int_0^{2\pi}(L_4L_7 - L_2L_6)d\varphi_1 \qquad (4.15g)$$

$$K_8 = \int_0^{2\pi} (L_1 L_2 + L_3 L_4) d\varphi_1 \tag{4.15h}$$

$$K_9 = \int_0^{2\pi} (L_2^2 + L_4^2) d\varphi_1 \tag{4.15i}$$

$$K_{10} = \int_0^{2\pi} (L_2 L_5 + L_4 L_8) d\varphi_1 \tag{4.15j}$$

$$K_{11} = \int_0^{2\pi} (L_1^2 + L_3^2) d\varphi_1 \tag{4.15k}$$

$$K_{12} = \int_0^{2\pi} (L_5^2 + L_8^2) d\varphi_1 \, . \tag{4.15l}$$

d. Optimization Equations

With the above simplifications, the set of five simultaneous optimization equations (4.10) - (4.14) appears as follows:

$$K_{11} + 2K_8 v_3 + K_9 v_3^2 = 2\pi q_1^2 \, f_{41_{RMS_u}}^2 \tag{4.16}$$

$$K_{12} + K_2 u_3^2 + K_2 t_3^2 + K_9 v_3^2 + 2K_6 u_3 + 2K_3 t_3 - 2K_{10} v_3 + 2K_7 u_3 v_3 - 2K_4 t_3 v_3 = 2\pi q_2^2 \, f_{43_{RMS_u}}^2 \tag{4.17}$$

$$K_1 + K_2 t_3 + \lambda_2 (K_3 + K_2 t_3 - K_4 v_3) = 0 \tag{4.18}$$

$$K_5 + K_2 u_3 + \lambda_2 (K_6 + K_2 u_3 + K_7 v_3) = 0 \tag{4.19}$$

$$\lambda_1 (K_8 + K_9 v_3) - \lambda_2 (K_{10} - K_7 u_3 + K_4 t_3 - K_9 v_3) = 0. \tag{4.20}$$

Solution of the above equations furnishes the optimum mass parameters u_3, t_3 and v_3 in addition to the Lagrange Multipliers λ_1 and λ_2.

3. Solution of Optimization Equations

Appendix E shows the solution of the optimization equations (4.16) - (4.20). While the Lagrange Multipliers λ_1 and λ_2 must be determined in order to obtain the optimum mass parameters u_3, t_3 and v_3, they serve no further purpose in the present investigation.

The results for u_3, t_3 and v_3 are listed below in the order necessary for numerical computation. It is to be noted that there are two solutions for v_3, and further, two solutions for u_3 and t_3 for each v_3. This gives rise to a total of four solutions.

Appendix F gives a theoretical proof that the two solutions associated with each v_3 represent a minimum and a maximum of the RMS shaking force. This is accomplished by showing that the constraint surface is represented by the circumferences of two possible circles, each corresponding to one of the v_3's, and that, therefore, the theorem which states that a continuous function has a minimum and a maximum on a closed and bounded set is satisfied.

According to the results represented by equations (E.6), (E.13) and (E.16) of Appendix E, one obtains

$$v_3^{(1)} = \frac{-K_8 + \sqrt{K_8^2 - K_9(K_{11} - 2\pi q_1^2 f_{41_{RMS_u}}^2)}}{K_9} \tag{4.21a}$$

$$v_3^{(2)} = \frac{-K_8 - \sqrt{K_8^2 - K_9(K_{11} - 2\pi q_1^2 f_{41_{RMS_u}}^2)}}{K_9} \tag{4.21b}$$

$$t_3^{(i,1)} = \frac{-H_2^{(i)} + \sqrt{H_2^{(i)2} - H_1^{(i)} H_3^{(i)}}}{H_3^{(i)}} \quad (i=1,2) \tag{4.22a}$$

$$t_3^{(i,2)} = \frac{-H_2^{(i)} - \sqrt{H_2^{(i)2} - H_1^{(i)} H_3^{(i)}}}{H_3^{(i)}} \quad (i=1,2) \tag{4.22b}$$

$$u_3^{(i,j)} = \frac{-(A_1^{(i)} + A_2^{(i)} t_3^{(j)})}{A_3^{(i)}} \quad (i=1,2;\ j=1,2) \tag{4.23}$$

where

$$A_1^{(i)} = K_3K_5 - K_4K_5v_3^{(i)} - K_1K_6 - K_1K_7v_3^{(i)} \quad (i=1,2) \tag{4.24a}$$

$$A_2^{(i)} = K_2K_5 - K_2K_6 - K_2K_7v_3^{(i)} \quad (i=1,2) \tag{4.24b}$$

$$A_3^{(i)} = K_2K_3 - K_1K_2 - K_2K_4v_3^{(i)} \quad (i=1,2) \tag{4.24c}$$

$$H_1^{(i)} = K_{12} + K_9 v_3^{(i)2} - 2K_{10} v_3^{(i)} - 2\pi q_2^2 f^2_{43_{RMS_u}} + \frac{A_1^{(i)2}}{A_3^{(i)2}} K_2 - 2 \frac{A_1^{(i)}}{A_3^{(i)}} (K_6 + K_7 v_3^{(i)}) \quad (i=1,2) \tag{4.24d}$$

$$H_2^{(i)} = K_2 \frac{A_1^{(i)} A_2^{(i)}}{A_3^{(i)2}} - (K_6 + K_7 v_3^{(i)}) \frac{A_2^{(i)}}{A_3^{(i)}} + K_3 - K_4 v_3^{(i)} \quad (i=1,2) \tag{4.24e}$$

$$H_3^{(i)} = \left(\frac{A_2^{(i)2}}{A_3^{(i)2}} + 1 \right) K_2 \quad (i=1,2) \; . \tag{4.24f}$$

4. Application of Solution to Design of Output Link Counterweight

The optimum mass parameters u_3, t_3 and v_3 are physically realized with the help of a counterweight, which is added to the already existing link 3. (See Fig. 6.) Parts 1 and 2a of Appendix G show how such a circular counterweight, which is tangent to the pivot A_3, must be designed when a standard configuration is used. (For standard linkage configuration, see [14] and Fig. 7.) The relevant design parameters are the dimensionless counterweight radius R_3^*, the counterweight angular position θ_3^* with respect to link 3, and the dimensionless counterweight thickness-density ratio D_3^*.

Expressed in terms of u_3, t_3 and v_3, the dimensionless

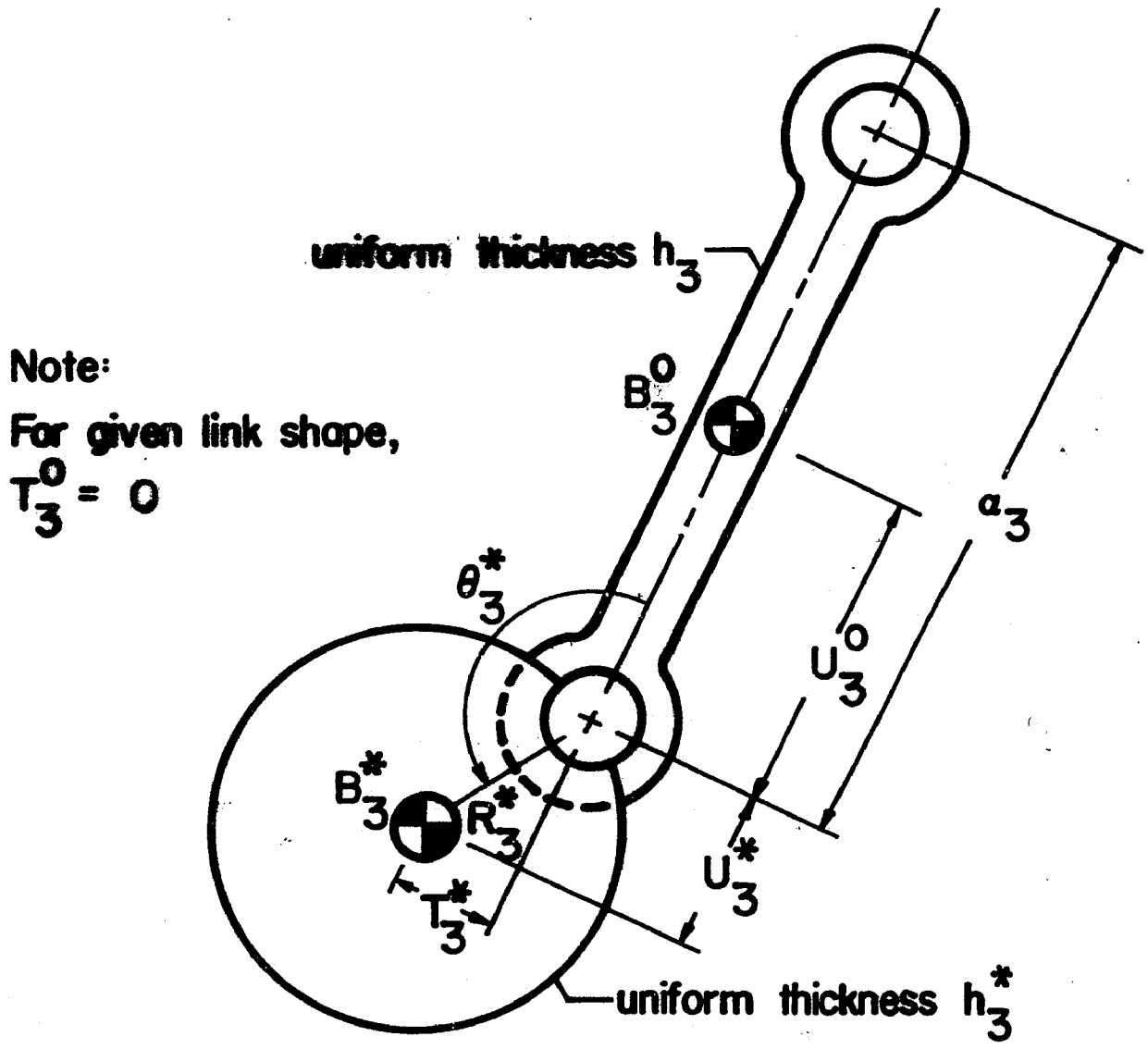

The superscript zero refers to the center of mass of the unbalanced link, and the superscript asterisk refers to the center of mass of the counterweight.

Fig. 6 Dimensionless parameters of output link with attached counterweight

radius according to equation (G.18) is given by:

$$R_3^* = \frac{r_3^*}{a_1} = (U_3^{*2} + T_3^{*2})^{1/2} = \frac{2\left[v_3 - \left(\frac{B_3^o \alpha_3^2}{4} + C_3^o\right)\right]}{3\left[t_3^2 + (u_3 - \frac{1}{2} B_3^o \alpha_3)^2\right]^{1/2}} \quad . \quad (4.25)$$

Similarly, the angular position according to equation (G.19) is given by:

$$\theta_3^* = \tan^{-1}\left(\frac{T_3^*}{U_3^*}\right) = \tan^{-1}\left(\frac{t_3}{u_3 - \frac{1}{2} B_3^o \alpha_3}\right) \quad . \quad (4.26)$$

Finally, the thickness-density ratio is shown by equation (G.20) to be

$$D_3^* = \delta_3\left(\frac{\rho_3^*}{\rho^o}\right) = \left(\frac{h_3^*}{h_3}\right)\left(\frac{\rho_3^*}{\rho^o}\right) = \frac{27\left[t_3^2 + (u_3 - \frac{1}{2} B_3^o \alpha_3)^2\right]^2}{8\pi\beta_3\gamma_3\left[v_3 - \left(\frac{B_3^o \alpha_3^2}{4} + C_3^o\right)\right]^3} \quad , \quad (4.27)$$

where

r_3^* = actual radius of counterweight

$U_3^* = R_3^* \cos\theta_3^*$, $T_3^* = R_3^* \sin\theta_3^*$ } dimensionless coordinates of position of counterweight center of mass

B_3^o, C_3^o = dimensionless mass and moment of inertia of existing link 3, respectively (see equations (A.119c) and (A.119e))

α_3, β_3, γ_3 = dimensionless parameters expressing geometry of link 3 (see equations (A.115))

δ_3 = ratio of counterweight thickness to thickness of link 3

h_3, h_3^* = thicknesses of link 3 and counterweight, respectively

ρ^o, ρ_3^* = mass densities of link 3 and counterweight, respectively.

5. Example of Optimization With Output Link Counterweight

a. Procedure

In order to apply the optimization procedure derived in the previous sections to an existing linkage, the following design steps must be followed:

(1) The range of meaningful constraint factors q_1 and q_2 must be determined from an inspection of the RMS ground bearing forces, both of the existing unbalanced mechanism as well as those which arise when the mechanism is fully force balanced by the Method of Linearly Independent Vectors [2]. To this end, use is made of equation (4.3).

(2) The counterweight radii R_3^*, the thickness-density ratios D_3^*, and the angles θ_3^*, as obtained from the optimum mass parameters u_3, t_3 and v_3, as well as the associated optimum dimensionless RMS shaking forces, are then computed as functions of the various combinations of constraint factors q_1 and q_2. In addition, the ratio

$$\nu_f = \frac{\text{RMS shaking force of partially balanced mechanism}}{\text{RMS shaking force of unbalanced mechanism}} , \tag{4.28}$$

which may serve as a measure of the reduction of the RMS shaking force, is introduced. Finally, design graphs, which are based upon the above information, permit the choice of the most practical configuration.

b. Numerical Example

The four-bar linkage of Fig. 7 with length dimensions listed in Table 3 will now be used for a numerical example. This mechanism is designed according to the standard configuration discussed in Appendix A.

Link i	1	2	3	4
Dimensionless link length $\alpha_i = a_i/a_1$	1.000	4.000	3.000	3.000
Dimensionless link width and end radius $\beta_i = d_i/a_1$	0.500	0.500	0.500	-
Dimensionless link thickness $\gamma_i = h_i/d_i$	0.400	0.400	0.400	-

Table 3 Dimensionless Length Parameters of Example Four-Bar Linkage

In order to determine the constraint factors q_1 and q_2, it is first necessary to know the magnitude of the dimensionless RMS ground bearing forces, both of the balanced and unbalanced mechanism. Furthermore, to judge the improvement of the RMS shaking force due to the optimization method, the RMS shaking force of the unbalanced mechanism must be known.

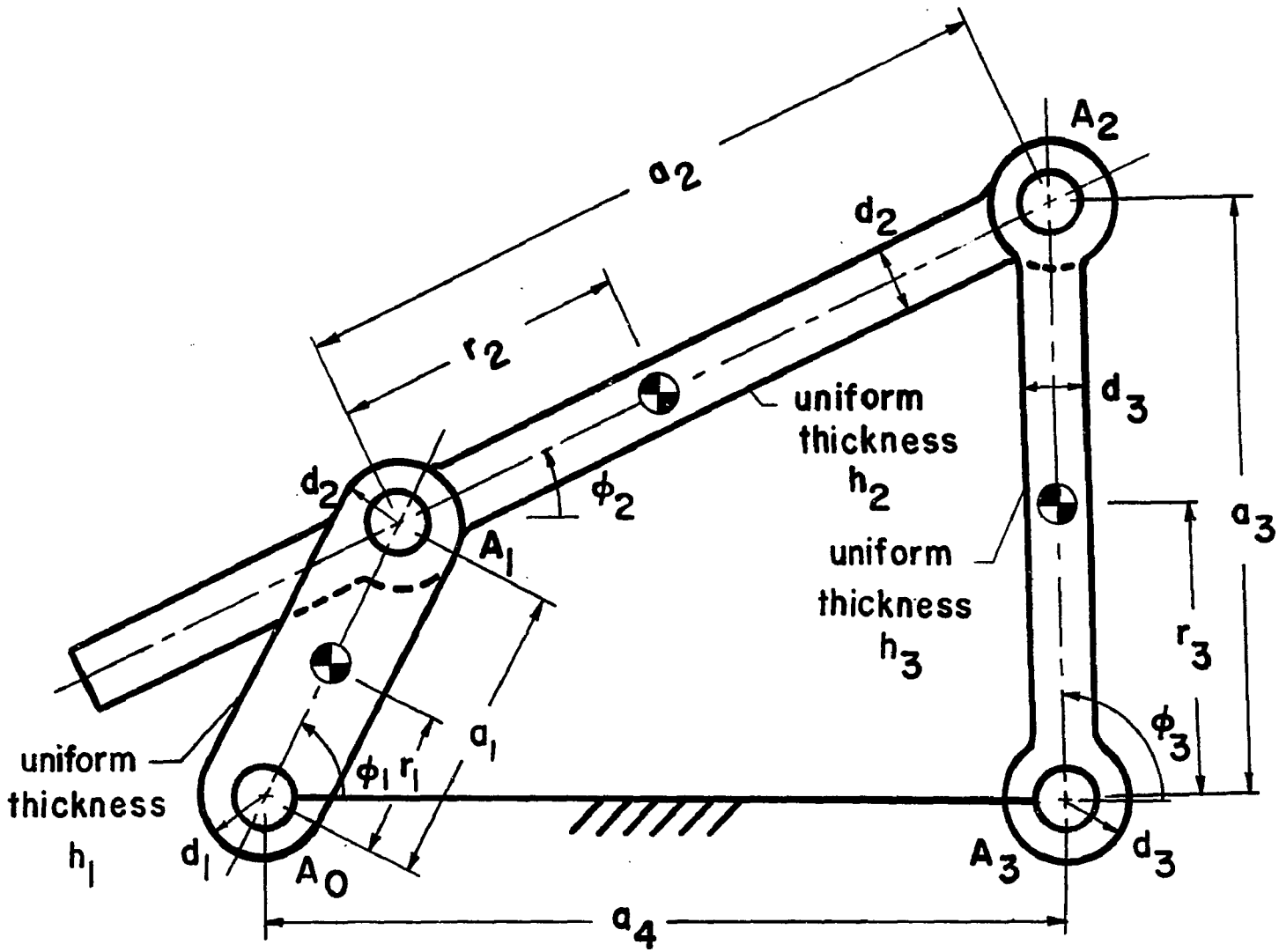

Fig. 7 Standard four-bar linkage configuration

(1) RMS Shaking and Ground Bearing Forces of Unbalanced Mechanism

To compute the dimensionless RMS ground bearing forces as well as the dimensionless RMS shaking force for the unbalanced mechanism, one first obtains values of the dimensionless components of both bearing forces, f_{4i_x} and f_{4i_y} (i=1,3), for equally spaced input angles with the help of equations (A.69) - (A.72). The necessary values of the link mass parameters are listed in Table 4.

The dimensionless RMS value of the individual ground bearing forces is given by:

$$f_{4i_{RMS}} = \sqrt{\frac{1}{2\pi}\int_0^{2\pi} (f_{4i_x}^2 + f_{4i_y}^2)d\varphi_1} \quad (i=1,3). \tag{4.29}$$

The dimensionless RMS shaking force of the unbalanced mechanism becomes:

$$f_{S_{RMS}} = \sqrt{\frac{1}{2\pi}\int_0^{2\pi} (f_{S_x}^2 + f_{S_y}^2)d\varphi_1} \tag{4.30a}$$

where

$$f_{S_x} = f_{14_x} + f_{34_x} \tag{4.30b}$$

$$f_{S_y} = f_{14_y} + f_{34_y} \, . \tag{4.30c}$$

Using intervals of 5°, the following values were obtained

	Unbalanced			Fully Balanced	
Link i	1	2	3	1	3
Dimensionless position of link center of mass along line joining pivots $U_i = b_i/a_1 = r_i/a_1$	0.500	3.000	1.500	-0.216	-0.691
Dimensionless position of link center of mass perpendicular to line joining pivots $T_i = c_i/a_1$	0.000	0.000	0.000	0.000	0.000
Dimensionless link mass B_i	0.357	0.845	0.514	0.977	2.753
Dimensionless link radius of gyration W_i	not needed	2.142	1.261	not needed	1.408
Dimensionless link moment of inertia $v_i = B_i(U_i^2 + T_i^2 + W_i^2)$	not needed	1.482	1.974	not needed	6.764

Table 4 Dimensionless Mass Parameters of Unbalanced and Fully Balanced Example Four-Bar Linkage

with the help of the above expressions[†]

$$f_{41_{RMS_u}} = 2.156, \quad f_{43_{RMS_u}} = 1.643, \quad f_{S_{RMS_u}} = 1.349 \ . \tag{4.31}$$

(2) RMS Ground Bearing Forces of Fully Force Balanced Mechanism

The dimensionless RMS ground bearing forces of the fully force balanced mechanism using circular tangent counterweights are given by:

$$f_{41_{RMS_b}} = f_{43_{RMS_b}} = 3.020 \ . \tag{4.32}$$

The above results were obtained with the help of equations (A.69) - (A.72) of Appendix A and equation (4.29), using 5^o intervals. The values of the link mass parameters of the fully balanced four-bar linkage, as shown in Table 4, were supplied by expressions derived in Appendix J. They are based upon a counterweight thickness-density ratio of 2.5, and the counterweight material is assumed to be identical with that of the links. The resulting dimensionless counterweight radii are:

$$R^*_{1_b} = 0.629, \quad R^*_{3_b} = 1.194 \ . \tag{4.33}$$

See also Table 15.

[†] All computations were performed on the City College IBM 360/50 Computer, with programs written in Fortran IV.

(3) Determination of Range of Constraint Factors q_1 and q_2

Using the criterion (4.3) for the range of meaningful constraint factors together with equations (4.31) and (4.32), one obtains

$$1 < q_1 < 1.40 \tag{4.34a}$$

$$1 < q_2 < 1.84 \ . \tag{4.34b}$$

(4) Design Method for Determination of Counterweight Radius, Thickness-Density Ratio and Angle

(a) Tabulation of Solutions

In order to obtain the values of R_3^*, D_3^* and θ_3^*, it is first necessary to determine the optimum mass parameters u_3, t_3 and v_3 for all desired combinations of q_1 and q_2, as well as the values listed in Table 3, with the help of equations (4.21) - (4.23). It must be recalled that there is a possibility of two pairs of answers, where each pair stems from one of the two possible values of v_3. Each of these pairs may produce a minimum or a maximum value for the RMS shaking force, and it is therefore necessary to determine which set of mass parameters is associated with the lowest RMS shaking force.†

---

† The magnitude of the dimensionless RMS shaking force of the partially balanced mechanism is obtained by substituting the optimum mass parameters t_3 and u_3 into the expressions for the components of the dimensionless shaking force given by equations (A.83) and (A.84). These are determined for equally spaced angles over a range of 360°. The dimensionless RMS shaking force is then obtained with the help of equation (4.30a).

Once this has been accomplished, equations (4.25) - (4.27) are used to obtain the counterweight parameters. Table 5 shows values for the optimum mass parameters v_3, t_3 and u_3 which are associated with the minimum dimensionless RMS shaking forces for the desired range of constraint factors. Table 6 then lists the corresponding dimensionless counterweight parameters R_3^*, D_3^* and θ_3^*, as well as the ratio ε_f, as functions of the indicated constraint factors.

In order to facilitate the selection of the most practical design from all the solutions of Table 6, the design graphs of Fig. 8 have been devised. The top graph shows values of D_3^* and R_3^* plotted against q_2 for various values of q_1. The bottom graph gives the ratio ε_f as a function of q_2, again for various values of q_1. The vertical line-up of the q_2 axes makes it easier to arrive at an engineering compromise.

(b) Choice of Solutions With Help of Design Graphs

Let it be required that the individual RMS ground bearing forces of the partially balanced mechanism have magnitudes no more than midway to 3/4 of the range between those of the unbalanced and the fully balanced mechanism. This corresponds to a maximum value of $q_1 = 1.30$ and $q_2 = 1.40$. Let it further be required that the thickness ratio δ_3 of the counterweight to the original link be no greater than 3 to 4, and let it be assumed that the original link is made of steel (density $\rho^o = 0.28$ lb/in.^{3}). If one uses a tungsten alloy (density $\rho_3^* \approx 0.7$ lb/in.^{3}) for the counterweight, then equation (4.27) shows that D_3^* must

q_1		q_2 = 1.10	1.20	1.30	1.40	1.50	1.60	1.70	1.80
1.05	v_3	2.443	2.443	2.443	2.443	2.443	2.443	2.443	2.443
	t_3	0.491	0.147	-0.192	-0.526	-0.857	-1.184	-1.510	-1.833
	u_3	-1.667	-1.916	-2.160	-2.402	-2.640	-2.877	-3.112	-3.346
1.10	v_3	2.912	2.912	2.912	2.912	2.912	2.912	2.912	2.912
	t_3	0.723	0.374	0.032	-0.305	-0.638	-0.967	-1.294	-1.618
	u_3	-1.498	-1.750	-1.998	-2.242	-2.482	-2.721	-2.958	-3.193
1.15	v_3	3.381	3.381	3.381	3.381	3.381	3.381	3.381	3.381
	t_3	0.956	0.603	0.257	-0.082	-0.417	-0.748	-1.078	-1.403
	u_3	-1.326	-1.583	-1.833	-2.080	-2.323	-2.564	-2.802	-3.039
1.20	v_3	3.849	3.849	3.849	3.849	3.849	3.849	3.849	3.849
	t_3	1.192	0.834	0.485	0.142	-0.195	-0.529	-0.859	-1.187
	u_3	-1.152	-1.413	-1.667	-1.916	-2.162	-2.405	-2.645	-2.884
1.25	v_3	4.316	4.316	4.316	4.316	4.316	4.316	4.316	4.316
	t_3	1.430	1.067	0.713	0.368	0.027	-0.308	-0.640	-0.970
	u_3	-0.976	-1.241	-1.499	-1.751	-1.999	-2.244	-2.486	-2.727
1.30	v_3	4.783	4.783	4.783	4.783	4.783	4.783	4.783	4.783
	t_3	1.672	1.302	0.944	0.595	0.251	-0.087	-0.421	-0.752
	u_3	-0.797	-1.067	-1.329	-1.584	-1.835	-2.082	-2.326	-2.568
1.35	v_3	5.250	5.250	5.250	5.250	5.250	5.250	5.250	5.250
	t_3	1.916	1.540	1.177	0.823	0.477	0.136	-0.200	-0.533
	u_3	-0.615	-0.891	-1.156	-1.415	-1.669	-1.919	-2.165	-2.409
1.40	v_3	5.717	5.717	5.717	5.717	5.717	5.717	5.717	5.717
	t_3	2.164	1.780	1.411	1.054	0.704	0.360	0.022	-0.313
	u_3	-0.430	-0.712	-0.982	-1.245	-1.501	-1.754	-2.002	-2.248

Table 5 Optimum Mass Parameters v_3, t_3 and u_3 (Associated With Lowest RMS Shaking Force) vs. q_1 and q_2

(Computations used 5^o intervals. Comparison showed that no greater accuracy was needed for the well behaved functions involved.)

q_1		q_2 = 1.10	1.20	1.30	1.40	1.50	1.60	1.70	1.80
1.05	R_3^*	0.126	0.116	0.107	0.097	0.089	0.082	0.075	0.069
	D_3^*	1,983	2,719	3,862	5,547	7,936	11,222	15,623	21,388
	θ_3^*	169°	177°	184°	189°	194°	198°	201°	204°
	ν_f	0.40	0.31	0.25	0.26	0.32	0.42	0.53	0.64
1.10	R_3^*	0.263	0.246	0.226	0.207	0.189	0.173	0.159	0.146
	D_3^*	209	274	381	546	785	1,120	1,576	2,183
	θ_3^*	162°	172°	179°	186°	191°	195°	199°	202°
	ν_f	0.48	0.37	0.28	0.25	0.28	0.35	0.45	0.57
1.15	R_3^*	0.407	0.386	0.358	0.329	0.300	0.274	0.251	0.231
	D_3^*	54	67	90	127	183	263	374	524
	θ_3^*	156°	166°	174°	182°	188°	193°	197°	200°
	ν_f	0.56	0.44	0.34	0.26	0.25	0.30	0.39	0.49
1.20	R_3^*	0.552	0.535	0.503	0.464	0.425	0.388	0.355	0.325
	D_3^*	21	24	31	42	61	88	125	178
	θ_3^*	148°	159°	169°	177°	184°	189°	194°	198°
	ν_f	0.65	0.52	0.40	0.31	0.25	0.26	0.33	0.42

Table 6 Counterweight Parameters R_3^*, D_3^* and θ_3^* and RMS Shaking Force Ratio ν_f vs. q_1 and q_2 for Values of Table 5

q_1		q_2 = 1.10	1.20	1.30	1.40	1.50	1.60	1.70	1.80
1.25	R_3^*	0.692	0.686	0.656	0.613	0.564	0.515	0.470	0.430
	D_3^*	10.858	11.242	13.395	17.640	24.623	35.272	50.771	72.544
	θ_3^*	141°	152°	163°	172°	179°	186°	191°	195°
	v_f	0.73	0.60	0.48	0.37	0.28	0.25	0.28	0.35
1.30	R_3^*	0.817	0.832	0.814	0.771	0.715	0.656	0.599	0.547
	D_3^*	6.682	6.235	6.804	8.434	11.381	16.083	23.130	33.260
	θ_3^*	133°	145°	156°	166°	174°	182°	187°	193°
	v_f	0.83	0.69	0.56	0.44	0.33	0.26	0.25	0.30
1.35	R_3^*	0.924	0.964	0.967	0.935	0.878	0.811	0.742	0.677
	D_3^*	4.777	4.023	3.973	4.551	5.837	8.036	11.458	16.510
	θ_3^*	126°	137°	149°	159°	169°	177°	184°	190°
	v_f	0.92	0.78	0.64	0.51	0.40	0.31	0.25	0.26
1.40	R_3^*	1.008	1.077	1.108	1.097	1.049	0.978	0.900	0.822
	D_3^*	3.844	2.952	2.630	2.743	3.283	4.334	6.061	8.696
	θ_3^*	119°	130°	141°	152°	163°	172°	180°	186°
	v_f	1.01	0.87	0.73	0.60	0.47	0.37	0.28	0.25

Table 6 continued

Fig. 8 Design graphs for counterweight attached to output link

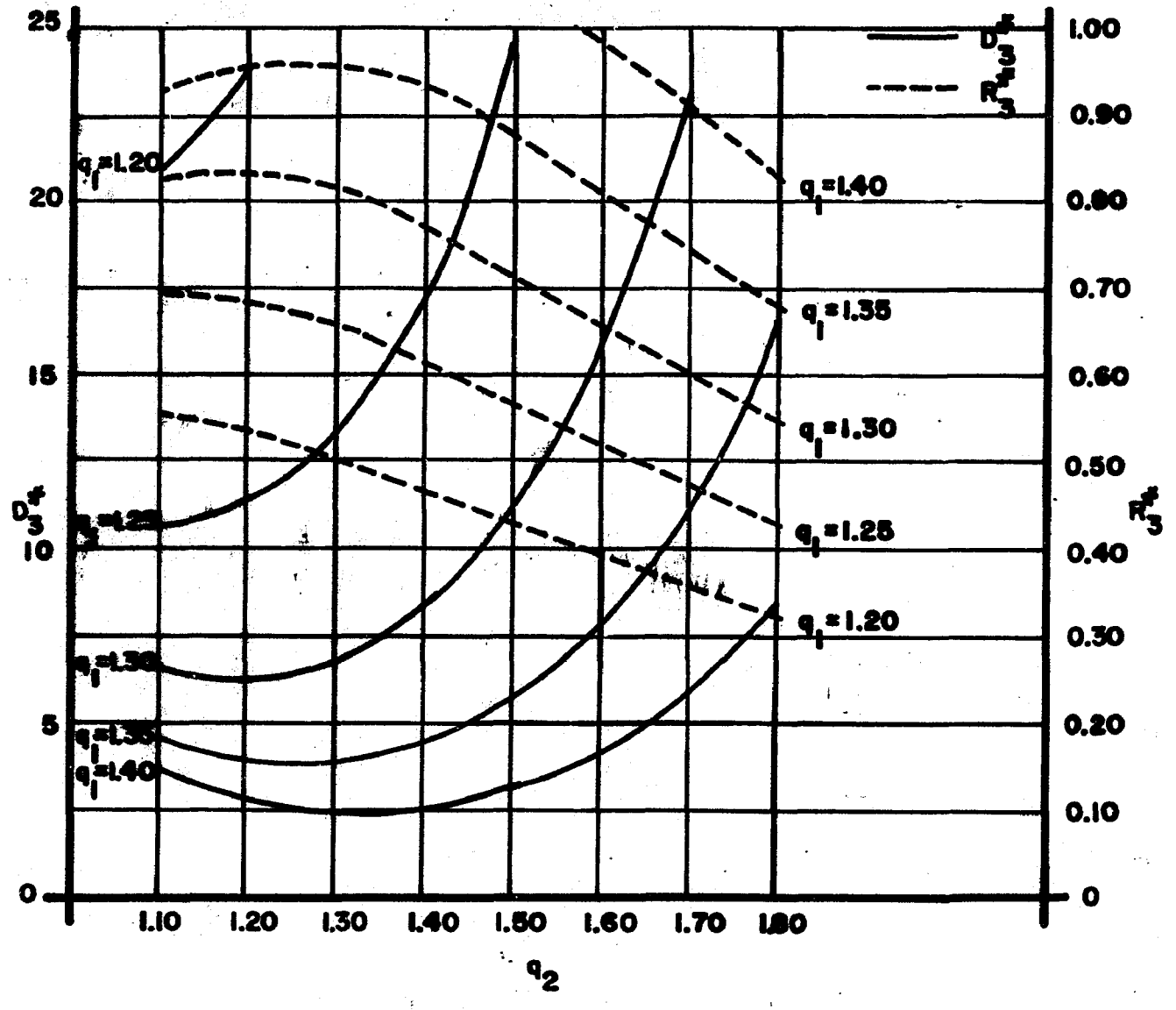

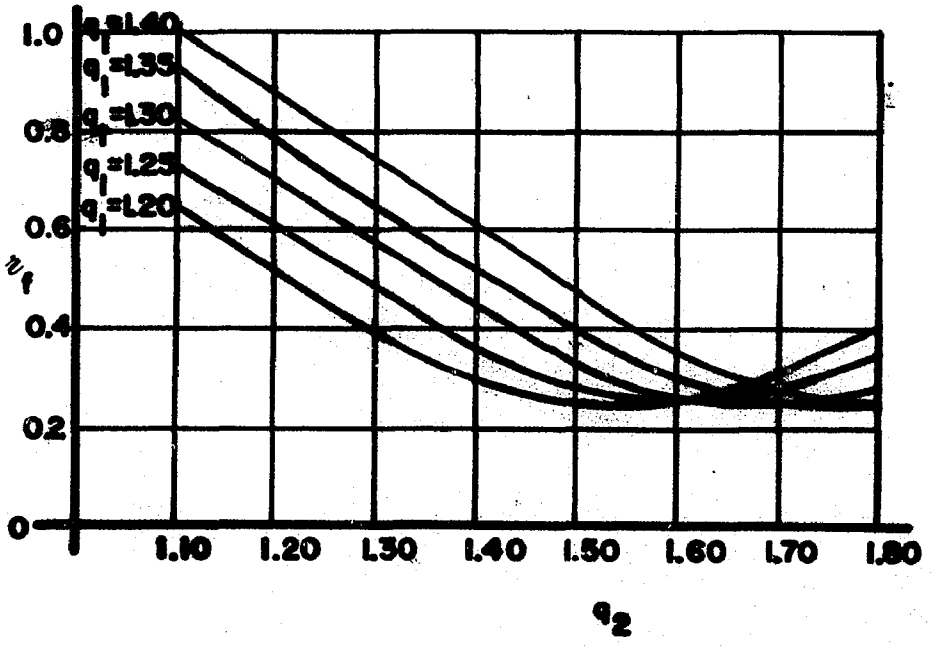

not exceed approximately 7.5.

In order to realize these requirements, the top graph of Fig. 8 is entered, and it is seen that the value of $D_3^* = 6.235$ may be obtained when $q_1 = 1.30$ and $q_2 = 1.20$. The top graph further indicates that these values correspond to a dimensionless counterweight radius $R_3^* = 0.832$. The bottom graph shows that for the same constraint factors, $\hat{r}_f = 0.69$. This represents a 31 % reduction in RMS shaking force. Finally, Table 6 furnishes $\theta_3^* = 145^\circ$. These values are listed in Table 7.

The design graphs suggest other feasible solutions containing reasonable counterweight dimensions. While these solutions will lead to slightly increased dimensionless RMS ground bearing forces, the dimensionless RMS shaking force will be much smaller. Table 7 gives two such examples, where in the first, $q_1 = q_2 = 1.30$, and in the second, $q_1 = 1.35$ and $q_2 = 1.50$.

D_3^*	q_1	q_2	$\hat{r}_f$	R_3^*	θ_3^*
6.235	1.30	1.20	0.69	0.832	145°
6.804	1.30	1.30	0.56	0.814	156°
5.837	1.35	1.50	0.40	0.878	169°

Table 7 Feasible Solutions Containing Reasonable Counterweight Dimensions

(c) Conclusions

Table 8 shows a comparison of the dimensionless

Balancing Condition	ν_f	$f_{41_{RMS}}$	$f_{43_{RMS}}$	R_1^*	R_3^*	D_1^*	D_3^*	θ_1^*	θ_3^*
Unbalanced	1.00	2.156	1.643	-	-	-	-	-	-
Fully Balanced ($\rho^*/\rho^o=1$)†	0.00	3.020	3.020	0.629	1.194	2.500	2.500	180°	180°
Partially Balanced ($\rho^*/\rho^o=2.5$)†									
$q_1=1.30$, $q_2=1.20$	0.69	2.802	1.972	-	0.832	-	6.235	-	145°
$q_1=1.30$, $q_2=1.30$	0.56	2.802	2.136	-	0.814	-	6.804	-	156°
$q_1=1.35$, $q_2=1.50$	0.40	2.910	2.465	-	0.878	-	5.837	-	169°

Table 8 Comparison of Dimensionless RMS Shaking Force, Dimensionless RMS Ground Bearing Forces and Counterweight Dimensions

† Counterweights are assumed to have the identical density as the links for the fully balanced case, while for the partially balanced case, a higher density material is used for the counterweights.

RMS shaking forces, the dimensionless RMS ground bearing forces, as well as the counterweight dimensions, of the three cases discussed above with those of the unbalanced and the fully balanced mechanism. This allows the following conclusions:

1. Comparatively small increases in the constraint factors, i.e. the permissible dimensionless RMS ground bearing forces, cause much larger decreases in the dimensionless RMS shaking forces of the partially balanced mechanisms.

2. There is very little difference in the counterweight dimensions of the three types of partially balanced mechanisms. The need for counterweight materials differing in density from that of the links in order to obtain reasonable dimensions represents an engineering compromise.

3. The attainable reduction of the dimensionless RMS ground bearing forces from those of the fully force balanced mechanism is modest when the present single counterweight method is used.

The two counterweight method described in the next section offers greatly improved results concerning dimensionless RMS ground bearing forces as well as counterweight density requirements.

C. Shaking Force Optimization With Counterweights Attached to Input and Output Links

1. Formulation of Lagrange Function

In order to apply the general formulation of equations (4.6) and (4.8) to the two counterweight optimization, the dimensionless forces of equation (4.8) must be written as explicit functions of the mass parameters of the two links, i.e. u_1, t_1, u_3, t_3 and v_3 (see equations (A.76) - (A.78), (A.95) and (A.96)). The Lagrange function (4.8) then becomes with the help of equations (A.97) - (A.102);*

$$
\begin{aligned}
E = (\rho a_1^4 \dot{\varphi}_1^2)^2 \Bigg\{ & \frac{1}{2\pi} \int_0^{2\pi} \Big[(N_{11} + N_2 u_1 - N_3 t_1 + N_8 u_3 + N_9 t_3)^2 \\
& + (N_{12} + N_3 u_1 + N_2 t_1 - N_9 u_3 + N_8 t_3)^2 \Big] d\varphi_1 \\
& + \lambda_1 \Bigg(\frac{1}{2\pi} \int_0^{2\pi} \Big[(N_1 + N_2 u_1 - N_3 t_1 + N_4 v_3)^2 \\
& + (N_5 + N_3 u_1 + N_2 t_1 + N_6 v_3)^2 \Big] d\varphi_1 - q_1^2 f_{41_{RMS_u}}^2 \Bigg) \\
& + \lambda_2 \Bigg(\frac{1}{2\pi} \int_0^{2\pi} \Big[(N_7 + N_8 u_3 + N_9 t_3 - N_4 v_3)^2 \\
& + (N_{10} - N_9 u_3 + N_8 t_3 - N_6 v_3)^2 \Big] d\varphi_1 - q_2^2 f_{43_{RMS_u}}^2 \Bigg) \Bigg\} .
\end{aligned}
\tag{4.35}
$$

*Equation (4.35) differs from equation (4.9) since u_1 and t_1 are not explicitly given in equation (4.9). Even though v_3 is not solved for in this procedure, it must be defined in the equations so that substitution of preassigned values is readily possible.

The N's are functions of the parameters of link 2 as well as the constant input angular velocity $\dot{\varphi}_1$, and are given by equations (A.103) - (A.114).

2. Derivation of Optimization Equations

The set of six optimization expressions which permit the solution for u_1, t_1, u_3, t_3, λ_1 and λ_2 are obtained in a manner similar to that of the previous section, i.e.

a. The two ground bearing constraint equations (4.6) are written in dimensionless form with the help of equations (A.97) - (A.100).

b. The Lagrange function (4.35) is differentiated in turn with respect to t_1, u_1, t_3 and u_3, and the results are set equal to zero.

a. Constraint Equations

The dimensionless form of the constraint equations (4.6) is obtained with the help of equations (A.97) - (A.100):

$$f_{41_{RMS}}^2 - q_1^2 f_{41_{RMS_u}}^2 = \frac{1}{2\pi}\int_0^{2\pi} \Big[(N_1 + N_2u_1 - N_3t_1 + N_4v_3)^2 + (N_5 + N_3u_1 + N_2t_1 + N_6v_3)^2\Big]d\varphi_1 - q_1^2 f_{41_{RMS_u}}^2 = 0 \qquad (4.36)$$

$$f^2_{43_{RMS}} - q_2^2 f^2_{43_{RMS_u}} = \frac{1}{2\pi}\int_0^{2\pi} \Big[(N_7 + N_8u_3 + N_9t_3 - N_4v_3)^2 + (N_{10} - N_9u_3 + N_8t_3 - N_6v_3)^2\Big]d\varphi_1 - q_2^2 f^2_{43_{RMS_u}} = 0 \; . \tag{4.37}$$

b. Differentiation of Lagrange Function With Respect to t_1, u_1, t_3 and u_3

$$\frac{\partial E}{\partial t_1} = 0 = (\rho a_1^{4\cdot 2}\varphi_1^2)^2\left\{\frac{1}{\pi}\int_0^{2\pi}\Big[-(N_{11} + N_2u_1 - N_3t_1 + N_8u_3 + N_9t_3)N_3 + (N_{12} + N_3u_1 + N_2t_1 - N_9u_3 + N_8t_3)N_2\Big]d\varphi_1 + \frac{\lambda_1}{\pi}\int_0^{2\pi}\Big[-(N_1 + N_2u_1 - N_3t_1 + N_4v_3)N_3 + (N_5 + N_3u_1 + N_2t_1 + N_6v_3)N_2\Big]d\varphi_1\right\} \tag{4.38}$$

$$\frac{\partial E}{\partial u_1} = 0 = (\rho a_1^4 \dot{\varphi}_1^2)^2 \left\{ \frac{1}{\pi} \int_0^{2\pi} \left[(N_{11} + N_2 u_1 - N_3 t_1 + N_8 u_3 + N_9 t_3) N_2 \right. \right.$$

$$\left. + (N_{12} + N_3 u_1 + N_2 t_1 - N_9 u_3 + N_8 t_3) N_3 \right] d\varphi_1$$

$$+ \frac{\lambda_1}{\pi} \int_0^{2\pi} \left[(N_1 + N_2 u_1 - N_3 t_1 + N_4 v_3) N_2 \right.$$

$$\left. \left. + (N_5 + N_3 u_1 + N_2 t_1 + N_6 v_3) N_3 \right] d\varphi_1 \right\}$$

(4.39)

$$\frac{\partial E}{\partial t_3} = 0 = (\rho a_1^4 \dot{\varphi}_1^2)^2 \left\{ \frac{1}{\pi} \int_0^{2\pi} \left[(N_{11} + N_2 u_1 - N_3 t_1 + N_8 u_3 + N_9 t_3) N_9 \right. \right.$$

$$\left. + (N_{12} + N_3 u_1 + N_2 t_1 - N_9 u_3 + N_8 t_3) N_8 \right] d\varphi_1$$

$$+ \frac{\lambda_2}{\pi} \int_0^{2\pi} \left[(N_7 + N_8 u_3 + N_9 t_3 - N_4 v_3) N_9 \right.$$

$$\left. \left. + (N_{10} - N_9 u_3 + N_8 t_3 - N_6 v_3) N_8 \right] d\varphi_1 \right\}$$

(4.40)

$$\frac{\partial E}{\partial u_3} = 0 = (\rho a_1^{4}\dot{\varphi}_1^{2})^2\left\{\frac{1}{\pi}\int_0^{2\pi}\Big[(N_{11} + N_2u_1 - N_3t_1 + N_8u_3 + N_9t_3)N_8 - (N_{12} + N_3u_1 + N_2t_1 - N_9u_3 + N_8t_3)N_9\Big]d\varphi_1 + \frac{\lambda_2}{\pi}\int_0^{2\pi}\Big[(N_7 + N_8u_3 + N_9t_3 - N_4v_3)N_8 - (N_{10} - N_9u_3 + N_8t_3 - N_6v_3)N_9\Big]d\varphi_1\right\}. \tag{4.41}$$

c. Simplification of Expressions

To facilitate solution of the above optimization equations (4.36) - (4.41), the following terms are defined:

$$I_1 = \int_0^{2\pi}(N_2N_{12} - N_3N_{11})d\varphi_1 \tag{4.42a}$$

$$I_2 = \int_0^{2\pi}(N_2^2 + N_3^2)d\varphi_1 \tag{4.42b}$$

$$I_3 = \int_0^{2\pi}(N_3N_8 + N_2N_9)d\varphi_1 \tag{4.42c}$$

$$I_4 = \int_0^{2\pi}(N_2N_8 - N_3N_9)d\varphi_1 \tag{4.42d}$$

$$I_5 = \int_0^{2\pi}\Big[N_2N_5 - N_1N_3 + (N_2N_6 - N_3N_4)v_3\Big]d\varphi_1 \tag{4.42e}$$

$$I_6 = \int_0^{2\pi}(N_2N_{11} + N_3N_{12})d\varphi_1 \tag{4.42f}$$

$$I_7 = \int_0^{2\pi}\left[N_1N_2 + N_3N_5 + (N_2N_4 + N_3N_6)v_3\right]d\varphi_1 \qquad (4.42g)$$

$$I_8 = \int_0^{2\pi}(N_9N_{11} + N_8N_{12})d\varphi_1 \qquad (4.42h)$$

$$I_9 = \int_0^{2\pi}(N_8^2 + N_9^2)d\varphi_1 \qquad (4.42i)$$

$$I_{10} = \int_0^{2\pi}\left[N_7N_9 + N_8N_{10} - (N_4N_9 + N_6N_8)v_3\right]d\varphi_1 \qquad (4.42j)$$

$$I_{11} = \int_0^{2\pi}(N_8N_{11} - N_9N_{12})d\varphi_1 \qquad (4.42k)$$

$$I_{12} = \int_0^{2\pi}\left[N_7N_8 - N_9N_{12} + (N_6N_9 - N_4N_8)v_3\right]d\varphi_1 \qquad (4.42l)$$

$$I_{13} = \int_0^{2\pi}\left[N_1^2 + N_5^2 + 2(N_1N_4 + N_5N_6)v_3 + (N_4^2 + N_6^2)v_3^2\right]d\varphi_1 \qquad (4.42m)$$

$$I_{14} = \int_0^{2\pi}\left[N_7^2 + N_{10}^2 - 2(N_4N_7 + N_6N_{10})v_3 + (N_4^2 + N_6^2)v_3^2\right]d\varphi_1 . \qquad (4.42n)$$

d. Optimization Equations

With the above simplifications, the set of six simultaneous optimization equations (4.36) - (4.41) appears as follows:

$$I_{13} + I_2t_1^2 + I_2u_1^2 + 2I_7u_1 + 2I_5t_1 = 2\pi q_1^2 f_{41_{RMS_u}}^2 \qquad (4.43)$$

$$I_{14} + I_9t_3^2 + I_9u_3^2 + 2I_{12}u_3 + 2I_{10}t_3 = 2\pi q_2^2 f_{43_{RMS_u}}^2 \qquad (4.44)$$

$$I_1 + I_2t_1 - I_3u_3 + I_4t_3 + \lambda_1(I_5 + I_2t_1) = 0 \qquad (4.45)$$

$$I_6 + I_2u_1 + I_4u_3 + I_3t_3 + \lambda_1(I_7 + I_2u_1) = 0 \qquad (4.46)$$

$$I_8 + I_3u_1 + I_4t_1 + I_9t_3 + \lambda_2(I_{10} + I_9t_3) = 0 \qquad (4.47)$$

$$I_{11} + I_4u_1 - I_3t_1 + I_9u_3 + \lambda_2(I_{12} + I_9u_3) = 0 \ . \qquad (4.48)$$

3. Solution of Optimization Equations

The following first outlines the solution of the optimization equations, and then discusses in detail the extent of its validity.

a. Steps of Solution

Appendix H shows that the solution of the optimization equations (4.43) - (4.48) leads to the following 16^{th} degree polynomial in u_3:

$$P_1u_3^{16} + P_2u_3^{15} + P_3u_3^{14} + P_4u_3^{13} + P_5u_3^{12} + P_6u_3^{11} + P_7u_3^{10}$$

$$+ P_8u_3^9 + P_9u_3^8 + P_{10}u_3^7 + P_{11}u_3^6 + P_{12}u_3^5 + P_{13}u_3^4 + P_{14}u_3^3$$

$$+ P_{15}u_3^2 + P_{16}u_3 + P_{17} = 0 \ , \qquad (4.49)$$

where P_1 to P_{17} are known constants for a specific value of v_3, and are given in Section 2 of Appendix H. After equation (4.49) is solved for u_3 by way of a numerical technique, the values of t_3, u_1 and t_1 may be found in the following order: According to equations (H.12)

$$t_3 = I_{93} \pm \sqrt{-u_3^2 + I_{94}u_3 + I_{95}} \qquad (4.50)$$

(Note that there are two possible solutions of t_3 for each u_3.)

Equation (H.8) gives

$$u_1 = \frac{-(I_{15} + I_{16}t_3 + I_{17}u_3 + I_{18}u_3t_3 + I_{19}u_3^2 + I_{20}t_3^2)}{I_{21} + I_{22}t_3 + I_{23}u_3}. \quad (4.51)$$

Finally, t_1 is found according to equation (H.9):

$$t_1 = \frac{I_{24} + I_{25}u_3 + I_{26}t_3 + I_{27}u_1 + I_{28}u_1u_3 + I_{29}u_1t_3}{I_{30} + I_{29}u_3 - I_{28}t_3}. \quad (4.52)$$

The constants I_{15} to I_{30} and I_{93} to I_{95} are given in Section 2 of Appendix H. The solutions for the Lagrange Multipliers λ_1 and λ_2, which serve no further purpose in this investigation, are listed for the sake of completeness by equations (H.15) and (H.16).

b. Discussion of Solution

In order to draw the correct conclusions from the solution of the 16^{th} degree polynomial, it is necessary to consider its origin.

Appendix H shows that the final solution steps of the optimization equations (H.1) - (H.6) lead to expressions for t_3 in terms of u_3 (see equations (H.12)), which are substituted into equation (H.11), an 8^{th} degree polynomial both in t_3 and u_3. The resulting expressions (H.13) represent an equality wherein the left-hand side constitutes one 8^{th} degree polynomial in u_3, while, due to the square root, the right-hand side contains positive and negative values of a second 8^{th} degree expression in the same variable.

Geometrically interpreted, the intersections of the above curves furnish those values of u_3 which lead to the extrema of the RMS shaking force. In order to avoid the difficulty of matching solutions, both sides of equations (H.13) are then squared (the opposite signs vanish), and the right-hand side of the ensuing expression is subtracted from that of the left-hand side, resulting in equation (4.49). It is to be noted that before subtracting, the intersections of the two 16^{th} degree polynomials furnish the same values of u_3 which are obtained from the intersections represented by equations (H.13). Finally, the real roots of the polynomial (4.49) are identical to the u_3's of the various intersection points. Each of the real u_3's will lead to two t_3's, which in turn will give rise to a u_1 and a t_1. Thus, there can be as many as 32 real solution sets when the method can only provide a maximum of 16. To separate valid from invalid sets, one must determine whether a given set satisfies the optimization equations (4.43) - (4.48).

All sets of solutions u_3, t_3, u_1 and t_1 which satisfy the optimization equations correspond to extrema of the RMS shaking force, and one of these represents the desired minimum solution. Appendix I proves that there is such a minimum amongst the true solutions. This is accomplished, in a manner similar to that of Section IVB-3, by showing the applicability of the theorem which states that a continuous function has a minimum and a maximum on a closed and bounded set.

4. Application of Solution to Design of Input and Output Link Counterweights

The optimum mass parameters u_1, t_1, u_3 and t_3, which are the result of the solution of the optimization equations, as well as the chosen parameter v_3, must now be physically realized with the help of counterweights which are attached to the already existing links 1 and 3. As in Section IVB-4, the counterweights are to be circular and tangent to the pivots.

a. Design of Counterweight for Output Link 3

In designing the counterweight for link 3, one has to satisfy the optimum mass parameters u_3 and t_3, which result from the optimization equations, as well as the mass parameter v_3, which is chosen in such a manner that a reasonable counterweight results. (See Section IVA-2.) To this end, the design equations of Section IVB-4 are used. (The fact that v_3 was obtained by way of the optimization equations in that section is of no consequence.)

b. Design of Counterweight for Input Link 1

In designing the counterweight for link 1, one has to satisfy only the mass parameters u_1 and t_1, which result from the optimization equations. The thickness-density ratio D_1^* is now chosen in such a manner that a reasonable counterweight results. Appendix G derives the appropriate design equations for the dimensionless radius R_1^* and the angular position θ_1^* of this counterweight. Thus,

according to equation (G.26):

$$R_1^* = \frac{r_1^*}{a_1} = (U_1^{*2} + T_1^{*2})^{1/2} = \left\{ \frac{\left[t_1^2 + (u_1 - \frac{1}{2} B_1^o)^2 \right]^{1/2}}{\pi \beta_1 \gamma_1 D_1^*} \right\}^{1/3}, \tag{4.53}$$

and according to equation (G.27):

$$\theta_1^* = \tan^{-1}\left(\frac{T_1^*}{U_1^*}\right) = \tan^{-1}\left(\frac{t_1}{u_1 - \frac{1}{2} B_1^o}\right). \tag{4.54}$$

In the above (see also Fig. 6)

r_1^* = actual radius of counterweight

$U_1^* = R_1^* \cos\theta_1^*$, $T_1^* = R_1^* \sin\theta_1^*$ } dimensionless coordinates of position of counterweight center of mass

B_1^o = dimensionless mass of link 1 (see equation (A.119a))

β_1, γ_1 = dimensionless parameters expressing the geometry of link 1 (see equations (A.115) and note that $\alpha_1 = 1$)

$D_1^* = \delta_1 \left(\frac{\rho_1^*}{\rho^o}\right)$ = dimensionless thickness-density ratio

δ_1 = ratio of the counterweight thickness to the thickness of link 1

ρ_1^*, ρ^o = mass densities of counterweight and link 1, respectively.

5. Example of Optimization With Input and Output Link Counterweights

a. Procedure

In order to employ the optimization procedure derived in the previous sections to an existing linkage, the following design steps must be followed:

(1) The range of meaningful constraint factors q_1 and q_2 which is to be examined is determined in the manner identical to that of Section IVB-5. Then the parameter v_3, which expresses the moment of inertia of the output link, is chosen. It has been found practical to examine the range of v_3 which varies from 1.5 to 3.5 times that of the original link. Finally, attention must be paid to the predetermined thickness-density ratio D_1^*, which is used in the computation of the counterweight parameters R_1^* and θ_1^*, so that the resulting design has a reasonable relationship between thickness and radius.

(2) The counterweight radii R_1^* and R_3^*, the thickness-density ratios D_3^*, and the angles θ_1^* and θ_3^*, as well as the ratios ϵ_f (see equation (4.28)), which correspond to the optimum dimensionless RMS shaking forces, are then computed. These values are found for the agreed upon range of v_3 from the optimum mass parameters u_1, t_1, u_3 and t_3, which are functions of the various combinations of constraint factors q_1 and q_2. As in Section IVB-5, design graphs, based upon the above information, are devised which permit the choice of the most practical optimum configuration.

b. Numerical Example

The four-bar linkage of Fig. 7, described in Section IVB-5, will be used as a numerical example to allow comparison between the one and two counterweight methods.

(1) Constraint Factors q_1 and q_2

The range of constraint factors remains as in Section IVB-5, i.e.

$$1 < q_1 < 1.40 \tag{4.55a}$$

$$1 < q_2 < 1.84 \ . \tag{4.55b}$$

All computations concerning the unbalanced and fully balanced mechanism, which lead to the above, of course, remain identical (see Section IVB-5), i.e.

$$f_{41_{RMS_u}} = 2.156, \quad f_{43_{RMS_u}} = 1.643, \quad f_{S_{RMS_u}} = 1.349 \tag{4.56}$$

$$f_{41_{RMS_b}} = f_{43_{RMS_b}} = 3.020 \ . \tag{4.57}$$

(2) Design Method for Determination of Counterweight Radius, Thickness-Density Ratio and Angle

(a) Tabulation of Solutions

In order to obtain the values of R_1^*, θ_1^*, R_3^*, D_3^* and θ_3^*, it is again first necessary to determine that set of optimum mass parameters u_1, t_1, u_3 and t_3 associated with given values of v_3, q_1 and q_2 which corresponds to the minimum RMS shaking force. (See equations (4.49) -

(4.52).) Once this has been accomplished, equations (4.25) - (4.27), (4.53) and (4.54) are used to obtain the counterweight parameters.

Tables 9 - 11 list the optimum mass parameters for $v_3 = 2.50v_3^o = 4.935$, $v_3 = 2.75v_3^o = 5.428$, and $v_3 = 3.00v_3^o = 5.921$ (v_3^o represents the moment of inertia of the unbalanced link, see Table 4) and constraint factors q_1 and q_2 as shown in equations (4.55). The above range of v_3 has been found to furnish meaningful results. Subsequently, Tables 12 - 14 list the corresponding counterweight parameters R_1^*, R_3^*, D_3^*, θ_1^* and θ_3^*, as well as the ratio ϵ_f, as functions of the indicated constraint factors. R_1^* and θ_1^* have been computed for a thickness-density ratio of $D_1^* = 2.5$. With this low value of D_1^*, the input link counterweight may be made of the same material as the input link.

In order to be able to select the most practical possibilities from all the solutions of Tables 12 - 14, the design graphs of Figs. 9 - 11 have been devised, each for a different value of v_3.

The top graph in each case shows values of R_1^* as a function of q_2 for various values of q_1 (and $D_1^* = 2.5$). The middle graph depicts the variation of D_3^* and R_3^* vs. q_2, again for various values of q_1. As in Section IVB-5, the vertical line-up of the q_2 axes makes it easier to arrive at an engineering solution.

q_1		q_2 = 1.10	1.20	1.30	1.40	1.50	1.60	1.70	1.80
1.05	u_3	-0.624	-0.859	-1.085	-1.305	-1.519	-1.729	-1.936	-2.140
	t_3	1.671	1.274	0.889	0.513	0.144	-0.220	-0.580	-0.937
	u_1	-0.923	-0.921	-0.920	-0.919	-0.919	-0.919	-0.920	-0.920
	t_1	-0.064	-0.037	-0.015	0.003	0.019	0.033	0.045	0.056
1.10	u_3	-0.696	-0.936	-1.165	-1.387	-1.603	-1.815	-2.024	-2.230
	t_3	1.721	1.323	0.942	0.568	0.200	-0.164	-0.523	-0.879
	u_1	-0.653	-0.650	-0.648	-0.647	-0.646	-0.647	-0.648	-0.648
	t_1	-0.105	-0.069	-0.039	-0.013	0.009	-0.029	0.046	0.061
1.15	u_3	-0.753	-0.995	-1.227	-1.452	-1.670	-1.884	-2.094	-2.302
	t_3	1.761	1.368	0.986	0.613	0.245	-0.118	-0.476	-0.832
	u_1	-0.432	-0.427	-0.424	-0.422	-0.422	-0.422	-0.422	-0.423
	t_1	-0.146	-0.101	-0.064	-0.032	-0.005	0.019	0.040	0.059
1.20	u_3	-0.800	-1.046	-1.280	-1.507	-1.727	-1.943	-2.155	-2.363
	t_3	1.797	1.405	1.205	0.652	0.285	-0.077	-0.435	-0.790
	u_1	-0.237	-0.230	-0.227	-0.225	-0.224	-0.223	-0.224	-0.224
	t_1	-0.187	-0.135	-0.091	-0.054	-0.022	0.007	0.032	0.054
1.25	u_3	-0.842	-1.091	-1.327	-1.556	-1.778	-1.995	-2.208	-2.418
	t_3	1.830	1.439	1.060	0.688	0.322	-0.039	-0.397	-0.752
	u_1	-0.059	-0.051	-0.046	-0.044	-0.042	-0.042	-0.042	-0.042
	t_1	-0.228	-0.169	-0.120	-0.077	-0.041	-0.008	0.020	0.046
1.30	u_3	-0.879	-1.131	-1.370	-1.600	-1.824	-2.043	-2.258	-2.469
	t_3	1.860	1.471	1.092	0.721	0.356	-0.005	-0.362	-0.716
	u_1	0.108	0.117	0.122	0.126	0.128	0.128	0.129	0.128
	t_1	-0.269	-0.204	-0.149	-0.102	-0.061	-0.025	0.007	0.036
1.35	u_3	-0.914	-1.168	-1.409	-1.642	-1.867	-2.087	-2.303	-2.516
	t_3	1.888	1.500	1.123	0.753	0.388	0.028	-0.328	-0.682
	u_1	0.265	0.275	0.281	0.286	0.288	0.290	0.290	0.290
	t_1	-0.311	-0.240	-0.180	-0.128	-0.083	-0.043	-0.008	0.024
1.40	u_3	-0.946	-1.202	-1.446	-1.680	-1.907	-2.129	-2.346	-2.559
	t_3	1.915	1.529	1.152	0.783	0.419	0.060	-0.296	-0.650
	u_1	0.415	0.427	0.434	0.439	0.442	0.444	0.444	0.444
	t_1	-0.353	-0.276	-0.211	-0.155	-0.106	-0.063	-0.024	0.010

Table 9 Optimum Mass Parameters u_3, t_3, u_1 and t_1 (Associated With Lowest RMS Shaking Force) vs. q_1 and q_2 for $v_3 = 4.935$

(Computations used 5° intervals. Comparison showed that no greater accuracy was needed for the well behaved functions involved.)

q_1		q_2 = 1.10	1.20	1.30	1.40	1.50	1.60	1.70	1.80
1.05	u_3	-0.344	-0.581	-0.808	-1.028	-1.243	-1.454	-1.662	-1.867
	t_3	1.874	1.468	1.076	0.694	0.321	-0.047	-0.410	-0.769
	u_1	-1.325	-1.324	-1.322	-1.321	-1.321	-1.320	-1.320	-1.320
	t_1	-0.033	-0.017	-0.005	0.006	0.015	0.023	0.030	0.036
1.10	u_3	-0.452	-0.694	-0.925	-1.149	-1.367	-1.581	-1.791	-1.998
	t_3	1.944	1.541	1.151	0.771	0.399	0.032	-0.330	-0.668
	u_1	-0.936	-0.933	-0.931	-0.930	-0.929	-0.929	-0.930	-0.930
	t_1	-0.084	-0.054	-0.030	-0.009	0.009	0.024	0.038	0.050
1.15	u_3	-0.520	-0.767	-1.002	-1.228	-1.449	-1.664	-1.876	-2.085
	t_3	1.992	1.591	1.203	0.824	0.453	0.087	-0.274	-0.632
	u_1	-0.670	-0.665	-0.662	-0.660	-0.660	-0.659	-0.660	-0.660
	t_1	-0.130	-0.090	-0.057	-0.029	-0.005	0.016	0.035	0.051
1.20	u_3	-0.574	-0.824	-1.062	-1.291	-1.514	-1.731	-1.945	-2.155
	t_3	2.032	1.632	1.245	0.868	0.498	0.133	-0.228	-0.585
	u_1	-0.449	-0.443	-0.439	-0.436	-0.435	-0.435	-0.435	-0.435
	t_1	-0.175	-0.127	-0.086	-0.052	-0.022	0.004	0.026	0.047
1.25	u_3	-0.620	-0.873	-1.114	-1.345	-1.570	-1.789	-2.004	-2.216
	t_3	2.067	1.669	1.283	0.907	0.537	0.173	-0.187	-0.544
	u_1	-0.254	-0.246	-0.241	-0.238	-0.236	-0.235	-0.235	-0.236
	t_1	-0.220	-0.163	-0.116	-0.077	-0.042	-0.012	0.015	0.039
1.30	u_3	-0.660	-0.917	-1.160	-1.393	-1.619	-1.840	-2.057	-2.270
	t_3	2.099	1.702	1.318	0.942	0.574	0.210	-0.149	-0.506
	u_1	-0.075	-0.066	-0.060	-0.056	-0.054	-0.052	-0.052	-0.052
	t_1	-0.264	-0.201	-0.148	-0.103	-0.063	-0.029	0.002	0.029
1.35	u_3	-0.697	-0.956	-1.201	-1.437	-1.665	-1.887	-2.105	-2.319
	t_3	2.128	1.733	1.350	0.976	0.608	0.245	-0.114	-0.470
	u_1	0.092	0.103	0.110	0.115	0.117	0.119	0.119	0.119
	t_1	-0.309	-0.239	-0.180	-0.130	-0.086	-0.048	-0.014	0.017
1.40	u_3	-0.730	-0.992	-1.239	-1.477	-1.707	-1.931	-2.150	-2.365
	t_3	2.156	1.762	1.380	1.007	0.640	0.277	-0.081	-0.437
	u_1	0.249	0.262	0.270	0.276	0.279	0.281	0.282	0.282
	t_1	-0.353	-0.277	-0.213	-0.158	-0.110	-0.068	-0.031	0.003

Table 10 Optimum Mass Parameters u_3, t_3, u_1 and t_1 (Associated With Lowest RMS Shaking Force) vs. q_1 and q_2 for $v_3 = 5.428$

(Computations used 5^o intervals.)

q_1		q_2 = 1.10	1.20	1.30	1.40	1.50	1.60	1.70	1.80
1.10	u_3	-0.176	-0.421	-0.654	-0.879	-1.098	-1.312	-1.523	-1.731
	t_3	2.156	1.742	1.344	0.959	0.582	0.211	-0.154	-0.515
	u_1	-1.319	-1.318	-1.316	-1.315	-1.314	-1.313	-1.313	-1.312
	t_1	-0.049	-0.030	-0.014	-0.002	0.010	0.019	0.027	0.035
1.15	u_3	-0.274	-0.524	-0.762	-0.991	-1.213	-1.430	-1.643	-1.853
	t_3	2.221	1.810	1.415	1.031	0.655	0.286	-0.079	-0.439
	u_1	-0.950	-0.946	-0.944	-0.942	-0.941	-0.940	-0.940	-0.940
	t_1	-0.107	-0.073	-0.022	-0.045	-0.003	0.015	0.030	0.043
1.20	u_3	-0.340	-0.594	-0.835	-1.066	-1.291	-1.510	-1.723	-1.937
	t_3	2.267	1.858	1.465	1.082	0.708	0.339	-0.024	-0.384
	u_1	-0.687	-0.681	-0.677	-0.675	-0.673	-0.673	-0.672	-0.673
	t_1	-0.158	-0.113	-0.077	-0.047	-0.020	0.002	0.023	0.040
1.25	u_3	-0.392	-0.650	-0.894	-1.128	-1.354	-1.576	-1.793	-2.006
	t_3	2.306	1.899	1.507	1.125	0.752	0.384	0.021	-0.338
	u_1	-0.467	-0.459	-0.454	-0.451	-0.449	-0.448	-0.448	-0.448
	t_1	-0.207	-0.154	-0.110	-0.073	-0.041	-0.013	0.011	0.033
1.30	u_3	-0.436	-0.697	-0.944	-1.180	-1.409	-1.632	-1.850	-2.065
	t_3	2.340	1.935	1.544	1.164	0.791	0.424	0.062	-0.297
	u_1	-0.272	-0.262	-0.256	-0.252	-0.249	-0.248	-0.247	-0.247
	t_1	-0.255	-0.194	-0.143	-0.100	-0.063	-0.031	-0.002	0.023
1.35	u_3	-0.475	-0.739	-0.988	-1.227	-1.458	-1.683	-1.902	-2.118
	t_3	2.371	1.967	1.578	1.199	0.827	0.461	0.099	-0.259
	u_1	-0.093	-0.081	-0.074	-0.069	-0.066	-0.064	-0.063	-0.063
	t_1	-0.303	-0.234	-0.177	-0.129	-0.087	-0.051	-0.018	0.011
1.40	u_3	-0.510	-0.777	-1.029	-1.270	-1.502	-1.729	-1.950	-2.167
	t_3	2.400	1.998	1.610	1.231	0.860	0.495	0.134	-0.224
	u_1	0.074	0.088	0.097	0.102	0.106	0.108	0.110	0.110
	t_1	-0.350	-0.275	-0.212	-0.159	-0.112	-0.072	-0.036	-0.004

Table 11 Optimum Mass Parameters u_3, t_3, u_1 and t_1 (Associated With Lowest RMS Shaking Force) vs. q_1 and q_2 for $v_3 = 5.921$*

(Computations used 5^o intervals.)

*No real solutions occurred for $q_1 = 1.05$.

q_1		q_2 = 1.10	1.20	1.30	1.40	1.50	1.60	1.70	1.80
1.05	R_1^*	0.889	0.888	0.888	0.887	0.887	0.888	0.888	0.888
	R_3^*	0.907	0.954	0.959	0.923	0.860	0.787	0.713	0.645
	D_3^*	4.646	3.794	3.717	4.327	5.735	8.209	12.156	18.108
	θ_1^*	183°	182°	181°	180°	179°	178°	178°	177°
	θ_3^*	130°	142°	154°	166°	176°	185°	192°	198°
	ν_f	0.60	0.51	0.46	0.45	0.47	0.53	0.62	0.71
1.10	R_1^*	0.811	0.809	0.807	0.807	0.807	0.807	0.807	0.808
	R_3^*	0.873	0.913	0.917	0.885	0.828	0.762	0.694	0.631
	D_3^*	5.413	4.515	4.449	5.131	6.670	9.336	13.534	19.798
	θ_1^*	187°	185°	183°	181°	179°	178°	177°	176°
	θ_3^*	130°	142°	154°	165°	175°	183°	191°	196°
	ν_f	0.57	0.45	0.35	0.29	0.28	0.33	0.42	0.53
1.15	R_1^*	0.736	0.731	0.728	0.726	0.726	0.726	0.726	0.727
	R_3^*	0.847	0.883	0.886	0.856	0.805	0.743	0.680	0.620
	D_3^*	6.090	5.158	5.105	5.849	7.499	10.326	14.734	21.258
	θ_1^*	193°	189°	186°	183°	180°	178°	176°	174°
	θ_3^*	131°	142°	154°	165°	174°	183°	189°	195°
	ν_f	0.60	0.46	0.33	0.21	0.14	0.17	0.27	0.39
1.20	R_1^*	0.662	0.650	0.642	0.637	0.635	0.635	0.636	0.637
	R_3^*	0.827	0.859	0.861	0.833	0.785	0.727	0.667	0.611
	D_3^*	6.721	5.762	5.724	6.524	8.275	11.246	15.843	22.598
	θ_1^*	204°	198°	193°	188°	183°	179°	176°	172°
	θ_3^*	131°	142°	153°	164°	173°	182°	188°	194°
	ν_f	0.66	0.51	0.37	0.24	0.10	0.03	0.16	0.29

Table 12 Counterweight Parameters R_1^*, R_3^*, D_3^*, θ_1^*, θ_3^* and RMS Shaking Force Ratio ν_f vs. q_1 and q_2 for $v_3 = 4.935$

q_1		q_2 = 1.10	1.20	1.30	1.40	1.50	1.60	1.70	1.80
1.25	R_1^*	0.594	0.566	0.545	0.531	0.523	0.520	0.520	0.524
	R_3^*	0.809	0.839	0.840	0.813	0.768	0.713	0.657	0.602
	D_3^*	7.325	6.345	6.322	7.176	9.021	12.126	16.897	23.867
	θ_1^*	224°	216°	208°	199°	190°	182°	175°	168°
	θ_3^*	131°	142°	153°	164°	173°	181°	188°	193°
	ε_f	0.73	0.59	0.45	0.32	0.20	0.11	0.14	0.25
1.30	R_1^*	0.562	0.514	0.466	0.418	0.370	0.329	0.318	0.340
	R_3^*	0.794	0.821	0.821	0.796	0.753	0.701	0.647	0.595
	D_3^*	7.913	6.915	6.908	7.815	9.749	12.981	17.916	25.088
	θ_1^*	255°	253°	249°	243°	230°	206°	172°	145°
	θ_3^*	132°	142°	153°	163°	172°	180°	187°	192°
	ε_f	0.82	0.68	0.55	0.43	0.32	0.24	0.22	0.27
1.35	R_1^*	0.590	0.548	0.509	0.474	0.444	0.423	0.414	0.417
	R_3^*	0.780	0.805	0.805	0.781	0.740	0.690	0.638	0.588
	D_3^*	8.488	7.477	7.488	8.446	10.467	13.820	18.912	26.277
	θ_1^*	285°	292°	300°	310°	323°	339°	356°	12°
	θ_3^*	132°	142°	153°	163°	172°	179°	186°	192°
	ε_f	0.91	0.77	0.65	0.53	0.43	0.36	0.32	0.33
1.40	R_1^*	0.647	0.618	0.595	0.578	0.566	0.558	0.554	0.553
	R_3^*	0.767	0.791	0.790	0.767	0.728	0.681	0.630	0.582
	D_3^*	9.057	8.034	8.064	9.073	11.178	14.648	19.892	27.444
	θ_1^*	304°	312°	320°	329°	338°	347°	355°	2°
	θ_3^*	132°	142°	153°	162°	171°	179°	185°	191°
	ε_f	1.00	0.87	0.75	0.64	0.54	0.47	0.42	0.42

Table 12 continued

q_1		q_2 = 1.10	1.20	1.30	1.40	1.50	1.60	1.70	1.80
1.05	R_1^*	0.986	0.985	0.985	0.985	0.985	0.984	0.984	0.985
	R_3^*	1.056	1.154	1.205	1.194	1.129	1.035	0.933	0.838
	D_3^*	2.947	2.066	1.737	1.803	2.256	3.199	4.831	7.436
	θ_1^*	181°	181°	180°	180°	179°	179°	179°	179°
	θ_3^*	121°	133°	146°	159°	171°	181°	190°	196°
	ε_f	0.78	0.73	0.70	0.71	0.73	0.78	0.85	0.93
1.10	R_1^*	0.893	0.892	0.891	0.890	0.890	0.890	0.890	0.891
	R_3^*	1.003	1.083	1.123	1.113	1.059	0.979	0.891	0.807
	D_3^*	3.626	2.662	2.303	2.391	2.919	3.991	5.805	8.644
	θ_1^*	184°	183°	182°	180°	180°	179°	178°	177°
	θ_3^*	122°	134°	146°	158°	169°	179°	187°	194°
	ε_f	0.67	0.57	0.50	0.46	0.46	0.50	0.56	0.65
1.15	R_1^*	0.818	0.814	0.812	0.811	0.811	0.811	0.811	0.812
	R_3^*	0.970	1.041	1.075	1.065	1.016	0.945	0.865	0.787
	D_3^*	4.141	3.123	2.745	2.851	3.434	4.598	6.540	9.545
	θ_1^*	189°	186°	184°	182°	180°	179°	178°	177°
	θ_3^*	123°	134°	146°	158°	168°	178°	186°	192°
	ε_f	0.66	0.53	0.42	0.33	0.28	0.30	0.37	0.46
1.20	R_1^*	0.746	0.739	0.735	0.732	0.731	0.731	0.731	0.732
	R_3^*	0.945	1.009	1.039	1.029	0.985	0.919	0.845	0.772
	D_3^*	4.597	3.537	3.145	3.267	3.898	5.140	7.192	10.337
	θ_1^*	196°	192°	188°	185°	182°	180°	178°	176°
	θ_3^*	124°	134°	146°	157°	168°	177°	185°	191°
	ε_f	0.69	0.55	0.41	0.29	0.18	0.14	0.21	0.32

Table 13 Counterweight Parameters R_1^*, R_3^*, D_3^*, θ_1^*, θ_3^* and RMS Shaking Force Ratio ε_f vs. q_1 and q_2 for $v_3 = 5.428$

q_1		q_2 = 1.10	1.20	1.30	1.40	1.50	1.60	1.70	1.80
1.25	R_1^*	0.676	0.661	0.652	0.646	0.643	0.641	0.641	0.642
	R_3^*	0.924	0.983	1.010	1.000	0.959	0.897	0.828	0.759
	D_3^*	5.023	3.926	3.524	3.663	4.336	5.649	7.800	11.070
	θ_1^*	207°	201°	196°	190°	186°	182°	178°	175°
	θ_3^*	124°	136°	146°	157°	167°	176°	184°	190°
	ε_f	0.75	0.61	0.46	0.33	0.19	0.06	0.08	0.21
1.30	R_1^*	0.615	0.586	0.563	0.546	0.535	0.529	0.528	0.529
	R_3^*	0.906	0.961	0.985	0.976	0.937	0.879	0.813	0.747
	D_3^*	5.429	4.302	3.892	4.047	4.761	6.140	8.382	11.768
	θ_1^*	226°	219°	212°	204°	195°	187°	180°	173°
	θ_3^*	124°	135°	146°	156°	167°	175°	183°	189°
	ε_f	0.83	0.68	0.54	0.41	0.28	0.16	0.10	0.17
1.35	R_1^*	0.589	0.542	0.497	0.452	0.407	0.365	0.338	0.340
	R_3^*	0.891	0.941	0.964	0.954	0.917	0.863	0.800	0.737
	D_3^*	5.823	4.669	4.253	4.424	5.178	6.619	8.947	12.444
	θ_1^*	254°	252°	249°	244°	235°	219°	193°	164°
	θ_3^*	126°	135°	146°	156°	166°	175°	182°	189°
	ε_f	0.91	0.77	0.63	0.50	0.39	0.28	0.22	0.22
1.40	R_1^*	0.612	0.569	0.529	0.491	0.456	0.428	0.410	0.404
	R_3^*	0.877	0.924	0.944	0.935	0.900	0.848	0.788	0.727
	D_3^*	6.209	5.031	4.610	4.798	5.590	7.092	9.503	13.105
	θ_1^*	281°	287°	293°	302°	312°	326°	343°	1°
	θ_3^*	125°	135°	146°	156°	166°	174°	182°	188°
	ε_f	1.00	0.86	0.73	0.61	0.50	0.40	0.33	0.31

Table 13 continued

q_1			q_2 = 1.10	1.20	1.30	1.40	1.50	1.60	1.70	1.80
	1.10	R_1^*	0.984	0.984	0.984	0.983	0.983	0.983	0.983	0.983
		R_3^*	1.118	1.247	1.344	1.379	1.345	1.257	1.144	1.030
		D_3^*	2.685	1.732	1.285	1.157	1.281	1.679	2.442	3.722
		θ_1^*	182°	181°	181°	180°	180°	179°	179°	179°
		θ_3^*	114°	124°	137°	150°	163°	174°	184°	192°
		ν_f	0.83	0.76	0.71	0.70	0.71	0.74	0.80	0.87
	1.15	R_1^*	0.897	0.895	0.894	0.894	0.893	0.893	0.893	0.893
		R_3^*	1.072	1.182	1.262	1.289	1.260	1.186	1.089	0.989
		D_3^*	3.171	2.143	1.653	1.515	1.664	2.119	2.973	4.378
		θ_1^*	185°	184°	182°	181°	180°	179°	178°	178°
		θ_3^*	115°	126°	137°	150°	162°	173°	182°	189°
		ν_f	0.75	0.64	0.55	0.49	0.46	0.47	0.52	0.60
	1.20	R_1^*	0.824	0.820	0.818	0.816	0.816	0.815	0.815	0.816
		R_3^*	1.042	1.141	1.211	1.234	1.207	1.141	1.054	0.962
		D_3^*	3.549	2.468	1.949	1.806	1.973	2.472	3.394	4.890
		θ_1^*	190°	188°	185°	183°	181°	180°	178°	177°
		θ_3^*	116°	126°	138°	150°	161°	172°	181°	188°
		ν_f	0.75	0.62	0.49	0.39	0.32	0.29	0.33	0.40

Table 14 Counterweight Parameters R_1^*, R_3^*, D_3^*, θ_1^*, θ_3^* and RMS Shaking Force Ratio ν_f vs. q_1 and q_2 for $v_3 = 5.921$

q_1		q_2 = 1.10	1.20	1.30	1.40	1.50	1.60	1.70	1.80
1.25	R_1^*	0.756	0.747	0.742	0.739	0.737	0.736	0.736	0.736
	R_3^*	1.019	1.110	1.172	1.192	1.167	1.107	1.027	0.941
	D_3^*	3.884	2.762	2.129	2.072	2.256	2.793	3.772	5.347
	θ_1^*	198°	194°	190°	187°	184°	181°	179°	177°
	θ_3^*	117°	127°	138°	149°	161°	170°	180°	187°
	ε_f	0.79	0.64	0.51	0.37	0.25	0.17	0.16	0.25
1.30	R_1^*	0.691	0.674	0.663	0.655	0.650	0.648	0.647	0.647
	R_3^*	1.000	1.084	1.140	1.158	1.135	1.078	1.004	0.923
	D_3^*	4.197	3.038	2.476	2.327	2.527	3.097	4.129	5.774
	θ_1^*	210°	204°	198°	193°	188°	184°	180°	176°
	θ_3^*	117°	127°	138°	149°	160°	170°	179°	186°
	ε_f	0.85	0.70	0.56	0.42	0.28	0.15	0.03	0.12
1.35	R_1^*	0.637	0.606	0.581	0.562	0.549	0.540	0.536	0.536
	R_3^*	0.983	1.061	1.113	1.129	1.107	1.054	0.984	0.907
	D_3^*	4.495	3.304	2.725	2.574	2.790	3.392	4.473	6.184
	θ_1^*	228°	222°	215°	208°	200°	192°	184°	177°
	θ_3^*	118°	128°	138°	149°	160°	169°	178°	185°
	ε_f	0.93	0.78	0.63	0.50	0.36	0.23	0.12	0.11
1.40	R_1^*	0.615	0.569	0.525	0.482	0.440	0.400	0.367	0.282
	R_3^*	0.967	1.041	1.090	1.104	1.083	1.033	0.966	0.893
	D_3^*	4.783	3.564	2.969	2.819	3.049	3.682	4.809	6.583
	θ_1^*	253°	252°	249°	244°	237°	225°	207°	183°
	θ_3^*	118°	128°	138°	149°	159°	169°	177°	184°
	ε_f	1.01	0.86	0.72	0.59	0.46	0.35	0.25	0.20

Table 14 continued

Fig. 9 Design graphs for counterweights for $v_3 = 4.935$

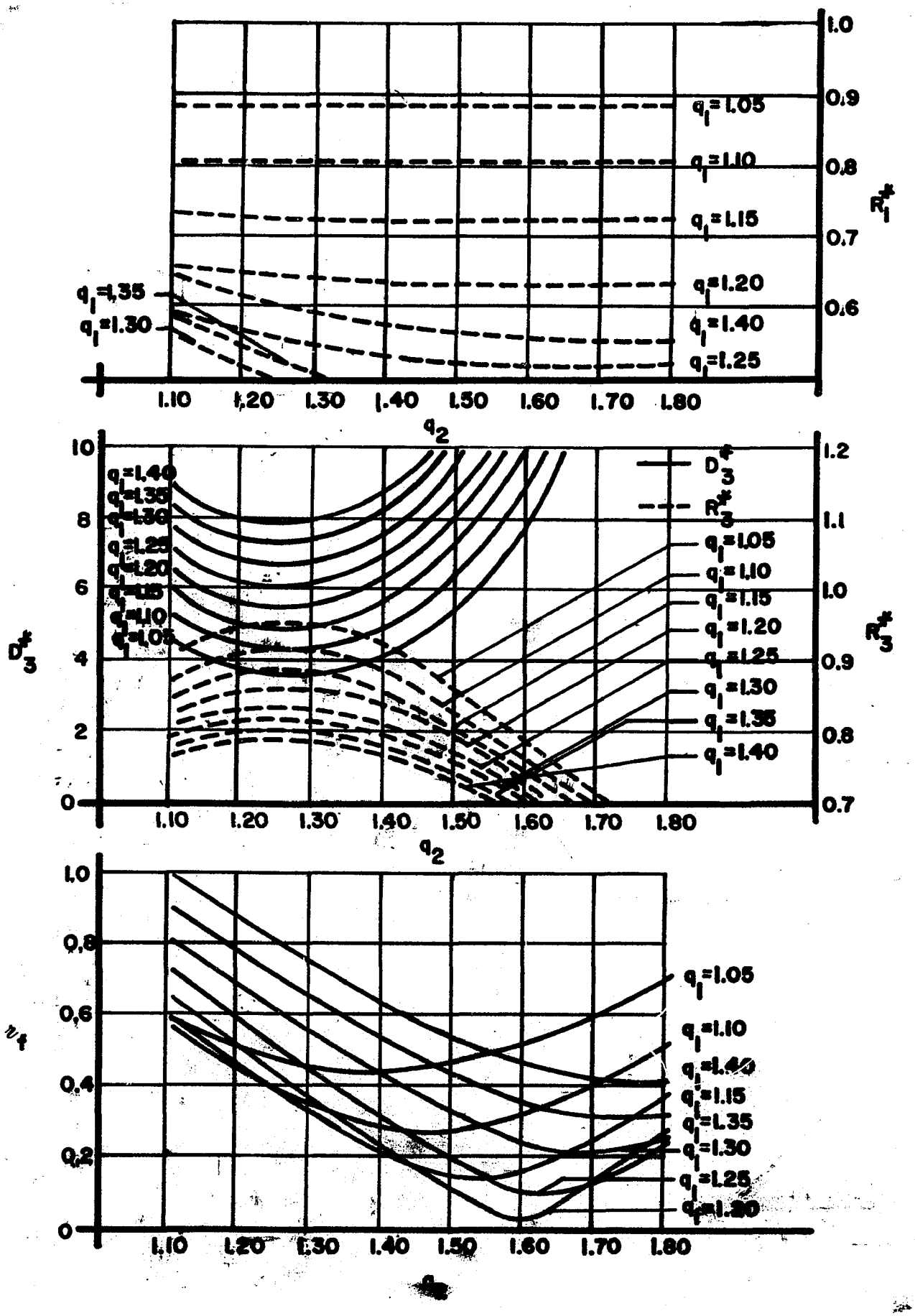

Fig. 10 Design graphs for counterweights for $v_3 = 5.428$

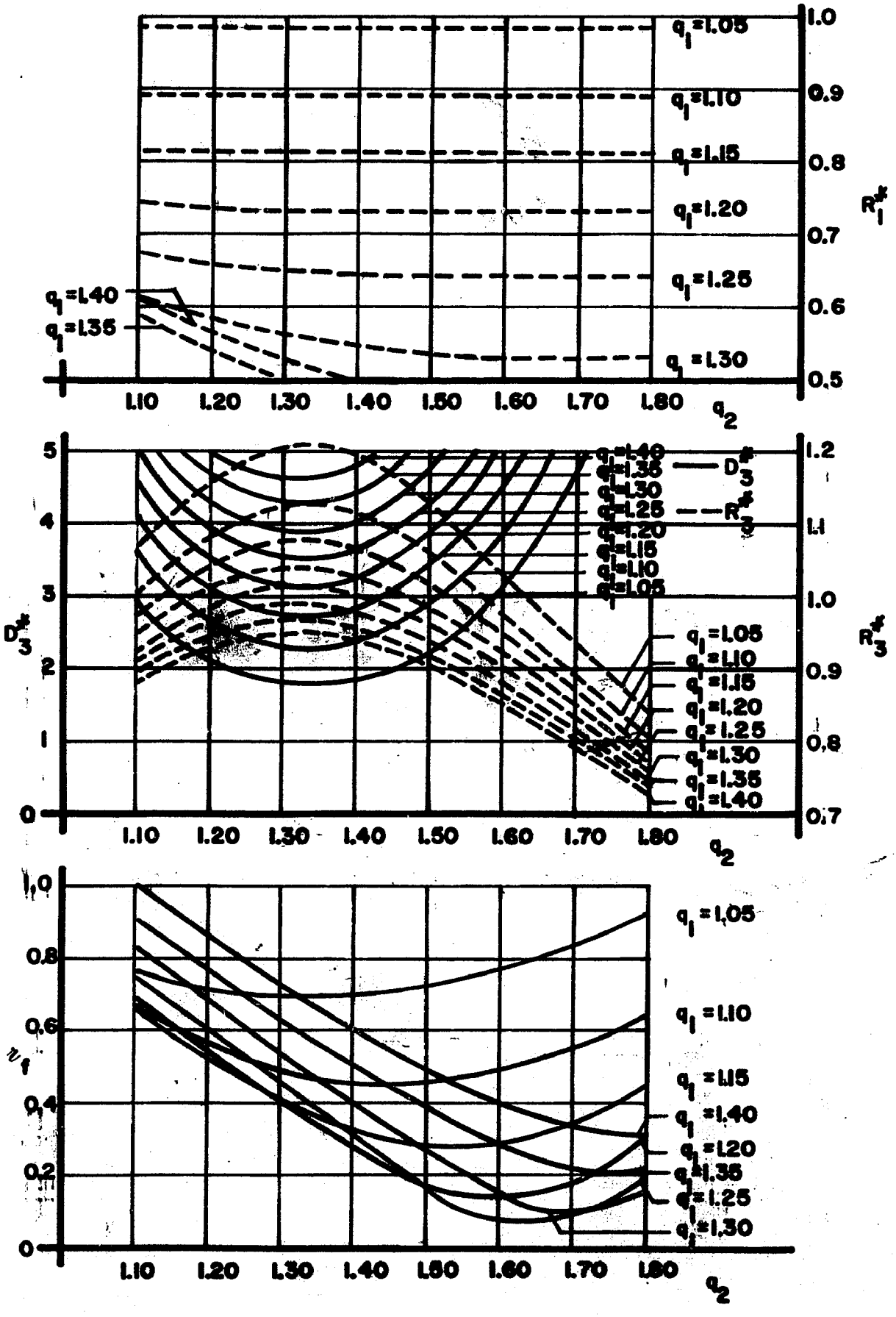

Fig. 11 Design graphs for counterweights for $v_3 = 5.921$

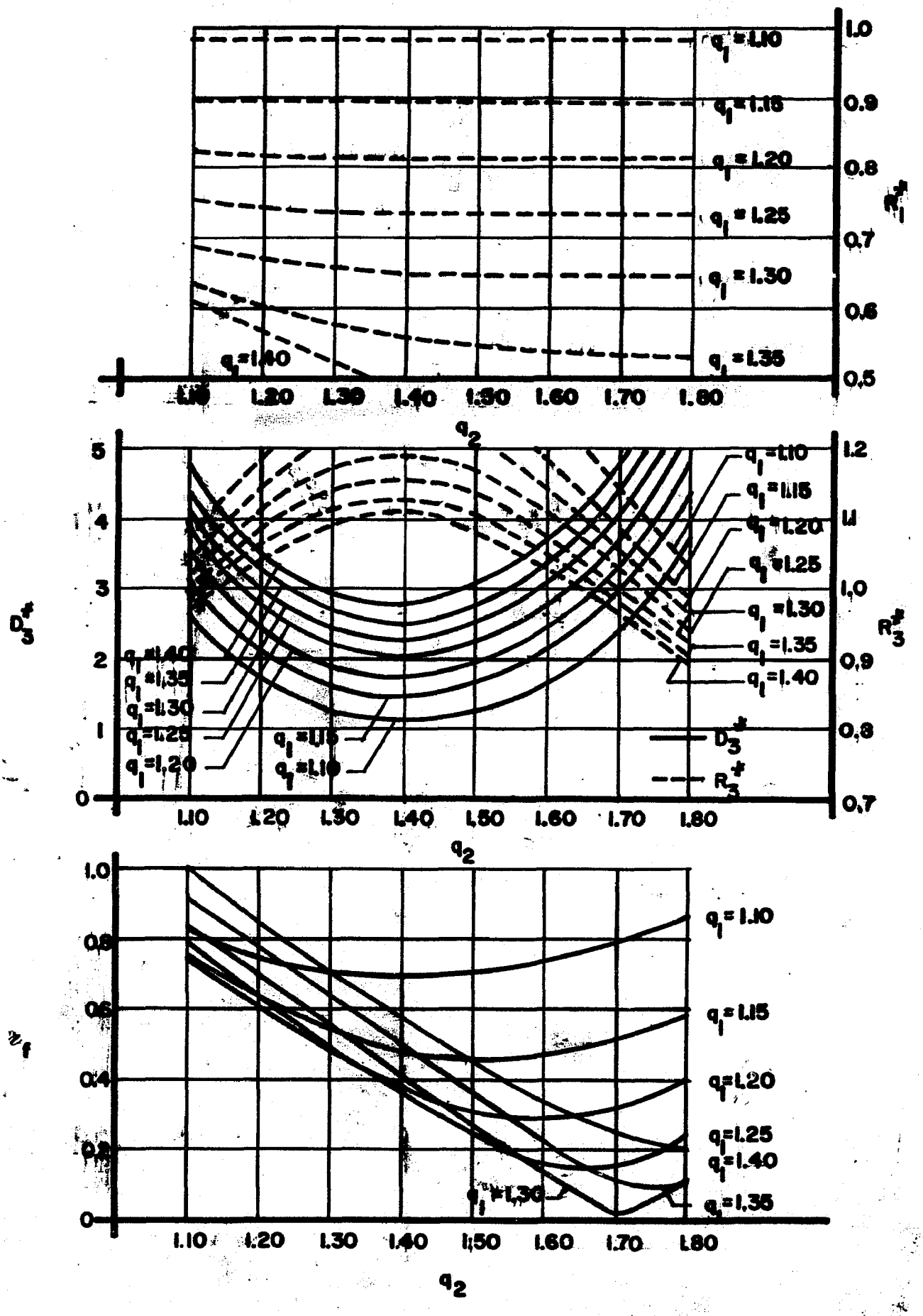

(b) Choice of Solutions With Help of Design Graphs

Let the approximate conditions specified in Section IVB-5 with respect to the constraint factors and thickness ratio δ_3 also prevail in the present case, i.e. the maximum values of q_1 and q_2 are not to exceed 1.30 and 1.40, respectively, and δ_3 is to be no greater than 3 to 4.

If one assumes that the original linkage and the counterweights are made of the same material, then the maximum value of D_3^* is also between 3 and 4. (See equation (4.27).) In order to realize the above requirements in the most favorable manner, the middle graph of Fig. 10, which represents $v_3 = 5.428$, is entered, and it is seen that the value of $D_3^* = 3.626$ may be obtained for $q_1 = 1.10$ and $q_2 = 1.10$. The top and middle graphs indicate that these values correspond to dimensionless counterweight radii $R_1^* = 0.893$ and $R_3^* = 1.003$. The lower graph shows that for the same constraint factors, $\epsilon_f = 0.67$. This represents a 33% reduction in RMS shaking force. Finally, Table 13 furnishes $\theta_1^* = 184^\circ$ and $\theta_3^* = 122^\circ$.

A further reduction in RMS shaking force may be obtained by again using a tungsten alloy for the counterweight attached to link 3. This allows D_3^* to be as large as 7.5. (Compare Section IVB-5.) Entering the middle graph of Fig. 9 ($v_3 = 4.935$), one obtains $D_3^* = 5.413$ when $q_1 = 1.10$ and $q_2 = 1.10$. The lower graph indicates that $\epsilon_f = 0.57$ for

the aforementioned constraint factors. Thus, the RMS shaking force is reduced by 43%. The counterweight radii, as obtained from the top and middle graphs, are $R_1^* = 0.811$ and $R_3^* = 0.873$. Finally, again from Table 13, $\theta_1^* = 187^\circ$ and $\theta_3^* = 130^\circ$.

As was the case in Section IVB-5, the present design graphs suggest other feasible solutions containing reasonable counterweight dimensions. While these solutions may lead to slightly increased dimensionless RMS ground bearing forces, the dimensionless RMS shaking force will be smaller. Table 15 gives a number of such solutions in addition to the two shown above. For purposes of comparison, this table also lists the values obtained from the single counterweight optimization described in Section IVB-5, as well as values of the unbalanced and fully balanced mechanism.

(c) Conclusions

Inspection of Table 15 allows the following conclusions concerning the application of the two counterweight method to the example mechanism:

1. The two counterweight method realizes a sizeable reduction in RMS shaking force while holding the RMS ground bearing forces very near those of the unbalanced mechanism.

2. While the single counterweight method only allows optimizations for constraint factors $q_1 \geq 1.30$ and $q_2 \geq 1.20$, the two counterweight method is useable for constraint

Balancing Condition		ν_f	f_{41RMS}	f_{43RMS}	R_1^*	R_3^*	D_1^*	D_3^*	θ_1^*	θ_3^*
Unbalanced		1.00	2.156	1.643	-	-	-	-	-	-
Fully Balanced (1)†		0.00	3.020	3.020	0.629	1.194	2.500	2.500	180°	180°
Partially Balanced										
q_1=1.10, q_2=1.10	1 cwt. (2.5)	n.a.[1]	n.a.	n.a.	n.a.	n.a.	n.a.	n.a.	n.a.	n.a.
	2 cwts. (1)	0.67	2.372	1.807	0.893	1.003	2.500	3.626	184°	122°
	2 cwts. (2.5)	0.57	2.372	1.807	0.811	0.873	2.500	5.413	187°	130°
q_1=1.10, q_2=1.20	1 cwt. (2.5)	n.a.	n.a.	n.a.	n.a.	n.a.	n.a.	n.a.	n.a.	n.a.
	2 cwts. (1)	0.57	2.372	1.972	0.892	1.083	2.500	2.662	183°	134°
	2 cwts. (2.5)	0.45	2.372	1.972	0.809	0.913	2.500	4.515	185°	142°
q_1=1.15, q_2=1.30	1 cwt. (2.5)	n.a.	n.a.	n.a.	n.a.	n.a.	n.a.	n.a.	n.a.	n.a.
	2 cwts. (1)	0.42	2.480	2.136	0.812	1.075	2.500	2.745	184°	146°
	2 cwts. (2.5)	0.33	2.480	2.136	0.728	0.886	2.500	5.105	186°	154°
q_1=1.20, q_2=1.40	1 cwt. (2.5)	n.a.	n.a.	n.a.	n.a.	n.a.	n.a.	n.a.	n.a.	n.a.
	2 cwts. (1)	0.29	2.587	2.300	0.732	1.029	2.500	3.267	185°	157°
	2 cwts. (2.5)	0.24	2.587	2.300	0.637	0.833	2.500	6.524	188°	164°
q_1=1.30, q_2=1.20	1 cwt. (2.5)	0.69	2.804	1.972	-	0.832	-	6.235	-	145°
	2 cwts. (1)	0.70	2.804	1.972	0.674	1.084	2.500	3.038	204°	127°
	2 cwts. (2.5)	0.68	2.804	1.972	0.586	0.961	2.500	4.302	219°	135°
q_1=1.30, q_2=1.30	1 cwt. (2.5)	0.56	2.804	2.136	-	0.814	-	6.804	-	156°
	2 cwts. (1)	0.56	2.804	2.136	0.663	1.140	2.500	2.476	198°	138°
	2 cwts. (2.5)	0.55	2.804	2.136	0.466	0.821	2.500	6.908	249°	153°
q_1=1.35, q_2=1.50	1 cwt. (2.5)	0.40	2.910	2.465	-	0.878	-	5.837	-	169°
	2 cwts. (1)	0.36	2.910	2.465	0.549	1.107	2.500	2.790	200°	160°
	2 cwts. (2.5)	0.39	2.910	2.465	0.407	0.917	2.500	5.178	235°	166°

Table 15 Comparison of RMS Shaking Force Ratio ν_f, Dimensionless RMS Ground Bearing Forces and Counterweight Dimensions

†Numbers in parenthesis indicate the value of the ratio ρ_3^*/ρ°. ρ_1^*/ρ° is always unity.

[1]n.a. = not attainable

factors as small as $q_1 = q_2 = 1.10$.

3. These desirable results are attainable without having to resort to a counterweight material denser than that of the link in order to obtain reasonable counterweight dimensions.

4. The introduction of a denser counterweight material generally leads to further reductions in the RMS shaking force for given values of RMS ground bearing forces.

5. When operating within the range of constraint factors applicable to the single counterweight method, the two counterweight method does not offer any appreciable advantages with respect to the reduction of the dimensionless RMS shaking force.

It is important to note that in all the cases considered, care has been taken to preserve practical counterweight dimensions.

V. APPENDICES

APPENDIX A

DERIVATION OF EXPRESSIONS FOR THE SHAKING FORCE, BEARING FORCES, AND INPUT MOMENT OF AN ARBITRARY FOUR-BAR LINKAGE

1. Introduction

In the present appendix, expressions are derived for the shaking force, the bearing forces, and the input moment of an arbitrary four-bar linkage using the method of superposition. In order to make the results of both the Lagrange optimization problems and the isomomental ellipse theory more general, the expressions for the shaking force, the ground bearing forces, and the input moment are put in dimensionless form. The equations for the ground bearing forces and shaking force are then rewritten in terms of the mass parameters of link 3 for the single counterweight Lagrange problem, and in terms of the mass parameters of links 1 and 3 for the two counterweight Lagrange problem. Finally, the dimensionless expressions for the ground bearing forces and input moment are rewritten in terms of the parameters of a standard linkage configuration, which was introduced in the section dealing with the distribution of the RMS shaking moment.

2. Force Analysis of Arbitrary Four-Bar Linkage

a. Description of Arbitrary Four-Bar Linkage and Associated Nomenclature

The force analysis is to be performed on the arbitrary four-bar linkage of Fig. A1. The following nomenclature is introduced for link j (j=1,2,3) of this mechanism:

a_j - pivot-to-pivot length

b_j, c_j - body-fixed x and y coordinates, respectively, of the position of the link center of mass

$\bar{F}_{D_j}$, $\bar{M}_{D_j}$ - D'Alembert force and D'Alembert moment, respectively, acting on the link

$\bar{i}$, $\bar{j}$, $\bar{k}$ - space-fixed unit vectors

m_j - link mass

φ_j - link angular position with respect to the x-axis.

Expressions will be derived for the following using the method of superposition:

F_{41_x}, F_{41_y} - components of bearing force at point A_0,

F_{21_x}, F_{21_y} - components of bearing force at point A_1,

F_{23_x}, F_{23_y} - components of bearing force at point A_2,

F_{43_x}, F_{43_y} - components of bearing force at point A_3,

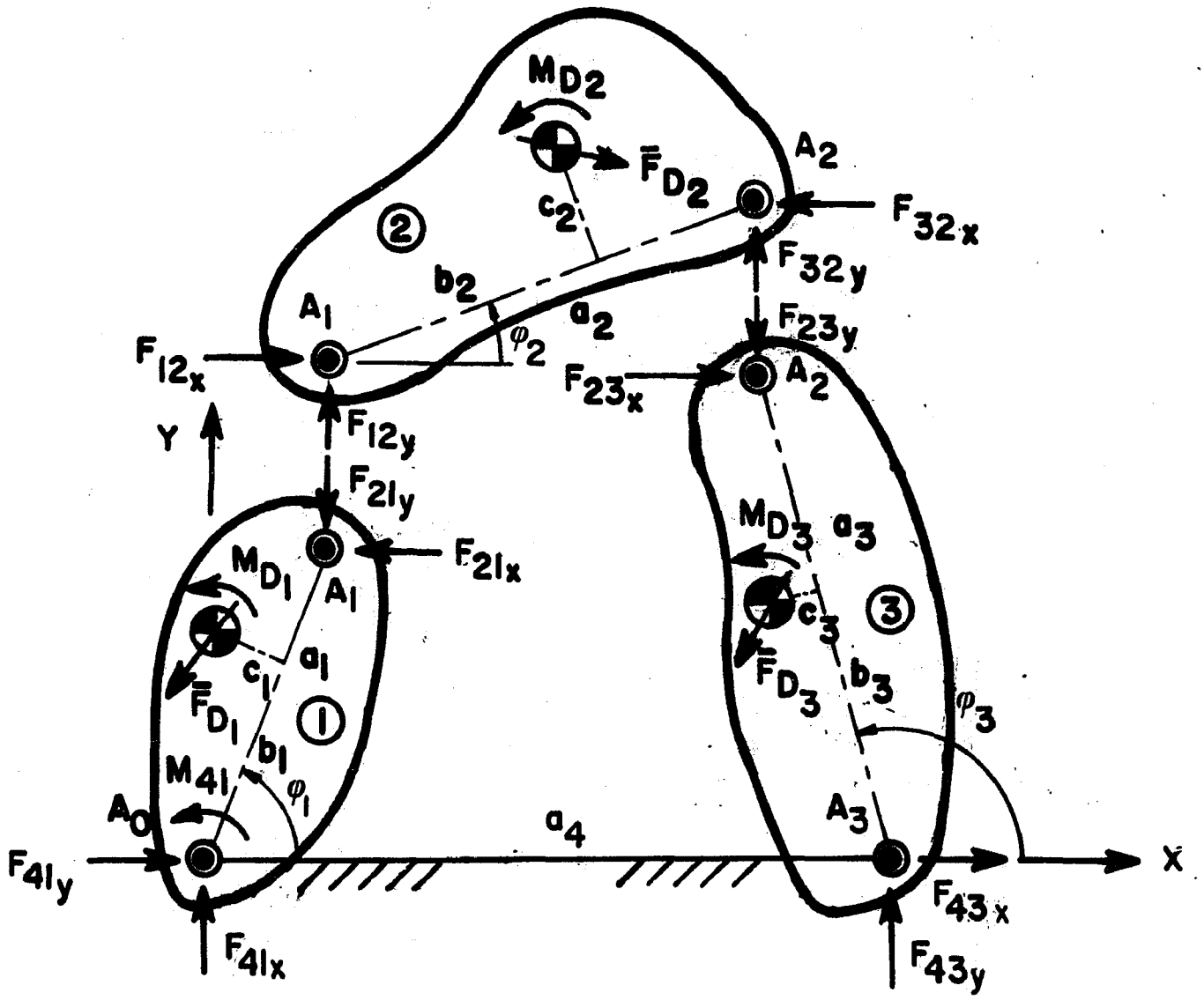

Fig. A1 Forces and moments acting on general four-bar linkage

$F_{S_x} = -(F_{41_x} + F_{43_x})$, $F_{S_y} = -(F_{41_y} + F_{43_y})$ - components of shaking force

M_{41} - input torque.

b. <u>D'Alembert Forces and Moments of Individual Links</u>

The D'Alembert forces and moments of the individual links are given by

$$\bar{F}_{D_j} = -m_j(\bar{\ddot{x}}_j + \bar{\ddot{y}}_j) \quad (j=1,2,3) \tag{A.1}$$

$$\bar{M}_{D_j} = -m_j\kappa_j^2\ddot{\varphi}_j\bar{k} \quad (j=1,2,3), \tag{A.2}$$

where κ_j is the radius of gyration of the j^{th} link with respect to its center of mass. The accelerations of the various centers of mass are given by:

$$\ddot{x}_1 = \frac{d^2}{dt^2}(b_1\cos\varphi_1 - c_1\sin\varphi_1)$$
$$= -\dot{\varphi}_1^2(b_1\cos\varphi_1 - c_1\sin\varphi_1) - \ddot{\varphi}_1(b_1\sin\varphi_1 + c_1\cos\varphi_1) \tag{A.3}$$

$$\ddot{y}_1 = \frac{d^2}{dt^2}(b_1\sin\varphi_1 + c_1\cos\varphi_1)$$
$$= -\dot{\varphi}_1^2(b_1\sin\varphi_1 + c_1\cos\varphi_1) + \ddot{\varphi}_1(b_1\cos\varphi_1 - c_1\sin\varphi_1) \tag{A.4}$$

$$\ddot{x}_2 = \frac{d^2}{dt^2}(a_1\cos\varphi_1 + b_2\cos\varphi_2 - c_2\sin\varphi_2)$$
$$= -a_1\sin\varphi_1\ddot{\varphi}_1 - a_1\dot{\varphi}_1^2\cos\varphi_1 - \ddot{\varphi}_2(b_2\sin\varphi_2 + c_2\cos\varphi_2)$$
$$- \dot{\varphi}_2^2(b_2\cos\varphi_2 - c_2\sin\varphi_2) \tag{A.5}$$

$$\ddot{y}_2 = \frac{d^2}{dt^2}(a_1\sin\varphi_1 + b_2\sin\varphi_2 + c_2\cos\varphi_2)$$

$$= a_1\cos\varphi_1\ddot{\varphi}_1 - a_1\dot{\varphi}_1^2\sin\varphi_1 + \ddot{\varphi}_2(b_2\cos\varphi_2 - c_2\sin\varphi_2)$$

$$- \dot{\varphi}_2^2(b_2\sin\varphi_2 + c_2\cos\varphi_2) \qquad (A.6)$$

$$\ddot{x}_3 = \frac{d^2}{dt^2}(b_3\cos\varphi_3 - c_3\sin\varphi_3 + a_4)$$

$$= -\ddot{\varphi}_3(b_3\sin\varphi_3 + c_3\cos\varphi_3) - \dot{\varphi}_3^2(b_3\cos\varphi_3 - c_3\sin\varphi_3) \qquad (A.7)$$

$$\ddot{y}_3 = \frac{d^2}{dt^2}(b_3\sin\varphi_3 + c_3\cos\varphi_3)$$

$$= \ddot{\varphi}_3(b_3\cos\varphi_3 - c_3\sin\varphi_3) - \dot{\varphi}_3^2(b_3\sin\varphi_3 + c_3\cos\varphi_3) \; . \qquad (A.8)$$

The expressions for φ_2, $\dot{\varphi}_2$, $\ddot{\varphi}_2$, φ_3, $\dot{\varphi}_3$ and $\ddot{\varphi}_3$ in terms of φ_1, $\dot{\varphi}_1$ and $\ddot{\varphi}_1$ may be found in [1].

c. Force Analysis By Superposition

Expressions for the shaking force, all bearing forces, and the input moment will now be derived by the method of superposition. This procedure consists of determining the input moment and all forces due to each D'Alembert force and moment acting separately. The resulting equations for the respective moment and forces are then summed to produce the desired expressions.

For the derivation of the aforementioned forces and moments, the following notation will be used:

$\bar{F}^{f(j)}_{rs}$ - the force exerted by the r^{th} link on the s^{th} link due to the D'Alembert force on the j^{th} link,

$\bar{F}^{m(j)}_{rs}$ - the force exerted by the r^{th} link on the s^{th} link due to the D'Alembert moment on the j^{th} link,

$M^{f(j)}_{41}$ - the input torque due to the D'Alembert force on the j^{th} link,

$M^{m(j)}_{41}$ - the input torque due to the D'Alembert moment on the j^{th} link.

(1) Effect of $\bar{F}_{D_1}$

When the only D'Alembert effect is that due to $\bar{F}_{D_1}$, links 2 and 3 cannot have forces acting on them. Hence,

$$\bar{F}^{f(1)}_{43} = \bar{F}^{f(1)}_{23} = \bar{F}^{f(1)}_{21} = 0 \ . \tag{A.9}$$

The force and moment equations for link 1 are

$$\bar{F}^{f(1)}_{41} + \bar{F}_{D_1} = 0 \tag{A.10}$$

$$M^{f(1)}_{41}\bar{k} + \left[b_1(\cos\varphi_1\bar{i} + \sin\varphi_1\bar{j}) + c_1(\cos(\varphi_1+\tfrac{\pi}{2})\bar{i} + \sin(\varphi_1+\tfrac{\pi}{2})\bar{j})\right] \times \bar{F}_{D_1} = 0 \ . \tag{A.11}$$

Substituting equation (A.1) into equations (A.10) and (A.11), performing the cross-multiplication in equation (A.11) and solving for $\bar{F}^{f(1)}_{41}$ and $M^{f(1)}_{41}$, one obtains

$$\bar{F}_{41}^{f(1)} = m_1(\ddot{\bar{x}}_1 + \ddot{\bar{y}}_1) \tag{A.12}$$

$$M_{41}^{f(1)} = m_1\left[\ddot{\bar{x}}_1(-b_1\sin\varphi_1 - c_1\cos\varphi_1) + \ddot{\bar{y}}_1(b_1\cos\varphi_1 - c_1\sin\varphi_1)\right]. \tag{A.13}$$

(2) Effect of M_{D_1}

Again, links 2 and 3 can have no forces acting on them. Thus,

$$\bar{F}_{43}^{m(1)} = \bar{F}_{23}^{m(1)} = \bar{F}_{21}^{m(1)} = 0 \ . \tag{A.14}$$

The force and moment equilibrium equations for link 1 are

$$\bar{F}_{41}^{m(1)} = 0 \tag{A.15}$$

$$M_{41}^{m(1)}\bar{k} + M_{D_1}\bar{k} = 0 \ ,$$

or using equation (A.2),

$$M_{41}^{m(1)} = m_1\kappa_1^2\ddot{\varphi}_1 \ . \tag{A.16}$$

(3) Effect of $\bar{F}_{D_2}$

The force and moment equilibrium equations for links 1, 2 and 3 can be written

$$\bar{F}_{41}^{f(2)} + \bar{F}_{21}^{f(2)} = 0 \tag{A.17}$$

$$M_{41}^{f(2)}\bar{k} + a_1(\cos\varphi_1\bar{i} + \sin\varphi_1\bar{j}) \times \bar{F}_{21}^{f(2)} = 0 \tag{A.18}$$

$$\bar{F}_{D_2} + \bar{F}_{12}^{f(2)} + \bar{F}_{32}^{f(2)} = 0 \tag{A.19}$$

$$\left[b_2(\cos\varphi_2\bar{i} + \sin\varphi_2\bar{j}) + c_2(\cos(\varphi_2+\tfrac{\pi}{2})\bar{i} + \sin(\varphi_2+\tfrac{\pi}{2})\bar{j})\right] \times \bar{F}_{D_2}$$

$$+ a_2(\cos\varphi_2\bar{i} + \sin\varphi_2\bar{j}) \times \bar{F}_{32}^{f(2)} = 0 \qquad \text{(A.20)}$$

$$\bar{F}_{23}^{f(2)} + \bar{F}_{43}^{f(2)} = 0 \ . \qquad \text{(A.21)}$$

Link 3 is a two force member. Thus, $\bar{F}_{32}^{f(2)}$ is directed along A_2A_3. Substituting equation (A.1) into equation (A.20), solving this equation for $\bar{F}_{23}^{f(2)}$, and then using the result in equation (A.21) yields the following:

$$\bar{F}_{23}^{f(2)} = -\bar{F}_{43}^{f(2)} = \frac{m_2}{a_2\tau_3}\Big[\ddot{x}_2(b_2\sin\varphi_2 + c_2\cos\varphi_2) - \ddot{y}_2(b_2\cos\varphi_2 - c_2\sin\varphi_2)\Big](\cos\varphi_3\bar{i} + \sin\varphi_3\bar{j}) \ , \qquad \text{(A.22)}$$

where

$$\tau_3 = \sin(\varphi_3 - \varphi_2).^* \qquad \text{(A.23)}$$

Now substitute equations (A.1) and (A.22) into equation (A.19), solve for $\bar{F}_{21}^{f(2)}$, and use the result in equation (A.17). This produces the following:

---

*Folding linkages, in which $\varphi_3 - \varphi_2 = 0$ or π, are excluded from this study since the motion becomes indeterminate.

$$\bar{F}_{21}^{f(2)} = -\bar{F}_{41}^{f(2)} = -\frac{m_2}{a_2\tau_3}\Big[\ddot{x}_2\big[(b_2\sin\varphi_2 + c_2\cos\varphi_2)\cos\varphi_3 + a_2\tau_3\big] - \ddot{y}_2(b_2\cos\varphi_2 - c_2\sin\varphi_2)\cos\varphi_3\Big]\bar{i} + \Big[\ddot{x}_2(b_2\sin\varphi_2 + c_2\cos\varphi_2)\sin\varphi_2 - \ddot{y}_2\big[(b_2\cos\varphi_2 - c_2\sin\varphi_2)\sin\varphi_3 - a_2\tau_3\big]\Big]\bar{j} \quad . \tag{A.24}$$

Solving equation (A.18) for $M_{41}^{f(2)}$ and substituting equation (A.24), one obtains

$$M_{41}^{f(2)} = \frac{a_1 m_2}{a_2\tau_3}\Big[\ddot{x}_2\big[(b_2\sin\varphi_2 + c_2\cos\varphi_2)\sin\varphi_3\big] - \ddot{y}_2\big[(b_2\cos\varphi_2 - c_2\sin\varphi_2)\sin\varphi_3 - a_2\tau_3\big]\Big]\cos\varphi_1 - \Big[\ddot{x}_2\big[(b_2\sin\varphi_2 + c_2\cos\varphi_2)\cos\varphi_3 + a_2\tau_3\big] - \ddot{y}_2\big[(b_2\cos\varphi_2 - c_2\sin\varphi_2)\cos\varphi_3\big]\Big]\sin\varphi_1 \quad . \tag{A.25}$$

(4) Effect of M_{D_2}

The force and moment equilibrium equations for links 1, 2 and 3 can be written as follows:

$$\bar{F}_{21}^{m(2)} + \bar{F}_{41}^{m(2)} = 0 \tag{A.26}$$

$$M_{41}^{m(2)}\bar{k} + a_1(\cos\varphi_1\bar{i} + \sin\varphi_1\bar{j}) \times \bar{F}_{21}^{m(2)} = 0 \tag{A.27}$$

$$\bar{F}_{12}^{m(2)} + \bar{F}_{32}^{m(2)} = 0 \tag{A.28}$$

$$a_2(\cos\varphi_2\bar{i} + \sin\varphi_2\bar{j}) \times \bar{F}_{32}^{m(2)} + M_{D_2}\bar{k} = 0 \tag{A.29}$$

$$\bar{F}_{23}^{m(2)} + \bar{F}_{43}^{m(2)} = 0 \ . \tag{A.30}$$

Since link 3 is a two force member, $\bar{F}_{23}^{m(2)}$ must be directed along A_2A_3. Substitute equation (A.2) into equation (A.29), solve this equation for $\bar{F}_{23}^{m(2)}$, and then use the result in equations (A.26), (A.28) and (A.30) to find $\bar{F}_{21}^{m(2)}$, $\bar{F}_{41}^{m(2)}$ and $\bar{F}_{43}^{m(2)}$. Thus, one obtains

$$\bar{F}_{23}^{m(2)} = -\bar{F}_{21}^{m(2)} = \bar{F}_{41}^{m(2)} = -\bar{F}_{43}^{m(2)} = \frac{-m_2 \kappa_2^2 \ddot{\varphi}_2}{a_2\tau_3}(\cos\varphi_3\bar{i} + \sin\varphi_3\bar{j}) \ . \tag{A.31}$$

Substitute equation (A.31) into equation (A.27) and solve for $M_{41}^{m(2)}$. Hence

$$M_{41}^{m(2)} = \frac{m_2 \kappa_2^2 a_1 \sin(\varphi_1-\varphi_3)\ddot{\varphi}_2}{a_2\tau_3} \ . \tag{A.32}$$

(5) Effect of $\bar{F}_{D_3}$

The force and moment equilibrium equations for links 1, 2 and 3 are

$$\bar{F}_{21}^{f(3)} + \bar{F}_{41}^{f(3)} = 0 \tag{A.33}$$

$$M_{41}^{f(3)}\bar{k} + a_1(\cos\varphi_1\bar{i} + \sin\varphi_1\bar{j}) \times \bar{F}_{21}^{f(3)} = 0 \tag{A.34}$$

$$\bar{F}_{12}^{f(3)} + \bar{F}_{32}^{f(3)} = 0 \tag{A.35}$$

$$\bar{F}_{D_3} + \bar{F}_{43}^{f(3)} + \bar{F}_{23}^{f(3)} = 0 \tag{A.36}$$

$$a_3(\cos\varphi_3\bar{i} + \sin\varphi_3\bar{j}) \times \bar{F}_{23}^{f(3)} + \Big[b_3(\cos\varphi_3\bar{i} + \sin\varphi_3\bar{j}) + c_3(\cos(\varphi_3+\tfrac{\pi}{2})\bar{i} + \sin(\varphi_3+\tfrac{\pi}{2})\bar{j})\Big] \times \bar{F}_{D_3} = 0 \; . \tag{A.37}$$

Link 2 is a two force member, and therefore, $\bar{F}_{23}^{f(3)}$ must be directed along A_1A_2. Substitute equation (A.1) into equations (A.36) and (A.37). These equations can be solved for $\bar{F}_{23}^{f(3)}$ and $\bar{F}_{43}^{f(3)}$. Using the expression for $\bar{F}_{23}^{f(3)}$ in equation (A.35) permits one to find $\bar{F}_{21}^{f(3)}$, which can then be used in equation (A.33) to solve for $\bar{F}_{41}^{f(3)}$. Thus,

$$\bar{F}_{23}^{f(3)} = -\bar{F}_{21}^{f(3)} = \bar{F}_{41}^{f(3)} = -\frac{m_3}{a_3\tau_3}\Big[\ddot{x}_3(b_3\sin\varphi_3 + c_3\cos\varphi_3) - \ddot{y}_3(b_3\cos\varphi_3 - c_3\sin\varphi_3)\Big](\cos\varphi_2\bar{i} + \sin\varphi_2\bar{j}) \tag{A.38}$$

$$\bar{F}_{43}^{f(3)} = -\frac{m_3}{a_3\tau_3}\Big\{\Big[\ddot{x}_3(b_3\sin\varphi_3 + c_3\cos\varphi_3 - a_3\tau_3) - \ddot{y}_3(b_3\cos\varphi_3 - c_3\sin\varphi_3)\Big]\cos\varphi_2\bar{i} + \Big[\ddot{x}_3(b_3\sin\varphi_3 + c_3\cos\varphi_3) - \ddot{y}_3(b_3\cos\varphi_3 - c_3\sin\varphi_3 + a_3\tau_3)\Big]\sin\varphi_2\bar{j}\Big\} \tag{A.39}$$

Now substitute equation (A.38) into equation (A.34) and

solve for $M_{41}^{f(3)}$. One obtains

$$M_{41}^{f(3)} = \frac{-m_3 a_1 \tau_1}{a_3 \tau_3}\left[\ddot{x}_3(b_3\sin\varphi_3 + c_3\cos\varphi_3) - \ddot{y}_3(b_3\cos\varphi_3 - c_3\sin\varphi_3)\right] \tag{A.40}$$

where

$$\tau_1 = \sin(\varphi_1 - \varphi_2). \tag{A.41}$$

(6) Effect of M_{D_3}

The force and moment equilibrium equations for links 1, 2 and 3 are

$$\bar{F}_{21}^{m(3)} + \bar{F}_{41}^{m(3)} = 0 \tag{A.42}$$

$$M_{41}^{m(3)}\bar{k} + a_1(\cos\varphi_1\bar{i} + \sin\varphi_1\bar{j}) \times \bar{F}_{21}^{m(3)} = 0 \tag{A.43}$$

$$\bar{F}_{12}^{m(3)} + \bar{F}_{32}^{m(3)} = 0 \tag{A.44}$$

$$\bar{F}_{43}^{m(3)} + \bar{F}_{23}^{m(3)} = 0 \tag{A.45}$$

$$M_{D_3}\bar{k} + a_3(\cos\varphi_3\bar{i} + \sin\varphi_3\bar{j}) \times \bar{F}_{23}^{m(3)} = 0 . \tag{A.46}$$

Link 2 is again a two force member. Hence, $\bar{F}_{23}^{m(3)}$ is directed along A_1A_2. After substituting equation (A.2) into equation (A.46), one can find $\bar{F}_{23}^{m(3)}$. This can then be used in equations (A.44) and (A.45) to obtain $\bar{F}_{43}^{m(3)}$ and $\bar{F}_{21}^{m(3)}$, which can now be substituted into equation (A.42)

to find $\bar{F}_{41}^{m(3)}$. Therefore,

$$\bar{F}_{23}^{m(3)} = -\bar{F}_{43}^{m(3)} = -\bar{F}_{21}^{m(3)} = \bar{F}_{41}^{m(3)} = \frac{-m_3\kappa_3\ddot{\varphi}_3}{a_3\tau_3}(\cos\varphi_2\bar{i} + \sin\varphi_2\bar{j}). \tag{A.47}$$

Substituting equation (A.47) into equation (A.43) and solving for $M_{41}^{m(3)}$, one obtains

$$M_{41}^{m(3)} = \frac{a_1\tau_1}{a_3\tau_3} m_3\kappa_3\ddot{\varphi}_3 . \tag{A.48}$$

(7) Superposition of Forces

The total bearing forces can now be determined by the method of superposition.

(a) Ground Bearing Force $\bar{F}_{41}$

F_{41_x} and F_{41_y}, the x and y components of $\bar{F}_{41}$, can be found by summing equations (A.12), (A.15), (A.24), (A.31), (A.38) and (A.47). Then substituting equations (A.3) - (A.8) and rearranging according to mass-distance products, one obtains

$$F_{41_x} = -m_2 a_1(\ddot{\varphi}_1 \sin\varphi_1 + \dot{\varphi}_1^2 \cos\varphi_1) - m_1 b_1(\dot{\varphi}_1^2 \cos\varphi_1 + \ddot{\varphi}_1 \sin\varphi_1)$$

$$+ m_1 c_1(\dot{\varphi}_1^2 \sin\varphi_1 - \ddot{\varphi}_1 \cos\varphi_1)$$

$$- m_2 b_2\left[\ddot{\varphi}_2 \sin\varphi_2 + \dot{\varphi}_2^2 \cos\varphi_2 - \frac{a_1 \cos\varphi_3}{a_2 \tau_3}(\dot{\varphi}_1^2 \tau_1 - \ddot{\varphi}_1 \tau_{11})\right]$$

$$- m_2 c_2\left[\ddot{\varphi}_2 \cos\varphi_2 - \dot{\varphi}_2^2 \sin\varphi_2 + \frac{a_1 \cos\varphi_3}{a_2 \tau_3}(\dot{\varphi}_1^2 \tau_{11} + \ddot{\varphi}_1 \tau_1)\right]$$

$$- m_2(b_2^2 + c_2^2 + \kappa_2^2)\frac{\ddot{\varphi}_2 \cos\varphi_3}{a_2 \tau_3} - m_3(b_3^2 + c_3^2 + \kappa_3^2)\frac{\ddot{\varphi}_3 \cos\varphi_2}{a_3 \tau_3} \tag{A.49}$$

$$F_{41_y} = m_2 a_1(\ddot{\varphi}_1 \cos\varphi_1 - \dot{\varphi}_1^2 \sin\varphi_1) - m_1 b_1(\dot{\varphi}_1^2 \sin\varphi_1 - \ddot{\varphi}_1 \cos\varphi_1)$$

$$- m_1 c_1(\dot{\varphi}_1^2 \cos\varphi_1 + \ddot{\varphi}_1 \sin\varphi_1)$$

$$+ m_2 b_2\left[\ddot{\varphi}_2 \cos\varphi_2 - \dot{\varphi}_2^2 \sin\varphi_2 + \frac{a_1 \sin\varphi_3}{a_2 \tau_3}(\dot{\varphi}_1^2 \tau_1 - \ddot{\varphi}_1 \tau_{11})\right]$$

$$- m_2 c_2\left[\ddot{\varphi}_2 \sin\varphi_2 + \dot{\varphi}_2^2 \cos\varphi_2 + \frac{a_1 \sin\varphi_3}{a_2 \tau_3}(\dot{\varphi}_1^2 \tau_{11} + \ddot{\varphi}_1 \tau_1)\right]$$

$$- m_2(b_2^2 + c_2^2 + \kappa_2^2)\frac{\ddot{\varphi}_2 \sin\varphi_3}{a_2 \tau_3} - m_3(b_3^2 + c_3^2 + \kappa_3^2)\frac{\ddot{\varphi}_3 \sin\varphi_2}{a_3 \tau_3} \tag{A.50}$$

where

$$\tau_{11} = \cos(\varphi_1 - \varphi_2) \ . \tag{A.51}$$

(b) Moving Bearing Force $\bar{F}_{21}$

The x and y components of $\bar{F}_{21}$ can be determined by adding equations (A.9), (A.14), (A.24), (A.31), (A.38) and (A.47). Substituting equations (A.3) - (A.8), and rearranging as above, one obtains

$$F_{21_x} = m_2 a_1(\ddot{\varphi}_1 \sin\varphi_1 + \dot{\varphi}_1^2 \cos\varphi_1) + m_2 b_2\Big[\ddot{\varphi}_2 \sin\varphi_2 + \dot{\varphi}_2^2 \cos\varphi_2 + \frac{a_1 \cos\varphi_3}{a_2 \tau_3}(\ddot{\varphi}_1 \tau_{11} - \dot{\varphi}_1^2 \tau_1)\Big] + m_2 c_2\Big[\ddot{\varphi}_2 \cos\varphi_2 - \dot{\varphi}_2^2 \sin\varphi_2 + \frac{a_1 \cos\varphi_3}{a_2 \tau_3}(\ddot{\varphi}_1 \tau_1 + \dot{\varphi}_1^2 \tau_{11})\Big] + m_2(b_2^2 + c_2^2 + \kappa_2^2)\frac{\ddot{\varphi}_2 \cos\varphi_3}{a_2 \tau_3} + m_3(b_3^2 + c_3^2 + \kappa_3^2)\frac{\ddot{\varphi}_3 \cos\varphi_2}{a_3 \tau_3} \tag{A.52}$$

$$F_{21_y} = m_2 a_1(-\ddot{\varphi}_1 \cos\varphi_1 + \dot{\varphi}_1^2 \sin\varphi_1) + m_2 b_2\Big[-\ddot{\varphi}_2 \cos\varphi_2 + \dot{\varphi}_2^2 \sin\varphi_2 + \frac{a_1 \sin\varphi_3}{a_2 \tau_3}(\ddot{\varphi}_1 \tau_{11} - \dot{\varphi}_1^2 \tau_1)\Big] + m_2 c_2\Big[\ddot{\varphi}_2 \sin\varphi_2 + \dot{\varphi}_2^2 \cos\varphi_2 + \frac{a_1 \sin\varphi_3}{a_2 \tau_3}(\ddot{\varphi}_1 \tau_1 + \dot{\varphi}_1^2 \tau_{11})\Big] + m_2(b_2^2 + c_2^2 + \kappa_2^2)\frac{\ddot{\varphi}_2 \sin\varphi_3}{a_2 \tau_3} + m_3(b_3^2 + c_3^2 + \kappa_3^2)\frac{\ddot{\varphi}_3 \sin\varphi_2}{a_3 \tau_3}\,. \tag{A.53}$$

(c) Moving Bearing Force $\bar{F}_{23}$

F_{23_x} and F_{23_y} can be found by summing equations (A.9), (A.14), (A.22), (A.31), (A.38) and (A.47). Again, substitute equations (A.3) - (A.8), and rearrange the results as indicated above. Thus, one obtains

$$F_{23_x} = m_2 b_2\left[\frac{a_1\cos\varphi_3}{a_2\tau_3}(\dot{\varphi}_1^2\tau_1 - \ddot{\varphi}_1\tau_{11})\right] + m_2 c_2\left[\frac{a_1\cos\varphi_3}{a_2\tau_3}(-\dot{\varphi}_1^2\tau_{11} + \ddot{\varphi}_1\tau_1)\right]$$
$$- m_2(b_2^2 + c_2^2 + \kappa_2^2)\frac{\ddot{\varphi}_2\cos\varphi_3}{a_2\tau_3} - m_3(b_3^2 + c_3^2 + \kappa_3^2)\frac{\ddot{\varphi}_3\cos\varphi_2}{a_3\tau_3} \qquad (A.54)$$

$$F_{23_y} = m_2 b_2\left[\frac{a_1\sin\varphi_3}{a_2\tau_3}(\dot{\varphi}_1^2\tau_1 - \ddot{\varphi}_1\tau_{11})\right] + m_2 c_2\left[\frac{a_1\sin\varphi_3}{a_2\tau_3}(-\dot{\varphi}_1^2\tau_{11} + \ddot{\varphi}_1\tau_1)\right]$$
$$- m_2(b_2^2 + c_2^2 + \kappa_2^2)\frac{\ddot{\varphi}_2\sin\varphi_3}{a_2\tau_3} - m_3(b_3^2 + c_3^2 + \kappa_3^2)\frac{\ddot{\varphi}_3\sin\varphi_2}{a_3\tau_3} . \qquad (A.55)$$

(d) Ground Bearing Force $\bar{F}_{43}$

F_{43_x} and F_{43_y} can be determined by summing equations (A.9), (A.14), (A.22), (A.31), (A.39) and (A.47). Once again, substitute equations (A.3) - (A.8), and rearrange the terms as above. F_{43_x} and F_{43_y} can now be written

$$F_{43_x} = m_2 b_2\left[\frac{a_1\cos\varphi_3}{a_2\tau_3}(-\dot{\varphi}_1^2\tau_1 + \ddot{\varphi}_1\tau_{11})\right] + m_2 c_2\left[\frac{a_1\cos\varphi_3}{a_2\tau_3}(\dot{\varphi}_1^2\tau_{11} + \ddot{\varphi}_1\tau_1)\right]$$

$$- m_3 b_3(\ddot{\varphi}_3\sin\varphi_3 + \dot{\varphi}_3^2\cos\varphi_3) - m_3 c_3(\ddot{\varphi}_3\cos\varphi_3 - \dot{\varphi}_3^2\sin\varphi_3)$$

$$+ m_2(b_2^2 + c_2^2 + \kappa_2^2)\frac{\ddot{\varphi}_2\cos\varphi_3}{a_2\tau_3} + m_3(b_3^2 + c_3^2 + \kappa_3^2)\frac{\ddot{\varphi}_3\cos\varphi_2}{a_3\tau_3}$$

(A.56)

$$F_{43_y} = m_2 b_2\left[\frac{a_1\sin\varphi_3}{a_2\tau_3}(-\dot{\varphi}_1^2\tau_1 + \ddot{\varphi}_1\tau_{11})\right] + m_2 c_2\left[\frac{a_1\sin\varphi_3}{a_2\tau_3}(\dot{\varphi}_1^2\tau_{11} + \ddot{\varphi}_1\tau_1)\right]$$

$$+ m_3 b_3(\ddot{\varphi}_3\cos\varphi_3 - \dot{\varphi}_3^2\sin\varphi_3) - m_3 c_3(\ddot{\varphi}_3\sin\varphi_3 + \dot{\varphi}_3^2\cos\varphi_3)$$

$$+ m_2(b_2^2 + c_2^2 + \kappa_2^2)\frac{\ddot{\varphi}_2\sin\varphi_3}{a_2\tau_3} + m_3(b_3^2 + c_3^2 + \kappa_3^2)\frac{\ddot{\varphi}_3\sin\varphi_2}{a_3\tau_3} \quad .$$

(A.57)

(e) Shaking Force $\bar{F}_S$

The x and y components of the shaking force can now be obtained with the help of the above. Thus,

$$F_{S_x} = F_{14_x} + F_{34_x}$$

$$= m_2a_1(\ddot{\varphi}_1\sin\varphi_1 + \dot{\varphi}_1^2\cos\varphi_1) + m_1b_1(\dot{\varphi}_1^2\cos\varphi_1 + \ddot{\varphi}_1\sin\varphi_1)$$

$$- m_1c_1(\dot{\varphi}_1^2\sin\varphi_1 - \ddot{\varphi}_1\cos\varphi_1) + m_2b_2(\ddot{\varphi}_2\sin\varphi_2 + \dot{\varphi}_2^2\cos\varphi_2)$$

$$+ m_2c_2(\ddot{\varphi}_2\cos\varphi_2 - \dot{\varphi}_2^2\sin\varphi_2) + m_3b_3(\ddot{\varphi}_3\sin\varphi_3 + \dot{\varphi}_3^2\cos\varphi_3)$$

$$+ m_3c_3(\ddot{\varphi}_3\cos\varphi_3 - \dot{\varphi}_3^2\sin\varphi_3) \qquad (A.58)$$

$$F_{S_y} = F_{14_y} + F_{34_y}$$

$$= -m_2a_1(\ddot{\varphi}_1\cos\varphi_1 - \dot{\varphi}_1^2\sin\varphi_1) + m_1b_1(\dot{\varphi}_1^2\sin\varphi_1 - \ddot{\varphi}_1\cos\varphi_1)$$

$$+ m_1c_1(\dot{\varphi}_1^2\cos\varphi_1 + \ddot{\varphi}_1\sin\varphi_1) - m_2b_2(\ddot{\varphi}_2\cos\varphi_2 - \dot{\varphi}_2^2\sin\varphi_2)$$

$$+ m_2c_2(\ddot{\varphi}_2\sin\varphi_2 + \dot{\varphi}_2^2\cos\varphi_2) - m_3b_3(\ddot{\varphi}_3\cos\varphi_3 - \dot{\varphi}_3^2\sin\varphi_3)$$

$$+ m_3c_3(\ddot{\varphi}_3\sin\varphi_3 + \dot{\varphi}_3^2\cos\varphi_3). \qquad (A.59)$$

(f) Input Torque M_{41}

The input torque can be determined by summing equations (A.13), (A.16), (A.25), (A.32), (A.40) and (A.48). Substituting equations (A.3) - (A.8) and rearranging the terms as before yields the following:

$$M_{41} = m_2 a_1^2 \ddot{\varphi}_1 + m_1(b_1^2 + c_1^2 + \kappa_1^2)\ddot{\varphi}_1$$

$$+ m_2 b_2 \left[a_1(\ddot{\varphi}_2 \tau_{11} + \dot{\varphi}_2^2 \tau_1) - \frac{a_1^2 \sin(\varphi_1 - \varphi_3)}{a_2 \tau_3}(\dot{\varphi}_1^2 \tau_1 - \ddot{\varphi}_1 \tau_{11}) \right]$$

$$+ m_2 c_2 \left[a_1(\ddot{\varphi}_2 \tau_1 - \dot{\varphi}_2^2 \tau_{11}) + \frac{a_1^2 \sin(\varphi_1 - \varphi_3)}{a_2 \tau_3}(\dot{\varphi}_1^2 \tau_{11} + \ddot{\varphi}_1 \tau_1) \right]$$

$$+ m_2(b_2^2 + c_2^2 + \kappa_2^2)\frac{\ddot{\varphi}_2 a_1 \sin(\varphi_1 - \varphi_3)}{a_2 \tau_3}$$

$$+ m_3(b_3^2 + c_3^2 + \kappa_3^2)\frac{\ddot{\varphi}_3 a_1 \tau_1}{a_3 \tau_3} \quad . \qquad \text{(A.60)}$$

3. Dimensionless Expressions for the Ground Bearing Forces, the Shaking Force, and the Input Moment in Terms of the Positions of the Link Centers of Mass

For purposes of the present work, the ground bearing forces, the shaking force, and the input moment will now be given in dimensionless form. This permits one to obtain identical expressions for all mechanisms with the same link length ratios [14]. Multiplication of the applicable expressions by the square of the input angular velocity $\dot{\varphi}_1$, the common link density ρ, and the suitable power of the length of the input link a_1, will produce the actual reactions. It is assumed throughout that the input angular velocity is constant.

The following need be defined:

$$\left.\begin{aligned} &\alpha_i = a_i/a_1 \text{ - dimensionless link length} \\ &B_i = m_i/\rho a_1^3 \text{ - dimensionless mass } (\rho \text{ - mass density}) \\ &\left.\begin{aligned} U_i &= b_i/a_1 \\ T_i &= c_i/a_1 \end{aligned}\right\} \text{dimensionless position of total center of mass of link} \\ &W_i = \kappa_i/a_1 \text{ - dimensionless radius of gyration} \\ &\qquad\qquad (i=1,2,3). \end{aligned}\right\} \quad (A.61)$$

The dimensionless reactions are obtained by substituting equations (A.61) into equations (A.49), (A.50), and (A.56) - (A.60). Subsequent multiplication and division of the results by $\dot{\varphi}_1^2$, as well as factoring $\rho a_1^4 \dot{\varphi}_1^2$ or $\rho a_1^5 \dot{\varphi}_1^2$, furnishes the actual

reactions:

$$F_{41_x} = \rho a_1^4 \dot{\varphi}_1^2 f_{41_x} \tag{A.62}$$

$$F_{41_y} = \rho a_1^4 \dot{\varphi}_1^2 f_{41_y} \tag{A.63}$$

$$F_{43_x} = \rho a_1^4 \dot{\varphi}_1^2 f_{43_x} \tag{A.64}$$

$$F_{43_y} = \rho a_1^4 \dot{\varphi}_1^2 f_{43_y} \tag{A.65}$$

$$F_{S_x} = \rho a_1^4 \dot{\varphi}_1^2 f_{S_x} \tag{A.66}$$

$$F_{S_y} = \rho a_1^4 \dot{\varphi}_1^2 f_{S_y} \tag{A.67}$$

$$M_{41} = \rho a_1^5 \dot{\varphi}_1^2 \mu_{41} \tag{A.68}$$

where

f_{41_x} = x component of dimensionless bearing force at A_0

$$= -B_2\cos\varphi_1 - B_1U_1\cos\varphi_1 + B_1T_1\sin\varphi_1$$

$$- B_2U_2\left[\frac{\ddot{\varphi}_2}{\dot{\varphi}_1^2}\sin\varphi_2 + \left(\frac{\dot{\varphi}_2}{\dot{\varphi}_1}\right)^2\cos\varphi_2 - \frac{\cos\varphi_3\tau_1}{\alpha_2\tau_3}\right]$$

$$- B_2T_2\left[\frac{\ddot{\varphi}_2}{\dot{\varphi}_1^2}\cos\varphi_2 - \left(\frac{\dot{\varphi}_2}{\dot{\varphi}_1}\right)^2\sin\varphi_2 + \frac{\cos\varphi_3\tau_{11}}{\alpha_2\tau_3}\right]$$

$$- B_2(U_2^2 + T_2^2 + W_2^2)\frac{\ddot{\varphi}_2}{\dot{\varphi}_1^2}\frac{\cos\varphi_3}{\alpha_2\tau_3} - B_3(U_3^2 + T_3^2 + W_3^2)\frac{\ddot{\varphi}_3}{\dot{\varphi}_1^2}\frac{\cos\varphi_2}{\alpha_3\tau_3} \tag{A.69}$$

f_{41_y} = y component of dimensionless bearing force at A_0

$$= -B_2\sin\varphi_1 - B_1U_1\sin\varphi_1 - B_1T_1\cos\varphi_1$$

$$+ B_2U_2\left[\frac{\ddot{\varphi}_2}{\dot{\varphi}_1^2}\cos\varphi_2 - \left(\frac{\dot{\varphi}_2}{\dot{\varphi}_1}\right)^2\sin\varphi_2 + \frac{\sin\varphi_3\tau_1}{\alpha_2\tau_3}\right]$$

$$- B_2T_2\left[\frac{\ddot{\varphi}_2}{\dot{\varphi}_1^2}\sin\varphi_2 + \left(\frac{\dot{\varphi}_2}{\dot{\varphi}_1}\right)^2\cos\varphi_2 + \frac{\sin\varphi_3\tau_{11}}{\alpha_2\tau_3}\right]$$

$$- B_2(U_2^2 + T_2^2 + W_2^2)\frac{\ddot{\varphi}_2}{\dot{\varphi}_1^2}\frac{\sin\varphi_3}{\alpha_2\tau_3} - B_3(U_3^2 + T_3^2 + W_3^2)\frac{\ddot{\varphi}_3}{\dot{\varphi}_1^2}\frac{\sin\varphi_2}{\alpha_3\tau_3} \tag{A.70}$$

f_{43_x} = x component of dimensionless bearing force at A_3

$$= -B_2U_2\frac{\tau_1\cos\varphi_3}{\alpha_2\tau_3} + B_2T_2\frac{\tau_{11}\cos\varphi_3}{\alpha_2\tau_3}$$

$$- B_3U_3\left[\frac{\ddot{\varphi}_3}{\dot{\varphi}_1^2}\sin\varphi_3 + \left(\frac{\dot{\varphi}_3}{\dot{\varphi}_1}\right)^2\cos\varphi_3\right] - B_3T_3\left[\frac{\ddot{\varphi}_3}{\dot{\varphi}_1^2}\cos\varphi_3 - \left(\frac{\dot{\varphi}_3}{\dot{\varphi}_1}\right)^2\sin\varphi_3\right]$$

$$+ B_2(U_2^2 + T_2^2 + W_2^2)\frac{\ddot{\varphi}_2}{\dot{\varphi}_1^2}\frac{\cos\varphi_3}{\alpha_2\tau_3} + B_3(U_3^2 + T_3^2 + W_3^2)\frac{\ddot{\varphi}_3}{\dot{\varphi}_1^2}\frac{\cos\varphi_2}{\alpha_3\tau_3} \tag{A.71}$$

f_{43_y} = y component of dimensionless bearing force at A_3

$$= -B_2U_2\frac{\tau_1\sin\varphi_3}{\alpha_2\tau_3} + B_2T_2\frac{\tau_{11}\sin\varphi_3}{\alpha_2\tau_3}$$

$$+ B_3U_3\left[\frac{\ddot{\varphi}_3}{\dot{\varphi}_1^2}\cos\varphi_3 - \left(\frac{\dot{\varphi}_3}{\dot{\varphi}_1}\right)^2\sin\varphi_3\right] - B_3T_3\left[\frac{\ddot{\varphi}_3}{\dot{\varphi}_1^2}\sin\varphi_3 + \left(\frac{\dot{\varphi}_3}{\dot{\varphi}_1}\right)^2\cos\varphi_3\right]$$

$$+ B_2(U_2^2 + T_2^2 + W_2^2)\frac{\ddot{\varphi}_2}{\dot{\varphi}_1^2}\frac{\sin\varphi_3}{\alpha_2\tau_3} + B_3(U_3^2 + T_3^2 + W_3^2)\frac{\ddot{\varphi}_3}{\dot{\varphi}_1^2}\frac{\sin\varphi_2}{\alpha_3\tau_3}$$

(A.72)

f_{S_x} = x component of dimensionless shaking force

$$= B_2\cos\varphi_1 + B_1U_1\cos\varphi_1 - B_1T_1\sin\varphi_1$$

$$+ B_2U_2\left[\frac{\ddot{\varphi}_2}{\dot{\varphi}_1^2}\sin\varphi_2 + \left(\frac{\dot{\varphi}_2}{\dot{\varphi}_1}\right)^2\cos\varphi_2\right] + B_2T_2\left[\frac{\ddot{\varphi}_2}{\dot{\varphi}_1^2}\cos\varphi_2 - \left(\frac{\dot{\varphi}_2}{\dot{\varphi}_1}\right)^2\sin\varphi_2\right]$$

$$+ B_3U_3\left[\frac{\ddot{\varphi}_3}{\dot{\varphi}_1^2}\sin\varphi_3 + \left(\frac{\dot{\varphi}_3}{\dot{\varphi}_1}\right)^2\cos\varphi_3\right] + B_3T_3\left[\frac{\ddot{\varphi}_3}{\dot{\varphi}_1^2}\cos\varphi_3 - \left(\frac{\dot{\varphi}_3}{\dot{\varphi}_1}\right)^2\sin\varphi_3\right]$$

(A.73)

f_{S_y} = y component of dimensionless shaking force

$$= B_2\sin\varphi_1 + B_1U_1\sin\varphi_1 + B_1T_1\cos\varphi_1$$

$$- B_2U_2\left[\frac{\ddot{\varphi}_2}{\dot{\varphi}_1^2}\cos\varphi_2 - \left(\frac{\dot{\varphi}_2}{\dot{\varphi}_1}\right)^2\sin\varphi_2\right] + B_2T_2\left[\frac{\ddot{\varphi}_2}{\dot{\varphi}_1^2}\sin\varphi_2 + \left(\frac{\dot{\varphi}_2}{\dot{\varphi}_1}\right)^2\cos\varphi_2\right]$$

$$- B_3U_3\left[\frac{\ddot{\varphi}_3}{\dot{\varphi}_1^2}\cos\varphi_3 - \left(\frac{\dot{\varphi}_3}{\dot{\varphi}_1}\right)^2\sin\varphi_3\right] + B_3T_3\left[\frac{\ddot{\varphi}_3}{\dot{\varphi}_1^2}\sin\varphi_3 + \left(\frac{\dot{\varphi}_3}{\dot{\varphi}_1}\right)^2\cos\varphi_3\right]$$

(A.74)

μ_{41} = dimensionless input moment

$$= B_2U_2\left[\frac{\ddot{\varphi}_2}{\dot{\varphi}_1^2}\tau_{11} + \left(\frac{\dot{\varphi}_2}{\dot{\varphi}_1}\right)^2\tau_1 - \frac{\tau_1\sin(\varphi_1-\varphi_3)}{\alpha_2\tau_3}\right]$$

$$+ B_2T_2\left[\frac{\ddot{\varphi}_2}{\dot{\varphi}_1^2}\tau_1 - \left(\frac{\dot{\varphi}_2}{\dot{\varphi}_1}\right)^2\tau_{11} + \frac{\tau_{11}\sin(\varphi_1-\varphi_3)}{\alpha_2\tau_3}\right]$$

$$+ B_2(U_2^2 + T_2^2 + W_2^2)\frac{\ddot{\varphi}_2}{\dot{\varphi}_1^2}\frac{\sin(\varphi_1-\varphi_3)}{\alpha_2\tau_3} + B_3(U_3^2 + T_3^2 + W_3^2)\frac{\ddot{\varphi}_3}{\dot{\varphi}_1^2}\frac{\tau_1}{\alpha_3\tau_3}\ .$$

(A.75)

4. Dimensionless Ground Bearing Forces and Shaking Force in Terms of the Mass Parameters u_3, t_3 and v_3 of Link 3 Only (Input Angular Velocity is Constant)

Since the single counterweight optimization problem is solved for the center of mass parameters u_3, t_3 and v_3 of link 3, the dimensionless ground bearing and shaking forces will now be rewritten as explicit functions of these parameters. With

$$u_3 = B_3 U_3 \qquad (A.76)$$

$$t_3 = B_3 T_3 \qquad (A.77)$$

$$v_3 = B_3(U_3^2 + T_3^2 + W_3^2), \qquad (A.78)$$

for definition, see equations (A.61)

one obtains

$$f_{41_x} = -(L_1 + L_2 v_3) \qquad (A.79)$$

$$f_{41_y} = -(L_3 + L_4 v_3) \qquad (A.80)$$

$$f_{43_x} = -(L_5 + L_6 u_3 + L_7 t_3 - L_2 v_3) \qquad (A.81)$$

$$f_{43_y} = -(L_8 - L_7 u_3 + L_6 t_3 - L_4 v_3) \qquad (A.82)$$

$$f_{S_x} = L_9 + L_6 u_3 + L_7 t_3 \qquad (A.83)$$

$$f_{S_y} = L_{10} - L_7 u_3 + L_6 t_3 , \qquad (A.84)$$

where

$$L_1 = B_2\cos\varphi_1 + B_1U_1\cos\varphi_1 - B_1T_1\sin\varphi_1$$
$$+ B_2U_2\left[\frac{\ddot{\varphi}_2}{\dot{\varphi}_1^2}\sin\varphi_2 + \left(\frac{\dot{\varphi}_2}{\dot{\varphi}_1}\right)^2\cos\varphi_2 - \frac{\tau_1\cos\varphi_3}{\alpha_2\tau_3}\right]$$
$$+ B_2T_2\left[\frac{\ddot{\varphi}_2}{\dot{\varphi}_1^2}\cos\varphi_2 - \left(\frac{\dot{\varphi}_2}{\dot{\varphi}_1}\right)^2\sin\varphi_2 + \frac{\tau_{11}\cos\varphi_3}{\alpha_2\tau_3}\right]$$
$$+ B_2(U_2^2 + T_2^2 + W_2^2)\frac{\ddot{\varphi}_2}{\dot{\varphi}_1^2}\frac{\cos\varphi_3}{\alpha_2\tau_3} \qquad \text{(A.85)}$$

$$L_2 = \frac{\ddot{\varphi}_3}{\dot{\varphi}_1^2}\frac{\cos\varphi_2}{\alpha_3\tau_3} \qquad \text{(A.86)}$$

$$L_3 = B_2\sin\varphi_1 + B_1U_1\sin\varphi_1 + B_1T_1\cos\varphi_1$$
$$- B_2U_2\left[\frac{\ddot{\varphi}_2}{\dot{\varphi}_1^2}\cos\varphi_2 - \left(\frac{\dot{\varphi}_2}{\dot{\varphi}_1}\right)^2\sin\varphi_2 + \frac{\tau_1\sin\varphi_3}{\alpha_2\tau_3}\right]$$
$$+ B_2T_2\left[\frac{\ddot{\varphi}_2}{\dot{\varphi}_1^2}\sin\varphi_2 + \left(\frac{\dot{\varphi}_2}{\dot{\varphi}_1}\right)^2\cos\varphi_2 + \frac{\tau_{11}\sin\varphi_3}{\alpha_2\tau_3}\right]$$
$$+ B_2(U_2^2 + T_2^2 + W_2^2)\frac{\ddot{\varphi}_2}{\dot{\varphi}_1^2}\frac{\sin\varphi_3}{\alpha_2\tau_3} \qquad \text{(A.87)}$$

$$L_4 = \frac{\ddot{\varphi}_3}{\dot{\varphi}_1^2} \frac{\sin\varphi_2}{\alpha_3 T_3} \tag{A.88}$$

$$L_5 = B_2 U_2 \frac{T_1 \cos\varphi_3}{\alpha_2 T_3} - B_2 T_2 \frac{T_{11} \cos\varphi_3}{\alpha_2 T_3} - B_2 (U_2^2 + T_2^2 + W_2^2) \frac{\ddot{\varphi}_2}{\dot{\varphi}_1^2} \frac{\cos\varphi_3}{\alpha_2 T_3} \tag{A.89}$$

$$L_6 = \frac{\ddot{\varphi}_3}{\dot{\varphi}_1^2} \sin\varphi_3 + \left(\frac{\dot{\varphi}_3}{\dot{\varphi}_1}\right)^2 \cos\varphi_3 \tag{A.90}$$

$$L_7 = \frac{\ddot{\varphi}_3}{\dot{\varphi}_1^2} \cos\varphi_3 - \left(\frac{\dot{\varphi}_3}{\dot{\varphi}_1}\right)^2 \sin\varphi_3 \tag{A.91}$$

$$L_8 = B_2 U_2 \frac{T_1 \sin\varphi_3}{\alpha_2 T_3} - B_2 T_2 \frac{T_{11} \sin\varphi_3}{\alpha_2 T_3} - B_2 (U_2^2 + T_2^2 + W_2^2) \frac{\ddot{\varphi}_2}{\dot{\varphi}_1^2} \frac{\sin\varphi_3}{\alpha_2 T_3} \tag{A.92}$$

$$L_9 = L_1 + L_5 \tag{A.93}$$

$$L_{10} = L_3 + L_8 \, . \tag{A.94}$$

5. Dimensionless Ground Bearing Forces and Shaking Force in Terms of the Mass Parameters u_1 and t_1 of Link 1 and u_3, t_3 and v_3 of Link 3 (Input Angular Velocity is Constant)

Since the two counterweight optimization problem is solved for the center of mass parameters u_1, t_1, u_3 and t_3 of links 1 and 3, respectively, for a predetermined value of v_3, the dimensionless ground bearing and shaking forces will now be rewritten as explicit functions of these parameters. With

$$\left.\begin{aligned} u_1 &= B_1 U_1 \\ t_1 &= B_1 T_1 \end{aligned}\right\} \text{ for definition, see equations (A.61)} \qquad \begin{matrix}(A.95)\\(A.96)\end{matrix}$$

in addition to equations (A.76) - (A.78), one obtains

$$f_{41_x} = -(N_1 + N_2 u_1 - N_3 t_1 + N_4 v_3) \qquad (A.97)$$

$$f_{41_y} = -(N_5 + N_3 u_1 + N_2 t_1 + N_6 v_3) \qquad (A.98)$$

$$f_{43_x} = -(N_7 + N_8 u_3 + N_9 t_3 - N_4 v_3) \qquad (A.99)$$

$$f_{43_y} = -(N_{10} - N_9 u_3 + N_8 t_3 - N_6 v_3) \qquad (A.100)$$

$$f_{S_x} = (N_{11} + N_2 u_1 - N_3 t_1 + N_8 u_3 + N_9 t_3) \qquad (A.101)$$

$$f_{S_y} = (N_{12} + N_3 u_1 + N_2 t_1 - N_9 u_3 + N_8 t_3) \qquad (A.102)$$

where

$$N_1 = B_2\cos\varphi_1 + B_2U_2\left[\frac{\ddot{\varphi}_2}{\dot{\varphi}_1^2}\sin\varphi_2 + \left(\frac{\dot{\varphi}_2}{\dot{\varphi}_1}\right)^2\cos\varphi_2 - \frac{\tau_1\cos\varphi_3}{\alpha_2\tau_3}\right]$$

$$+ B_2T_2\left[\frac{\ddot{\varphi}_2}{\dot{\varphi}_1^2}\cos\varphi_2 - \left(\frac{\dot{\varphi}_2}{\dot{\varphi}_1}\right)^2\sin\varphi_2 + \frac{\tau_{11}\cos\varphi_3}{\alpha_2\tau_3}\right]$$

$$+ B_2(U_2^2 + T_2^2 + W_2^2)\frac{\ddot{\varphi}_2}{\dot{\varphi}_1^2}\frac{\cos\varphi_3}{\alpha_2\tau_3} \qquad \text{(A.103)}$$

$$N_2 = \cos\varphi_1 \qquad \text{(A.104)}$$

$$N_3 = \sin\varphi_1 \qquad \text{(A.105)}$$

$$N_4 = \frac{\ddot{\varphi}_3}{\dot{\varphi}_1^2}\frac{\cos\varphi_2}{\alpha_3\tau_3} \qquad \text{(A.106)}$$

$$N_5 = B_2\sin\varphi_1 + B_2U_2\left[-\frac{\ddot{\varphi}_2}{\dot{\varphi}_1^2}\cos\varphi_2 + \left(\frac{\dot{\varphi}_2}{\dot{\varphi}_1}\right)^2\sin\varphi_2 - \frac{\tau_1\sin\varphi_3}{\alpha_2\tau_3}\right]$$

$$+ B_2T_2\left[\frac{\ddot{\varphi}_2}{\dot{\varphi}_1^2}\sin\varphi_2 + \left(\frac{\dot{\varphi}_2}{\dot{\varphi}_1}\right)^2\cos\varphi_2 + \frac{\tau_{11}\sin\varphi_3}{\alpha_2\tau_3}\right]$$

$$+ B_2(U_2^2 + T_2^2 + W_2^2)\frac{\ddot{\varphi}_2}{\dot{\varphi}_1^2}\frac{\sin\varphi_3}{\alpha_2\tau_3} \qquad \text{(A.107)}$$

$$N_6 = \frac{\ddot{\varphi}_3}{\dot{\varphi}_1^2} \frac{\sin\varphi_2}{\alpha_3 T_3} \tag{A.108}$$

$$N_7 = B_2U_2 \frac{T_1\cos\varphi_3}{\alpha_2 T_3} - B_2T_2 \frac{T_{11}\cos\varphi_3}{\alpha_2 T_3} - B_2(U_2^2 + T_2^2 + W_2^2)\frac{\ddot{\varphi}_2}{\dot{\varphi}_1^2} \frac{\cos\varphi_3}{\alpha_2 T_3} \tag{A.109}$$

$$N_8 = \frac{\ddot{\varphi}_3}{\dot{\varphi}_1^2} \sin\varphi_3 + \left(\frac{\dot{\varphi}_3}{\dot{\varphi}_1}\right)^2 \cos\varphi_3 \tag{A.110}$$

$$N_9 = \frac{\ddot{\varphi}_3}{\dot{\varphi}_1^2} \cos\varphi_3 - \left(\frac{\dot{\varphi}_3}{\dot{\varphi}_1}\right)^2 \sin\varphi_3 \tag{A.111}$$

$$N_{10} = B_2U_2 \frac{T_1\sin\varphi_3}{\alpha_2 T_3} - B_2T_2 \frac{T_{11}\sin\varphi_3}{\alpha_2 T_3} - B_2(U_2^2 + T_2^2 + W_2^2)\frac{\ddot{\varphi}_2}{\dot{\varphi}_1^2} \frac{\sin\varphi_3}{\alpha_2 T_3} \tag{A.112}$$

$$N_{11} = N_1 + N_7 \tag{A.113}$$

$$N_{12} = N_5 + N_{10} \cdot \tag{A.114}$$

6. Dimensionless Expressions for the Ground Bearing Forces and Input Moment for a Four-Bar Linkage of Standard Configuration (Input Angular Velocity is Constant)

This section of the appendix presents dimensionless expressions for the ground bearing forces and the input moment of a standard four-bar linkage configuration. This standard configuration, which has been introduced in [1,14], is shown again in Fig. A2: d_1 represents the width of the links as well as the radius at the pin joints (where applicable); h_1 stands for the thickness (normal to the mechanism plane) of the individual links.

To modify the dimensionless expressions for the ground bearing forces and input moment of equations (A.69) - (A.75) in terms of the link geometry of the above configuration, the following parameters are introduced as functions of the length of the input link a_1:

$$\left.\begin{aligned} \text{link length ratio:} \quad & \alpha_i = a_i/a_1 \\ \text{link width ratio:} \quad & \beta_1 = d_1/a_1 \\ \text{link thickness ratio:} \quad & \gamma_1 = h_1/d_1 \\ \text{position of link center of mass ratio:} \quad & \sigma_i = b_1/a_i = r_1/a_i \ . \end{aligned}\right\} \quad (A.115)$$

The standard configuration of Fig. A2 assumes that the center of mass of links 1 and 3 are located at the centers of the links, and that only the center of mass of link 2 is variable (i.e., the coupler may overhang either of the pivots A_1 or A_2). Thus, σ_2 remains variable while

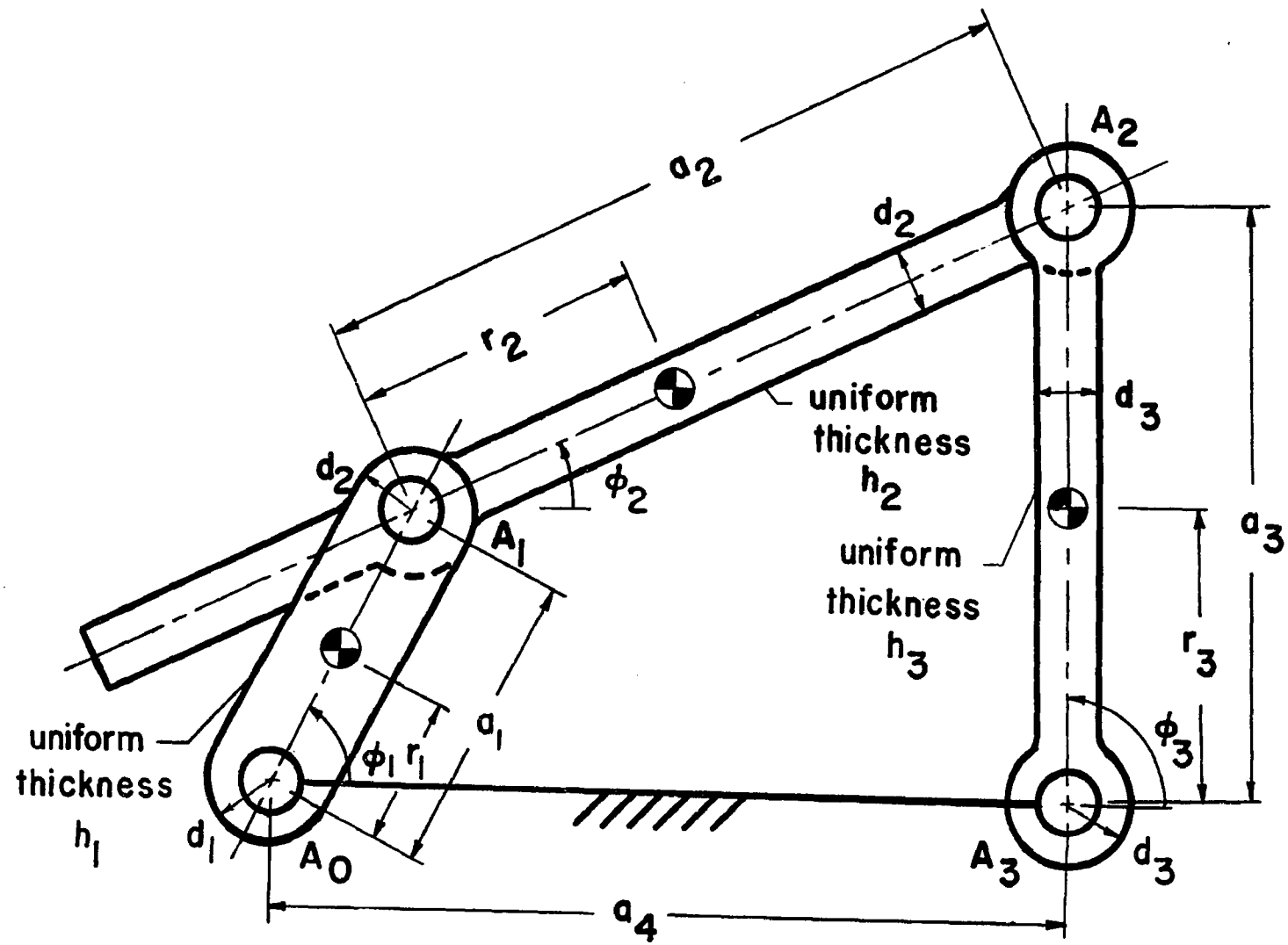

Fig. A2 Standard four-bar linkage configuration

$$\sigma_1 = \sigma_3 = \frac{1}{2} \, . \tag{A.116}$$

Since the link centers of mass lie on the line joining the pivots, certain expressions of equations (A.61) must be modified:

$$U_1 = \frac{b_1}{a_1} = \frac{r_1}{a_1} = \sigma_1 \alpha_1 \tag{A.117a}$$

$$T_1 = \frac{c_1}{a_1} = 0 \, . \tag{A.117b}$$

In addition, the link masses and the link moments of inertia (with respect to the individual link centers of mass) may be expressed according to [14] and equations (A.61) in the following manner, if one assumes that the mass density ρ is the same for all links:

$$m_1 = \rho a_1^3 B_1 \tag{A.118a}$$

$$m_2 = \rho a_1^3 B_2 \tag{A.118b}$$

$$m_3 = \rho a_1^3 B_3 \tag{A.118c}$$

$$\mathscr{I}_2 = m_2 \kappa_2^2 = \rho a_1^5 B_2 W_2^2 = \rho a_1^5 C_2 \tag{A.118d}$$

$$\mathscr{I}_3 = m_3 \kappa_3^2 = \rho a_1^5 B_3 W_3^2 = \rho a_1^5 C_3 \, , \tag{A.118e}$$

where the dimensionless B's and C's are as follows:

$$B_1 = \beta_1^2 \gamma_1 (\pi \beta_1 + 2) \quad \text{(not contained in [14], but simply obtained)} \tag{A.119a}$$

$$B_2 = \beta_2^2 \gamma_2 \left[V_2 + \alpha_2 + 2\beta_2 (\pi - 1) \right] \tag{A.119b}$$

$$B_3 = \beta_3^2\gamma_3\left[\alpha_3 + 2\beta_3(\pi - 1)\right] \tag{A.119c}$$

$$C_2 = \beta_2^2\gamma_2\left\{\frac{1}{12}\,V_2\left[\beta_2^2 + V_2^2 + 3(V_2 + 2\beta_2 + 2\sigma_2\alpha_2)^2\right]\right.$$
$$+ \frac{1}{12}\,(\alpha_2 - 2\beta_2)\left[(\alpha_2 - 2\beta_2)^2 + \beta_2^2 + 3\alpha_2^2(1 - 2\sigma_2)^2\right]$$
$$\left. + \pi\beta_2\left[\beta_2^2 + \alpha_2^2(2\sigma_2^2 - 2\sigma_2 + 1)\right]\right\} \tag{A.119d}$$

$$C_3 = \beta_3^2\gamma_3\left\{\frac{1}{12}\,(\alpha_3 - 2\beta_3)\left[(\alpha_3 - 2\beta_3)^2 + \beta_3^2\right] + \pi\beta_3(\beta_3^2 + \tfrac{1}{2}\alpha_3^2)\right\} \tag{A.119e}$$

and

$$V_2 = \sqrt{\alpha_2^2(1 - \sigma_2)^2 + (\alpha_2 - \beta_2)^2 - \alpha_2^2 + 2\alpha_2\beta_2\left[\pi - \sigma_2(2\pi - 3)\right]}$$
$$- \sigma_2\alpha_2 - \beta_2\,. \tag{A.119f}$$

Using equations (A.115) - (A.119) in equations (A.69) - (A.72) and (A.75), one obtains the following dimensionless forms for the ground bearing forces and input moment of the standard four-bar linkage configuration:

$$f_{14_x} = \left(\frac{B_1}{2} + B_2\right)\cos\varphi_1 + B_2\alpha_2\sigma_2\left[\frac{\ddot{\varphi}_2}{\dot{\varphi}_1^2}\sin\varphi_2 + \left(\frac{\dot{\varphi}_2}{\dot{\varphi}_1}\right)^2\cos\varphi_2 - \frac{\tau_1\cos\varphi_3}{\alpha_2\tau_3}\right]$$
$$+ (B_2\alpha_2^2\sigma_2^2 + C_2)\frac{\ddot{\varphi}_2}{\dot{\varphi}_1^2}\,\frac{\cos\varphi_3}{\alpha_2\tau_3} + \left(\frac{B_3\alpha_3^2}{4} + C_3\right)\frac{\ddot{\varphi}_3}{\dot{\varphi}_1^2}\,\frac{\cos\varphi_2}{\alpha_3\tau_3} \tag{A.120}$$

$$f_{14_y} = \left(\frac{B_1}{2} + B_2\right)\sin\varphi_1 - B_2\alpha_2\sigma_2\left[\frac{\ddot{\varphi}_2}{\dot{\varphi}_1^2}\cos\varphi_2 - \left(\frac{\dot{\varphi}_2}{\dot{\varphi}_1}\right)^2 \sin\varphi_2 + \frac{\tau_1\sin\varphi_3}{\alpha_2\tau_3}\right]$$

$$+ (B_2\alpha_2^2\sigma_2^2 + C_2)\frac{\ddot{\varphi}_2}{\dot{\varphi}_1^2}\frac{\sin\varphi_3}{\alpha_2\tau_3} + \left(\frac{B_3\alpha_3^2}{4} + C_3\right)\frac{\ddot{\varphi}_3}{\dot{\varphi}_1^2}\frac{\sin\varphi_2}{\alpha_3\tau_3} \qquad \text{(A.121)}$$

$$f_{34_x} = \frac{B_2\alpha_2\sigma_2\tau_1\cos\varphi_3}{\tau_3} + \frac{B_3\alpha_3}{2}\left[\frac{\ddot{\varphi}_3}{\dot{\varphi}_1^2}\sin\varphi_3 + \left(\frac{\dot{\varphi}_3}{\dot{\varphi}_1}\right)^2 \cos\varphi_3\right]$$

$$- (B_2\alpha_2^2\sigma_2^2 + C_2)\frac{\ddot{\varphi}_2}{\dot{\varphi}_1^2}\frac{\cos\varphi_3}{\alpha_2\tau_3} - \left(\frac{B_3\alpha_3^2}{4} + C_3\right)\frac{\ddot{\varphi}_3}{\dot{\varphi}_1^2}\frac{\cos\varphi_2}{\alpha_3\tau_3} \qquad \text{(A.122)}$$

$$f_{34_y} = \frac{B_2\alpha_2\sigma_2\tau_1\sin\varphi_3}{\tau_3} - \frac{B_3\alpha_3}{2}\left[\frac{\ddot{\varphi}_3}{\dot{\varphi}_1^2}\cos\varphi_3 - \left(\frac{\dot{\varphi}_3}{\dot{\varphi}_1}\right)^2 \sin\varphi_3\right]$$

$$- (B_2\alpha_2^2\sigma_2^2 + C_2)\frac{\ddot{\varphi}_2}{\dot{\varphi}_1^2}\frac{\sin\varphi_3}{\alpha_2\tau_3} - \left(\frac{B_3\alpha_3^2}{4} + C_3\right)\frac{\ddot{\varphi}_3}{\dot{\varphi}_1^2}\frac{\sin\varphi_2}{\alpha_3\tau_3} \qquad \text{(A.123)}$$

$$\mu_{14} = -B_2\alpha_2\sigma_2\left[\tau_{11}\frac{\ddot{\varphi}_2}{\dot{\varphi}_1^2} + \tau_1\left(\frac{\dot{\varphi}_2}{\dot{\varphi}_1}\right)^2 - \frac{\tau_1\sin(\varphi_1 - \varphi_3)}{\alpha_2\tau_3}\right]$$

$$- (B_2\alpha_2^2\sigma_2^2 + C_2)\frac{\ddot{\varphi}_2}{\dot{\varphi}_1^2}\frac{\sin(\varphi_1 - \varphi_3)}{\alpha_2\tau_3} - \left(\frac{B_3\alpha_3^2}{4} + C_3\right)\frac{\ddot{\varphi}_3}{\dot{\varphi}_1^2}\frac{\tau_1}{\alpha_3\tau_3} \; . \qquad \text{(A.124)}$$

APPENDIX B

PROOF OF BALANCEABILITY CRITERION (CONTOUR THEOREM) FOR PLANE MECHANISMS

It will now be proven that whenever a mechanism without axi-symmetric link groupings does not contain a contour from each link to the ground by way of revolutes only, it cannot be completely force balanced. This will be accomplished by showing that the replacement of terms with time dependent coefficients in the center of mass trajectory equation by terms with constant coefficients is not possible because the applicable loop equations cannot be solved simultaneously to produce this effect. The reason for the above lies in the fact that the coefficient matrix resulting from the loop equations is of lower rank than the number of terms with time dependent coefficients, and therefore, these terms are not linearly independent. The method of the general proof will first be demonstrated by means of an example.

1. Specific Mechanism Which Cannot Be Balanced

Fig. B1 shows a mechanism wherein no path can be found from link 4 to the ground by way of revolutes only, and according to the contour theorem, the mechanism cannot be fully force balanced. (Note that link 4 is surrounded by sliders.) The center of mass trajectory of this linkage can be written in the following form:

$$\bar{r}_S = \frac{1}{M}\Big[(m_1 r_1 e^{i\theta_1} + m_2 a_1)e^{i\varphi_1} + m_2 r_2 e^{i\theta_2} e^{i\varphi_2} + m_3 r_3 e^{i\theta_3} e^{i\varphi_3} + m_{4_T} r_4 e^{i\theta_4} e^{i\varphi_4} + m_{4_T} a_1'(t) e^{i\varphi_1} + m_3 a_8 \Big] , \tag{B.1}$$

where m_{4_T} represents the total mass of links 4, 5, 6 and 7. The relevant loop equations are given by:

$$\text{Loop 1:}\quad a_3'(t)e^{i\varphi_3} - a_2'(t)e^{i\varphi_2} = a_3 e^{i\varphi_3} - a_2 e^{i\varphi_2} - d_4 e^{i(\varphi_4+\gamma_4)} \tag{B.2}$$

$$\text{Loop 2:}\quad a_2'(t)e^{i\varphi_2} - a_1'(t)e^{i\varphi_1} = b_4 e^{i(\varphi_4+\alpha_4)} - a_1 e^{i\varphi_1} \tag{B.3}$$

$$\text{Loop 3:}\quad a_1'(t)e^{i\varphi_1} - a_3'(t)e^{i\varphi_3} = a_8 - a_4 e^{i\varphi_4} . \tag{B.4}$$

The trajectory equation (B.1) contains the term $m_{4_T} a_1'(t) e^{i\varphi_1}$, which has a time dependent coefficient. There is no simple way of replacing $a_1'(t)e^{i\varphi_1}$ by a sum of terms with constant coefficients with the help of the loop equations, and thus make it possible to balance the mechanism by setting all of the resultant constant coefficients of the $e^{i\varphi_j}$-terms equal to zero.

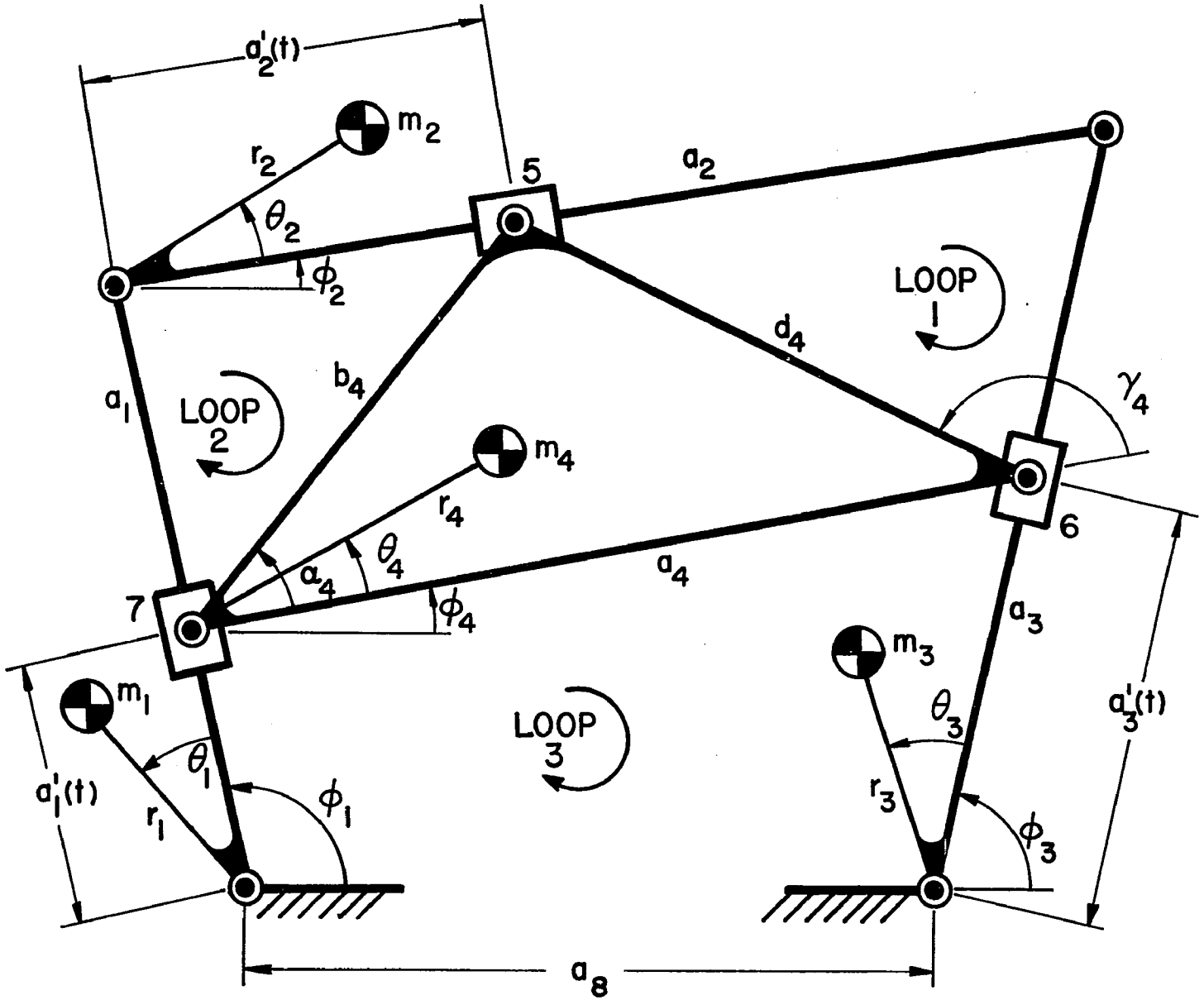

Fig. B1 Eight link mechanism

If one attempts to solve equations (B.2)-(B.4) simultaneously for the terms $a_1'(t)e^{i\varphi_1}$, $a_2'(t)e^{i\varphi_2}$, $a_3'(t)e^{i\varphi_3}$ as a function of the constant coefficient terms of the respective right-hand sides, the following coefficient matrix results after suitable ordering of terms:

$$\begin{bmatrix} 0 & -1 & 1 \\ -1 & 1 & 0 \\ 1 & 0 & -1 \end{bmatrix} . \qquad \text{(B.5)}$$

Since the above 3 x 3 matrix is only of rank 2, the aforementioned three terms are not linearly independent, and they cannot be solved for simultaneously. Thus, $a_1'(t)e^{i\varphi_1}$ cannot be replaced by a sum of terms with constant coefficients, and the mechanism cannot be balanced.

2. Generalization

The generalization of the contour theorem is also based on showing that whenever a loop equation contains more than one term with a time dependent coefficient, and one or more of the identical terms appear in the center of mass trajectory equation, the loop equations cannot be solved simultaneously for these terms in order to replace them in the trajectory equation with terms containing constant coefficients only. It will be demonstrated that under the above circumstances, these terms with time dependent coefficients are not linearly independent. To this end, it has been found advantageous to introduce the concepts of "surrounding" prismatic pairs, as well as "other" prismatic pairs, and to assign certain associated link lengths in a predetermined way.

A "surrounding" prismatic pair is associated with a "surrounded" link or group of links, and occurs whenever a loop equation unavoidably contains at least two sets of sliders, and thus there is no contour to the ground from any of the "surrounded" links by way of revolutes only. For example, in Fig. B2 links 3 and 4 together are surrounded by prismatic pairs 1 and 2, or link 3 alone is surrounded by prismatic pairs 2 and 3. (Note that in Fig. B1 there are three "surrounding" prismatic pairs.)

Whenever a loop equation which contains a "surrounded" link or a "surrounded" group of links is traced out, two time dependent terms of the form $a'_{\mu}(t)e^{i\varphi_{\mu}}$ will appear in the loop equation, one upon entering and one upon leaving

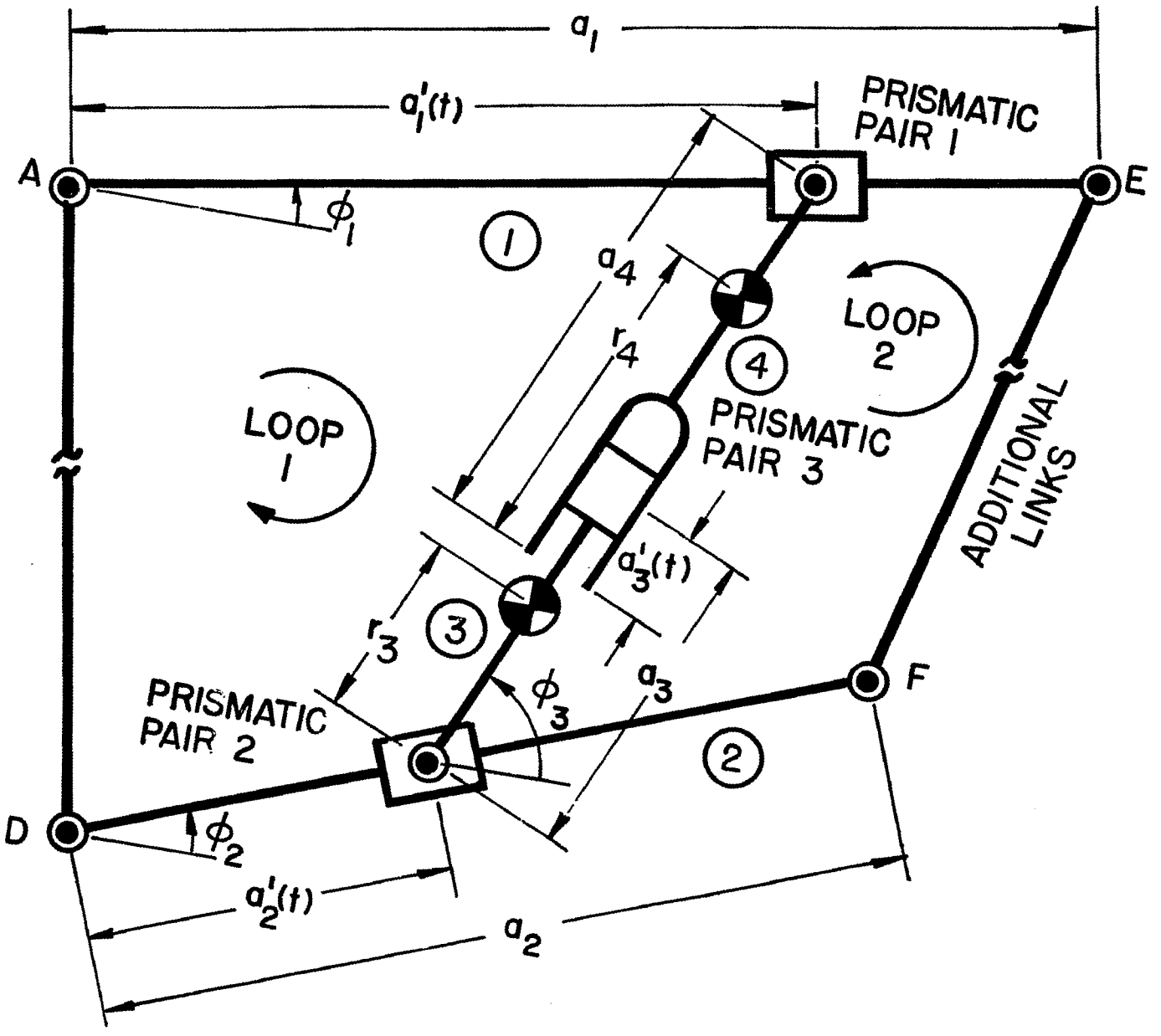

Fig. B2 Three-slider configuration for determination of sign convention

the associated "surrounding" prismatic pairs. For example, if links 3 and 4 of Fig. B2 are assumed to be the "surrounded" group, $a_1'(t)e^{i\varphi_1}$ occurs in the loop equation upon entering slider 1, and $a_2'(t)e^{i\varphi_2}$ occurs when leaving slider 2. Similarly, if link 3 is designated as the "surrounded" link, then $a_3'(t)e^{i\varphi_3}$ occurs upon entering and $a_2'(t)e^{i\varphi_2}$ upon leaving the "surrounded" group.

If one now chooses the $a_\mu'(t)$'s such that in each loop the terms $a_\mu'(t)e^{i\varphi_\mu}$ have a positive sign upon entering a "surrounding" prismatic pair and a negative sign upon leaving such a pair, one assures that these terms appear with alternate signs.

"Other" prismatic pairs are those which are not defined as "surrounding" pairs.

Consider Fig. B2 to clarify the above. Assuming that prismatic pairs 1 and 2 represent the "surrounding" ones, the center of mass trajectory with respect to point D for the combined links 3 and 4 may be written in the following way:

$$\bar{r} = \frac{1}{(m_3 + m_4)}\left[(m_3 + m_4)a_2'(t)e^{i\varphi_2} - m_4 a_3'(t)e^{i\varphi_3} + m_3 r_3 e^{i\varphi_3} + m_4(a_3 + r_4)e^{i\varphi_3}\right] . \qquad (B.6)$$

r_3 and r_4 represent the center of mass locations of the respective links. Equation (B.6) shows that the position of the center of mass of any link within a "surrounded" group, such as those of links 3 and 4, can be expressed with the help of only one term, i.e. $a_2'(t)e^{i\varphi_2}$, of the associated

"surrounding" prismatic pairs. The quantity $a_3'(t)e^{i\varphi_3}$ refers to the "other" prismatic pair. The $a_\mu'(t)$ terms are assigned in Fig. B2 in the previously agreed upon manner, and the resulting two loop equations appear with the desired sign alternation:

$$\text{Loop 1:}\quad \underbrace{a_1'(t)e^{i\varphi_1} - a_2'(t)e^{i\varphi_2}}_{\text{"surrounding" prismatic pairs}} + \underbrace{a_3'(t)e^{i\varphi_3}}_{\text{"other" prismatic pair}} = (a_3 + a_4)e^{i\varphi_3} - \overline{DA} \qquad \text{(B.7)}$$

$$\text{Loop 2:}\quad \underbrace{a_1'(t)e^{i\varphi_1} - a_2'(t)e^{i\varphi_2}}_{\text{"surrounding" prismatic pairs}} + \underbrace{a_3'(t)e^{i\varphi_3}}_{\text{"other" prismatic pair}} = a_1e^{i\varphi_1} - a_2e^{i\varphi_2} + (a_3 + a_4)e^{i\varphi_3} - \overline{FE} \qquad \text{(B.8)}$$

Assume that an arbitrary n-linked mechanism without axi-symmetric links contains g groups of links, each "surrounded" by an arbitrary number of prismatic pairs (p_g). The center of mass trajectory equation will then appear in the following form if the "surrounding" and "other" prismatic pairs are separated in the same manner as in equation (B.6):

$$\bar{r}_S = \frac{1}{\mathcal{M}}\left\{\sum_{j=1}^{n-1}\left[\left(m_j r_j e^{i\theta_j} + \sum_{k=1}^{k^*}(mhe^{i\alpha})_{kj}\right)e^{i\varphi_j} + \underbrace{\sum_{\mu=1}^{g}(ma'(t)e^{i\beta})_{\mu j}e^{i\varphi_j}}_{\text{(contains "surrounding" prismatic pairs only)}} + \underbrace{\sum_{\mu=g+1}^{\mu^*}(ma'(t)e^{i\beta})_{\mu j}e^{i\varphi_j}}_{\text{(contains "other" prismatic pairs)}}\right] + \bar{d}\right\}. \qquad \text{(B.9)}$$

Note that for each of the g groups of "surrounded" links, there will be only one term containing the factor $a'(t)e^{i\beta}e^{i\varphi}$, and this term is due to one of the p_g terms with time dependent coefficients of one of the p_g "surrounding" sliders of the particular group. This means that a specific "surrounded" group is always entered by way of a single "surrounding" slider when describing its center of mass trajectories.

While it may be possible to eliminate some of the terms with time dependent coefficients due to the "other" prismatic pairs from the center of mass trajectory equation (if there is only one prismatic pair in a loop), it will now be shown that it is never possible to eliminate terms with time dependent coefficients due to "surrounding" prismatic pairs. This will be accomplished by proving that the p_μ terms with time dependent coefficients of the μ^{th} "surrounded" group are <u>not</u> linearly independent, and therefore, in any simultaneous solution of the system of loop equations, one of them will have to be expressed in terms of another in addition to terms with time dependent coefficients due to "other" prismatic pairs, if present. To this end, the loop equations are divided into two separate sets, one of which contains all possible loop equations, i.e. $p_\mu(p_\mu - 1)/2$ equations, referring to the p_μ "surrounding" sliders of the μ^{th} "surrounded" group. The second set contains the L possible remaining mechanism loop equations, and by definition of the first set, none of the above p_μ terms appear in it. With the agreed upon sign convention used in the first set, the mechanism loop equations appear in the following way:

$$(a_1'(t)e^{i\beta_1})e^{i\varphi_1} - (a_2'(t)e^{i\beta_2})e^{i\varphi_2} + \sum_{j=1}^{n-1} a_{1j}'(t)e^{i(\beta_{1j}+\varphi_j)} = -\sum_{j=1}^{n} h_{1j}e^{i(\alpha_{1j}+\varphi_j)}$$

$$(a_1'(t)e^{i\beta_1})e^{i\varphi_1} - (a_3'(t)e^{i\beta_3})e^{i\varphi_3} + \sum_{j=1}^{n-1} a_{2j}'(t)e^{i(\beta_{2j}+\varphi_j)} = -\sum_{j=1}^{n} h_{2j}e^{i(\alpha_{2j}+\varphi_j)}$$

$$\vdots$$

$$(a_1'(t)e^{i\beta_1})e^{i\varphi_1} - (a_{p_\mu}'(t)e^{i\beta_{p_\mu}})e^{i\varphi_{p_\mu}} + \sum_{j=1}^{n-1} a_{p_\mu-1,j}'(t)e^{i(\beta_{p_\mu-1,j}+\varphi_j)} = -\sum_{j=1}^{n} h_{p_\mu-1,j}e^{i(\alpha_{p_\mu-1,j}+\varphi_j)}$$

$$(a_2'(t)e^{i\beta_2})e^{i\varphi_2} - (a_3'(t)e^{i\beta_3})e^{i\varphi_3} + \sum_{j=1}^{n-1} a_{p_\mu j}'(t)e^{i(\beta_{p_\mu j}+\varphi_j)} = -\sum_{j=1}^{n} h_{p_\mu j}e^{i(\alpha_{p_\mu j}+\varphi_j)}$$

$$\vdots$$

$$(a_2'(t)e^{i\beta_2})e^{i\varphi_2} - (a_{p_\mu}'(t)e^{i\beta_{p_\mu}})e^{i\varphi_{p_\mu}} + \sum_{j=1}^{n-1} a_{2p_\mu-3,j}'(t)e^{i(\beta_{2p_\mu-3,j}+\varphi_j)} = -\sum_{j=1}^{n} h_{2p_\mu-3,j}e^{i(\alpha_{2p_\mu-3,j}+\varphi_j)}$$

$$\vdots$$

Terms due to "surrounding" prismatic pairs | Terms due to "other" prismatic pairs | Constant coefficient terms

Set 1

$$\vdots$$

$$\sum_{j=1}^{n-1} a_{\lambda j}'(t)e^{i(\beta_{\lambda j}+\varphi_j)} = -\sum_{j=1}^{n} h_{\lambda j}e^{i(\alpha_{\lambda j}+\varphi_j)}$$

$$\vdots$$

Time dependent terms of set 2—they do not contain "surrounding" pairs of set 1.

$$\vdots$$

$$0 = -\sum_{j=1}^{n} h_{Lj}e^{i(\alpha_{Lj}+\varphi_j)}$$

Set 2

(B.10)

The scheme of set 1 is continued without repeating a previously stated combination, producing a pattern of alternating signs for the terms with time dependent coefficients associated with the "surrounding" prismatic pairs of the group considered.* Terms of the type $\sum_{j=1}^{n-1} a_{rj}(t)e^{i(\beta_{rj}+\varphi_j)}$ are due to the "other" prismatic pairs, which may appear in the r^{th} loop equation of the first set.

The second set of loop equations consists of equations with and without time dependent coefficients. Terms with time dependent coefficients are of the form $\sum_{j=1}^{n-1} a_{\lambda j}(t)e^{i(\beta_{\lambda j}+\varphi_j)}$. These represent all prismatic pairs in the λ^{th} loop equation, but do not contain, as stated before, any terms due to the "surrounding" sliders of the first set of loop equations.

The terms with constant coefficients are represented in both sets by terms of the type $\sum_{j=1}^{n} h_{rj}e^{i(\alpha_{rj}+\varphi_j)}$. There are $p_\mu(p_\mu - 1)/2$ such terms in the first set and L such terms in the second.

To show that the p_μ terms due to the p_μ "surrounding" sliders are <u>not</u> linearly independent, it will now be proven that the rank of the submatrix due to these terms is less than p_μ. The submatrix associated with the μ^{th} group of "surrounding" sliders can be written as follows:

---

*While more than one independent loop equation may contain a given set of two sliders, only one is necessary to determine the rank of the coefficient submatrix corresponding to the "surrounding" sliders (no linearly independent rows would be added).

$$
\left[\begin{array}{ccccccc}
1 & -1 & 0 & 0 & 0 \ldots & 0 & 0 \\
1 & 0 & -1 & 0 & 0 \ldots & 0 & 0 \\
1 & 0 & 0 & -1 & 0 \ldots & 0 & 0 \\
\vdots & \vdots & \vdots & \vdots & \vdots & \vdots & \vdots \\
1 & 0 & 0 & 0 & 0 \ldots & 0 & -1 \\
0 & 1 & -1 & 0 & 0 \ldots & 0 & 0 \\
0 & 1 & 0 & -1 & 0 \ldots & 0 & 0 \\
0 & 1 & 0 & 0 & -1 \ldots & 0 & 0 \\
\vdots & \vdots & \vdots & \vdots & \vdots & \vdots & \vdots \\
0 & 1 & 0 & 0 & 0 \ldots & 0 & -1 \\
0 & 0 & 1 & -1 & 0 \ldots & 0 & 0 \\
0 & 0 & 1 & 0 & -1 \ldots & 0 & 0 \\
\vdots & \vdots & \vdots & \vdots & \vdots & \vdots & \vdots \\
0 & 0 & 1 & 0 & 0 \ldots & 0 & -1 \\
\vdots & \vdots & \vdots & \vdots & \vdots & \vdots & \vdots \\
0 & 0 & 0 & 0 & 0 \ldots & 1 & -1 \\
0 & 0 & 0 & 0 & 0 \ldots & 0 & 0 \\
\vdots & \vdots & \vdots & \vdots & \vdots & \vdots & \vdots \\
0 & 0 & 0 & 0 & 0 \ldots & 0 & 0
\end{array}\right]
$$

rows due to first set of loop equations

rows due to second set of loop equations

(B.11)

This submatrix with p_μ columns can be transformed by successively adding the second, third, ..., and $p_\mu{}^{th}$ columns to the first column. In this manner, the first column will only contain zero elements. Accordingly, the p_μ columns are <u>not</u> linearly independent, and the submatrix is of rank lower than p_μ. Similar proofs are readily obtained for the terms with time dependent coefficients arising from the "surrounding" sliders of any of the other g - 1 "surrounded" groups. Because

of the above, the complete system of loop equations, i.e. equations (B.10), cannot be solved for any of the terms with time dependent coefficients in terms of constant coefficients only, if these terms are associated with loops containing more than one prismatic pair. This applies equally to terms with time dependent coefficients arising from "surrounding", as well as "other" prismatic pairs. Under these circumstances, the centers of mass of the associated mechanisms cannot be made stationary, and the contour theorem is proven.

APPENDIX C

EXAMPLE CONCERNING THE THEORETICAL POSSIBILITY OF FULL FORCE BALANCING WITH LESS THAN n/2 COUNTERWEIGHTS

Fig. C1 represents a six-bar linkage which has been fully force balanced in [2] according to the Method of Linearly Independent Vectors by attaching counterweights to links 1, 3 and 5. It will now be shown that it is theoretically possible to obtain full force balance by mass rearrangements confined to links 2 and 4 (which are not attached to the ground). This leads to the related groups of unknowns m_2, $m_2r_2\cos\theta_2$, $m_2r_2\sin\theta_2$, and m_4, $m_4r_4\cos\theta_4$, $m_4r_4\sin\theta_4$. When $e^{i\varphi_1}$ and $e^{i\varphi_5}$ are eliminated by way of the loop equations from the center of mass trajectory equation (16) of [2], and the result is written in the matrix form of equation (2.13), one obtains:

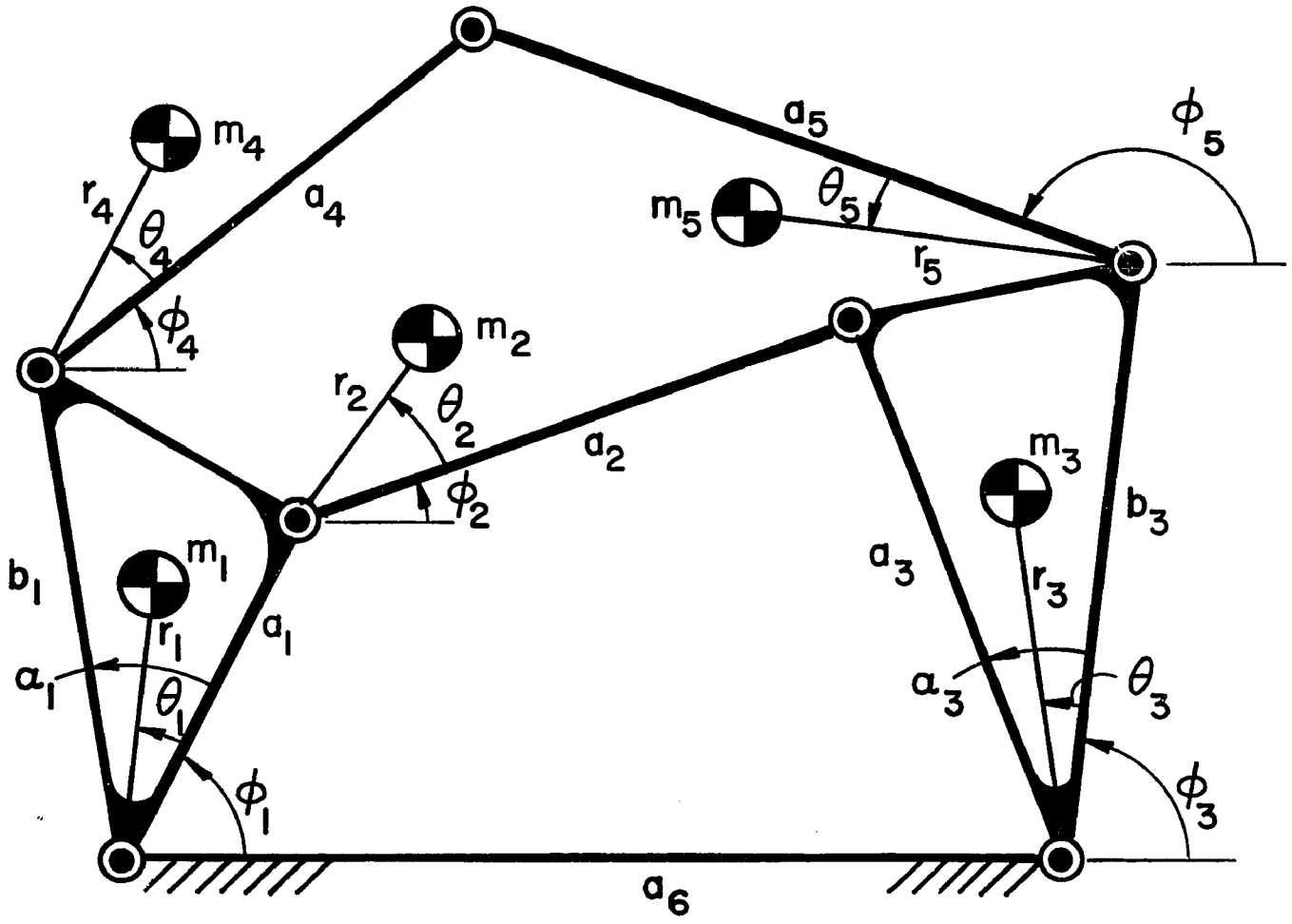

Fig. C1 Six-bar linkage with arbitrary link mass distribution [2]

$$\begin{bmatrix} 1 & 0 & 0 & 0 & -a_2 & -a_2b_1\cos\alpha_1/a_1 \\ 0 & 1 & 0 & 0 & 0 & -a_2b_1\sin\alpha_1/a_1 \\ 0 & 0 & 1 & 0 & 0 & 0 \\ 0 & 0 & 0 & 1 & 0 & 0 \\ 0 & 0 & 0 & 0 & a_3\cos\alpha_3 & b_1a_3\cos(\alpha_1+\alpha_3)/a_1 \\ 0 & 0 & 0 & 0 & a_3\sin\alpha_3 & b_1a_3\sin(\alpha_1+\alpha_3)/a_1 \end{bmatrix} \begin{bmatrix} m_2r_2\cos\theta_2 \\ m_2r_2\sin\theta_2 \\ m_4r_4\cos\theta_4 \\ m_4r_4\sin\theta_4 \\ m_2 \\ m_4 \end{bmatrix} \qquad (C.1)$$

$$= \begin{bmatrix} a_2m_1r_1\cos\theta_1/a_1 + b_1a_2m_5r_5\cos(\theta_5+\alpha_1)/a_1a_5 \\ a_2m_1r_1\sin\theta_1/a_1 + b_1a_2m_5r_5\sin(\theta_5+\alpha_1)/a_1a_5 \\ -a_4m_5r_5\cos\theta_5/a_5 \\ -a_4m_5r_5\sin\theta_5/a_5 \\ -m_5b_3 - m_3r_3\cos\theta_3 - a_3m_1r_1\cos(\theta_1+\alpha_3)/a_1 - a_3b_1m_5r_5\cos(\theta_5+\alpha_1+\alpha_3)/a_1a_5 + b_3m_5r_5\cos\theta_5/a_5 \\ - m_3r_3\sin\theta_3 - a_3m_1r_1\sin(\theta_1+\alpha_3)/a_1 - a_3b_1m_5r_5\sin(\theta_5+\alpha_1+\alpha_3)/a_1a_5 + b_3m_5r_5\sin\theta_5/a_5 \end{bmatrix}$$

For the above coefficient matrix

$$\mathscr{D} = a_3^2 b_1 \sin\alpha_1 / a_1 \quad . \tag{C.2}$$

Hence, the matrix is nonsingular (unless $\alpha_1 = 0$), and the balancing equations can be solved for the designated unknowns.

If links 2 and 5, which again are not attached to the ground, are chosen for the mass rearrangements, equation (2.14) will be of the type

$$\mathscr{D} = -a_3 b_3 \sin\alpha_3 \quad . \tag{C.3}$$

Again, since the matrix is nonsingular (unless $\alpha_3 = 0$), the balancing equations can be solved for the unknowns m_2, $m_2 r_2 \cos\theta_2$, $m_2 r_2 \sin\theta_2$, m_5, $m_5 r_5 \cos\theta_5$, and $m_5 r_5 \sin\theta_5$.

Finally, if links 4 and 5 are chosen for the mass rearrangements, equation (2.14) becomes

$$\mathscr{D} = 0 \ , \tag{C.4}$$

and the mechanism cannot be force balanced with counterweights on links 4 and 5 only, regardless of α_1 and α_3. (This is due to the fact that the y-component of the appropriate balancing equation does not contain m_4 and m_5. Thus, the coefficient matrix will contain a row of zeroes.)

APPENDIX D

PROOF THAT J_8 AND J_9 ARE NONZERO POSITIVE QUANTITIES AND THAT J_9 IS LARGER THAN J_8

The denominator of equation (3.14d) for J_8 can be rewritten with the help of equation (3.12) and certain trigonometric identities as follows:

$$J_1\cos^2\Theta + J_2\sin^2\Theta + 2J_3\sin\Theta\cos\Theta = \frac{1}{2}\left[J_1 + J_2 + \sqrt{(J_1 - J_2)^2 + 4J_3^2}\right] . \tag{D.1}$$

Since for unbalanced mechanisms, $J_1 + J_2 > 0$ (see equations (3.6a) and (3.6b)), this expression, and hence J_8, is proven to be a nonzero positive quantity.

In order to demonstrate that $J_9 > 0$, the denominator of equation (3.14e) is similarly rewritten:

$$J_1\sin^2\Theta + J_2\cos^2\Theta - 2J_3\sin\Theta\cos\Theta = \frac{1}{2}\left[J_1 + J_2 - \sqrt{(J_1 - J_2)^2 + 4J_3^2}\right] . \tag{D.2}$$

Since $J_1 + J_2 > 0$ (for unbalanced mechanisms), it is sufficient to show that

$$(J_1 + J_2)^2 > (J_1 - J_2)^2 + 4J_3^2 \tag{D.3}$$

in order to prove that $J_9 > 0$.

By adding and subtracting $2J_1J_2$, the right-hand side of inequality (D.3) may be written in the following manner:

$$(J_1 - J_2)^2 + 4J_3^2 = (J_1 + J_2)^2 + 4(J_3^2 - J_1J_2) . \tag{D.4}$$

Inequality (D.3) may now be rewritten:

$$(J_1 + J_2)^2 > (J_1 + J_2)^2 + 4(J_3^2 - J_1J_2) \ . \qquad (D.5)$$

The above can only hold true if $J_3^2 - J_1J_2$ is a negative quantity. Since this point has been proven with the help of inequalities (3.9) and (3.10), $J_9 > 0$.

Inspection of the right-hand sides of equations (D.1) and (D.2) shows, in light of the above, that J_9 is larger than J_8.

APPENDIX E

SOLUTION OF OPTIMIZATION EQUATIONS FOR SINGLE COUNTERWEIGHT PROBLEM

The method of solution of the optimization equations (4.16) - (4.20) will now be presented. They are rewritten below for convenience:

$$K_{11} + 2K_8 v_3 + K_9 v_3^2 = 2\pi q_1^2 f_{41_{RMS_u}}^2 \tag{E.1}$$

$$K_{12} + K_2 u_3^2 + K_2 t_3^2 + K_9 v_3^2 + 2K_6 u_3 + 2K_3 t_3 - 2K_{10} v_3 + 2K_7 u_3 v_3 - 2K_4 t_3 v_3 = 2\pi q_2^2 f_{43_{RMS_u}}^2 \tag{E.2}$$

$$K_1 + K_2 t_3 + \lambda_2 (K_3 + K_2 t_3 - K_4 v_3) = 0 \tag{E.3}$$

$$K_5 + K_2 u_3 + \lambda_2 (K_6 + K_2 u_3 + K_7 v_3) = 0 \tag{E.4}$$

$$\lambda_1 (K_8 + K_9 v_3) - \lambda_2 (K_{10} - K_7 u_3 + K_4 t_3 - K_9 v_3) = 0. \tag{E.5}$$

Equation (E.1) may be solved for v_3.

$$v_3^{(1)} = \frac{-K_8 + \sqrt{K_8^2 - K_9 (K_{11} - 2\pi q_1^2 f_{41_{RMS_u}}^2)}}{K_9} \tag{E.6a}$$

$$v_3^{(2)} = \frac{-K_8 - \sqrt{K_8^2 - K_9 (K_{11} - 2\pi q_1^2 f_{41_{RMS_u}}^2)}}{K_9} . \tag{E.6b}$$

Now solve equation (E.3) for λ_2.

$$\lambda_2^{(i)} = \frac{-(K_1 + K_2 t_3)}{K_3 + K_2 t_3 - K_4 v_3^{(i)}} , \qquad (i=1,2) . \qquad (E.7)$$

This furnishes an expression for λ_2 in terms of the unknown t_3.

λ_1 may be determined by substituting equation (E.7) into equation (E.5). Thus:

$$\lambda_1^{(i)} = \frac{-(K_{10} - K_7 u_3 + K_4 t_3 - K_9 v_3^{(i)})(K_1 + K_2 t_3)}{(K_8 + K_9 v_3^{(i)})(K_3 + K_2 t_3 - K_4 v_3^{(i)})} \qquad (E.8)$$

$$(i=1,2) .$$

Substitution of equation (E.7) into equation (E.4) yields an equation in terms of the unknowns t_3 and u_3.

$$K_5 + K_2 u_3 - (K_6 + K_2 u_3 + K_7 v_3^{(i)}) \frac{(K_1 + K_2 t_3)}{K_3 + K_2 t_3 - K_4 v_3^{(i)}} = 0 . \qquad (E.9)$$

This can be rewritten as follows:

$$(K_3 K_5 - K_4 K_5 v_3^{(i)} - K_1 K_6 - K_1 K_7 v_3^{(i)}) + (K_2 K_5 - K_2 K_6 - K_2 K_7 v_3^{(i)}) t_3 + (K_2 K_3 - K_1 K_2 - K_2 K_4 v_3^{(i)}) u_3 = 0 . \qquad (E.10)$$

Let

$$A_1^{(i)} = K_3 K_5 - K_4 K_5 v_3^{(i)} - K_1 K_6 - K_1 K_7 v_3^{(i)} \qquad (E.11a)$$

$$A_2^{(i)} = K_2K_5 - K_2K_6 - K_2K_7v_3^{(i)} \qquad \text{(E.11b)}$$

$$A_3^{(i)} = K_2K_3 - K_1K_2 - K_2K_4v_3^{(i)} \qquad \text{(E.11c)}$$

$$(i=1,2) .$$

With equations (E.11), equation (E.10) becomes

$$A_1^{(i)} + A_2^{(i)}t_3 + A_3^{(i)}u_3 = 0 . \qquad \text{(E.12)}$$

Equations (E.2) and (E.12) are two equations in terms of t_3 and u_3. Solving equation (E.12) for u_3 in terms of t_3, one obtains

$$u_3 = \frac{-(A_1^{(i)} + A_2^{(i)}t_3)}{A_3^{(i)}} . \qquad \text{(E.13)}$$

Now substitute equation (E.13) into equation (E.2). Thus

$$(K_{12} + K_9v_3^{(i)^2} - 2K_{10}v_3^{(i)}) + K_2\frac{(A_1^{(i)} + A_2^{(i)}t_3)^2}{A_3^{(i)^2}} + K_2t_3^2$$

$$- \frac{2K_6(A_1^{(i)} + A_2^{(i)}t_3)}{A_3^{(i)}} + 2K_3t_3 - 2K_7v_3^{(i)}\frac{(A_1^{(i)} + A_2^{(i)}t_3)}{A_3^{(i)}}$$

$$- 2K_4v_3^{(i)}t_3 = 2\pi q_2^2 f_{43}^2{}_{RMS_u} . \qquad \text{(E.14)}$$

Expanding and collecting like terms yields

$$(K_{12} + K_9 v_3^{(i)2} - 2K_{10} v_3^{(i)} - 2\pi q_2^2 f_{43_{RMS_u}}^2 + \frac{A_1^{(i)2}}{A_3^{(i)2}} K_2$$

$$- 2K_6 \frac{A_1^{(i)}}{A_3^{(i)}} - 2K_7 v_3^{(i)} \frac{A_1^{(i)}}{A_3^{(i)}}) + 2(K_2 \frac{A_1^{(i)} A_2^{(i)}}{A_3^{(i)2}} - K_6 \frac{A_2^{(i)}}{A_3^{(i)}}$$

$$+ K_3 - K_7 v_3^{(i)} \frac{A_2^{(i)}}{A_3^{(i)}} - K_4 v_3^{(i)}) t_3 + K_2 (\frac{A_2^{(i)2}}{A_3^{(i)2}} + 1) t_3^2 = 0 \qquad \text{(E.15)}$$

$$(i=1,2) .$$

Equation (E.15) is a quadratic equation whose solution is

$$t_3^{(i,1)} = \frac{-H_2^{(i)} + \sqrt{H_2^{(i)2} - H_1^{(i)} H_3^{(i)}}}{H_3^{(i)}} \qquad (i=1,2) \qquad \text{(E.16a)}$$

$$t_3^{(i,2)} = \frac{-H_2^{(i)} - \sqrt{H_2^{(i)2} - H_1^{(i)} H_3^{(i)}}}{H_3^{(i)}} \qquad (i=1,2) , \qquad \text{(E.16b)}$$

where

$$H_1^{(i)} = K_{12} + K_9 v_3^{(i)^2} - 2K_{10} v_3^{(i)} - 2\pi q_2^2 f_{43_{RMS_u}}^2 + \frac{A_1^{(i)^2}}{A_3^{(i)^2}} K_2$$

$$- 2\frac{A_1^{(i)}}{A_3^{(i)}} (K_6 + K_7 v_3^{(i)}) \qquad \text{(E.17a)}$$

$$H_2^{(i)} = K_2 \frac{A_1^{(i)} A_2^{(i)}}{A_3^{(i)^2}} - (K_6 + K_7 v_3^{(i)}) \frac{A_2^{(i)}}{A_3^{(i)}} + K_3 - K_4 v_3^{(i)} \qquad \text{(E.17b)}$$

$$H_3^{(i)} = \left(\frac{A_2^{(i)^2}}{A_3^{(i)^2}} + 1 \right) K_2 \qquad \text{(E.17c)}$$

$$(i=1,2) \ .$$

Substitution of equations (E.16) into equation (E.13) will then furnish the values for u_3. Therefore, equations (E.6), (E.7), (E.8), (E.13) and (E.16) represent the solution to the problem.

APPENDIX F

PROOF OF THE EXISTENCE OF A MINIMUM FOR THE SINGLE COUNTERWEIGHT OPTIMIZATION PROBLEM

It will now be shown that two of the four extrema found in Section IVB are minima. This will be accomplished by way of the following theorem:

If a set is closed and bounded, and a function is continuous on that set, then the function takes a minimum and a maximum somewhere on that set [4].

In the present case, the function under consideration is represented by the RMS shaking force, whose value must be minimized in such a way that the prescribed magnitudes of the RMS bearing forces are satisfied. The set of points under consideration are those points which satisfy the constraint equations. Since the RMS shaking force is continuous everywhere, one only needs to show that all points which satisfy the constraint equations represent a closed and bounded set to prove that the above theorem is applicable.

To prove this point, one proceeds in the following manner: All t_3, u_3, and v_3 which satisfy the constraint equations simultaneously, must lie on their intersections. Equations (4.16) and (4.17) give the constraint equations:

$$K_{11} + 2K_8 v_3 + K_9 v_3^2 = 2\pi q_1^2 f_{41_{RMS_u}}^2 \qquad (F.1)$$

and

$$K_{12} + K_2 u_3^2 + K_2 t_3^2 + K_9 v_3^2 + 2K_6 u_3 + 2K_3 t_3 - 2K_{10} v_3$$

$$+ 2K_7 u_3 v_3 - 2K_4 t_3 v_3 = 2\pi q_2^2 \, f_{43_{RMS_u}}^2 \, . \qquad (F.2)$$

Since equation (F.1) may readily be solved for $v_3^{(i)}$ (i=1,2), this parameter may be considered known in equation (F.2). Under these circumstances, equation (F.2) represents the equation of the intersection of the constraint equations. When this expression is rearranged to read

$$\left[u_3 + \frac{K_6 + K_7 v_3^{(i)}}{K_2}\right]^2 + \left[t_3 + \frac{K_3 - K_4 v_3^{(i)}}{K_2}\right]^2$$

$$= \left\{ \frac{2\pi q_2^2 \, f_{43_{RMS_u}}^2 - K_{12} - K_9 v_3^{(i)^2} + 2K_{10} v_3^{(i)}}{K_2} \right.$$

$$\left. + \left[\frac{K_6 + K_7 v_3^{(i)}}{K_2}\right]^2 + \left[\frac{K_3 - K_4 v_3^{(i)}}{K_2}\right]^2 \right\} \quad (i=1,2), \qquad (F.3)$$

one may show that one is dealing with the equations of the circumferences of two different offset circles in the u_3, t_3 coordinate system (one each for $v_3^{(1)}$ and $v_3^{(2)}$). Since the circumferences of circles represent closed and bounded sets, the existence of one maximum and one minimum per circumference is assured.

APPENDIX G

DESIGN OF COUNTERWEIGHTS

The present appendix will first describe the relationship of the optimum mass parameters u_i, t_i and v_i, which are the results of the optimization process, to the parameters of the already existing link and of the counterweight which is to be designed. Design equations are then developed for the case when u_i, t_i and v_i are prescribed and must be physically realized, as well as when only u_i and t_i are given. Finally, these counterweight design equations are adapted to the standard four-bar linkage configuration, which was introduced in [14], and is also described in Appendix A.

1. Relationship of Optimum Mass Parameters to Existing Link and Counterweight

Since the optimum mass parameters u_i, t_i and v_i (i=1,3) refer to the mass properties which the total link must have in order to realize the optimization, the following relationships between them and the parameters of the original link and the counterweight must hold (see Fig. G1):†

$$u_i = B_i^o U_i^o + B_i^* U_i^* \tag{G.1}$$

$$t_i = B_i^o T_i^o + B_i^* T_i^* \tag{G.2}$$

$$v_i = B_i^o (U_i^{o2} + T_i^{o2} + W_i^{o2}) + B_i^* (U_i^{*2} + T_i^{*2} + W_i^{*2}) \tag{G.3}$$

$$(i=1,3)$$

where

$$u_i = B_i U_i \tag{G.4}$$

$$t_i = B_i T_i \tag{G.5}$$

$$v_i = B_i (U_i^2 + T_i^2 + W_i^2) \tag{G.6}$$

} refer to equations (A.61)

Further

B_i^o = dimensionless mass of existing link (actual mass $= \rho^o a_1^3 B_i^o$)

---

†While Fig. G1 shows a circular counterweight which is tangent to the pivot, equations (G.1) - (G.3) apply to any shape of counterweight.

The superscript zero refers to the center of mass of the unbalanced link, and the superscript asterisk refers to the center of mass of the counterweight.

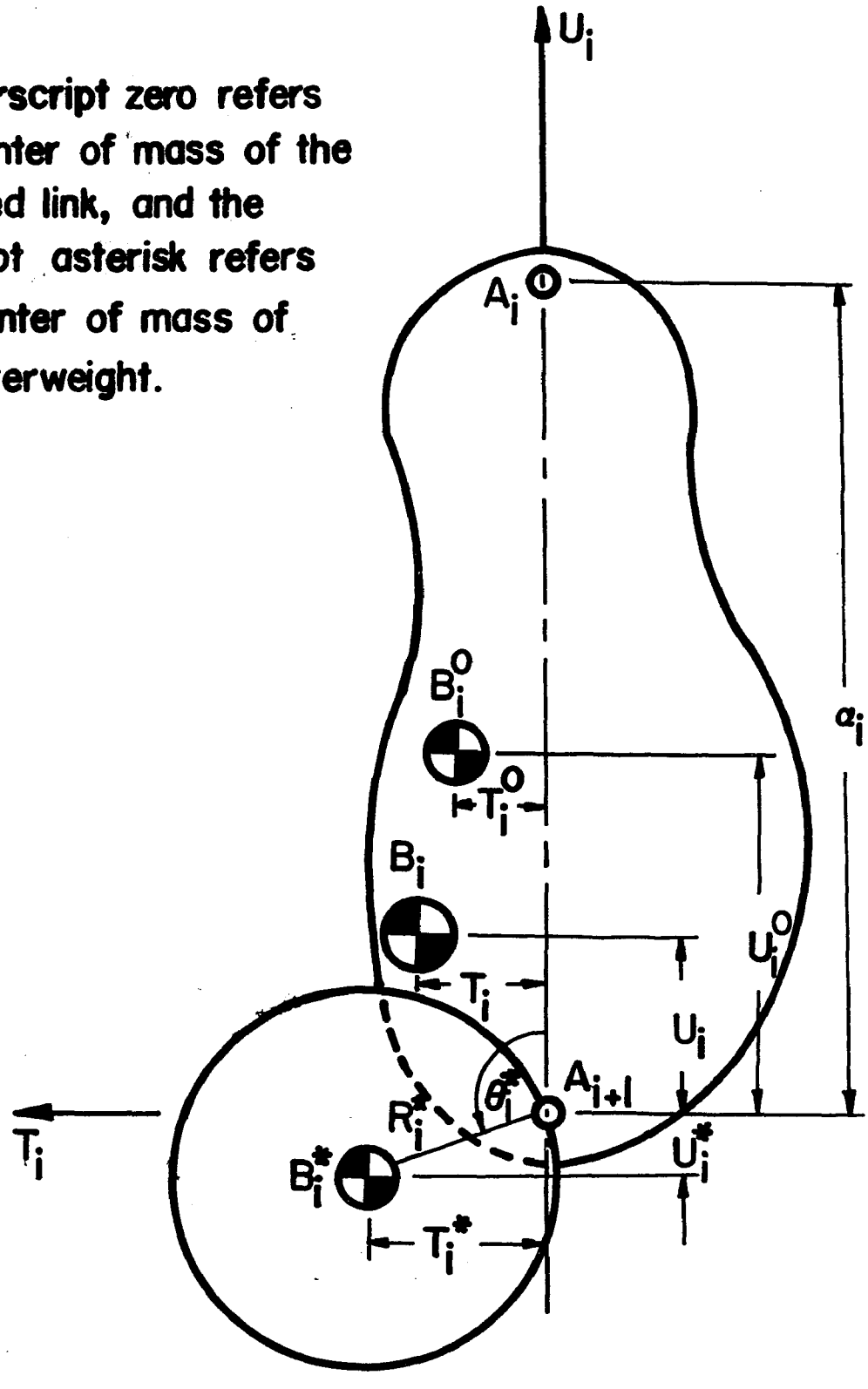

Fig. G1 Dimensionless parameters of link i with attached counterweight

$U_i^o = b_i/a_1$
$T_i^o = c_i/a_1$
} dimensionless coordinates of center of mass of existing link (see Figs. 6 and G1)

$W_i^o = \sqrt{C_i^o/B_i^o}$ = dimensionless radius of gyration of existing link

C_i^o = dimensionless moment of inertia of existing link with respect to link center of mass

B_i^* = dimensionless mass of counterweight (actual mass = $\rho^o a_1^3 B_i^*$, see also equation (G.7d))

U_i^*
T_i^*
} dimensionless coordinates of center of mass of counterweight

W_i^* = dimensionless radius of gyration of counterweight.

Once the configuration of the counterweight has been decided on, and the shape and mass of the original link are known, equations (G.1) - (G.3) can be solved for $B_i^* U_i^*$, $B_i^* T_i^*$ and W_i^*, or other equivalently suitable counterweight parameters.

2. Counterweight Design Equations for Standard Four-Bar Linkage Configuration

Equations (G.1) - (G.3) will now be used to design counterweights for a mechanism with the standard configuration of Fig. A2. The counterweights are chosen to be circular and tangent to the pivots A_0 and A_3 of the input and output links, respectively.

Certain counterweight parameters will now be defined:

the dimensionless radius of the counterweight is given by:

$$R_i^* = r_i^*/a_1 = (T_i^{*2} + U_i^{*2})^{1/2}, \qquad \text{(G.7a)}$$

where r_i^* is the actual radius of the counterweight;

the dimensionless radius of gyration of the circular counterweight is given by:

$$W_i^* = \frac{1}{\sqrt{2}} R_i^* = \frac{1}{\sqrt{2}} (T_i^{*2} + U_i^{*2})^{1/2}; \qquad \text{(G.7b)}$$

the angular position of the counterweight is given by:

$$\theta_i^* = \tan^{-1}\left(\frac{T_i^*}{U_i^*}\right); \qquad \text{(G.7c)}$$

and finally, the dimensionless mass of the counterweight is given by:

$$B_i^* = \frac{\rho_i^* \pi r_i^{*2} h_i^*}{\rho^o a_1^3}, \qquad \text{(G.7d)}$$

where

h_i^* = actual thickness of the counterweight

ρ_i^* = mass density of the counterweight which may be different from ρ^o, the density of the original link.

The introduction of the ratio ρ_i^*/ρ^o permits the counterweight to be made of a denser material, and therefore, a smaller counterweight will result.

If one further introduces the ratios[†]

$$\beta_i = \frac{d_i}{a_1}, \quad \gamma_i = \frac{h_i}{d_i}, \quad \delta_i = \frac{h_i^*}{h_i} \text{ (see Fig. 6),} \tag{G.8a}$$

equation (G.7d) may be rewritten with the help of equation (G.7a):

$$B_i^* = \pi(T_i^{*2} + U_i^{*2})\beta_i\gamma_i D_i^*, \tag{G.8b}$$

where

$$D_i^* = \delta_i\left(\frac{\rho_i^*}{\rho^o}\right) \tag{G.8c}$$

is defined as the counterweight thickness-density ratio.

For the given linkage configuration, the link mass parameters become:

$$U_i^o = \frac{1}{2}\alpha_i \tag{G.9a}$$

$$T_i^o = 0 \tag{G.9b}$$

$$W_i^o = \sqrt{C_i^o/B_i^o}, \tag{G.9c}$$

where α_i represents the dimensionless link length a_i/a_1

[†] See also equations (A.115) in Appendix A. This means of expressing the mass of the counterweight has been chosen because it allows one to relate the counterweight thickness to the thickness of the existing link.

(see equations (A.115)). The dimensionless moment of inertia C_i^o and dimensionless mass B_i^o are given by equations (A.119) of Appendix A. (The superscript o was not used in these equations.)

When the three optimum mass parameters u_i, t_i and v_i are prescribed, the three desirable counterweight parameters are represented by the dimensionless counterweight radius R_i^*, the angular position θ_i^* with respect to link i, and the thickness-density ratio D_i^*. When only the parameters u_i and t_i are prescribed, it is best to choose a practical thickness-density ratio D_i^*, and solve only for R_i^* and θ_i^*.

a. Optimum Mass Parameters u_i, t_i and v_i are Prescribed by Solution of Optimization Equations

When u_i, t_i and v_i are prescribed by the solution of the optimization equations, equations (G.1) - (G.3) may be rewritten with the help of equations (G.7b), (G.8) and (G.9) as follows:

$$(T_i^{*2} + U_i^{*2})D_i^*U_i^* = \frac{u_i - \frac{1}{2} B_i^o\alpha_i}{\pi\beta_i\gamma_i} \tag{G.10}$$

$$(T_i^{*2} + U_i^{*2})D_i^*T_i^* = \frac{t_i}{\pi\beta_i\gamma_i} \tag{G.11}$$

$$(T_i^{*2} + U_i^{*2})^2 D_i^* = \frac{v_i - \left(\frac{B_i^o\alpha_i^2}{4} + C_i^o\right)}{\frac{3}{2}\pi\beta_i\gamma_i} \quad . \tag{G.12}$$

By combining equations (G.10) and (G.11), U_i^* is obtained in terms of T_i^*. Thus

$$U_i^* = \left(\frac{u_i - \frac{1}{2} B_i^o \alpha_i}{t_i} \right) T_i^* \quad . \tag{G.13}$$

By substituting equation (G.13) into equations (G.10) and (G.12), the following results:

$$D_i^* T_i^{*3} = \frac{t_i^3}{\pi \beta_i \gamma_i \left[t_i^2 + (u_i - \frac{1}{2} B_i^o \alpha_i)^2 \right]} \tag{G.14}$$

$$D_i^* T_i^{*4} = \frac{2 t_i^4 \left[v_i - \left(\frac{B_i^o \alpha_i^2}{4} + C_i^o \right) \right]}{3 \pi \beta_i \gamma_i \left[t_i^2 + (u_i - \frac{1}{2} B_i^o \alpha_i)^2 \right]^2} \quad . \tag{G.15}$$

Equations (G.14) and (G.15) may be combined to produce the following expression for T_i^*:

$$T_i^* = \frac{2 t_i \left[v_i - \left(\frac{B_i^o \alpha_i^2}{4} + C_i^o \right) \right]}{3 \left[t_i^2 + (u_i - \frac{1}{2} B_i^o \alpha_i)^2 \right]} \quad . \tag{G.16}$$

Substituting equation (G.16) into equation (G.13) yields U_i^*:

$$U_i^* = \frac{2 (u_i - \frac{1}{2} B_i^o \alpha_i) \left[v_i - \left(\frac{B_i^o \alpha_i^2}{4} + C_i^o \right) \right]}{3 \left[t_i^2 + (u_i - \frac{1}{2} B_i^o \alpha_i)^2 \right]} \quad . \tag{G.17}$$

Equations (G.16) and (G.17) can now be substituted into equation (G.7a) to find the dimensionless counterweight radius. Thus

$$R_i^* = (U_i^{*2} + T_i^{*2})^{1/2} = \frac{2\left[v_i - \left(\frac{B_i^o \alpha_i^2}{4} + C_i^o\right)\right]}{3\left[t_i^2 + (u_i - \frac{1}{2} B_i^o \alpha_i)^2\right]^{1/2}} \quad . \quad (G.18)$$

The angular position of the center of mass of the counterweight can be found by substituting equations (G.16) and (G.17) into equation (G.7c). This yields

$$\theta_i^* = \tan^{-1}\left(\frac{T_i^*}{U_i^*}\right) = \tan^{-1}\left(\frac{t_i}{u_i - \frac{1}{2} B_i^o \alpha_i}\right) \quad . \quad (G.19)$$

Finally, the dimensionless counterweight thickness-density ratio D_i^* can be found by substituting equation (G.16) into equation (G.14). Hence

$$D_i^* = \delta_i\left(\frac{\rho_i^*}{\rho^o}\right) = \frac{27\left[t_i^2 + (u_i - \frac{1}{2} B_i^o \alpha_i)^2\right]^2}{8\pi\beta_i\gamma_i\left[v_i - \left(\frac{B_i^o \alpha_i^2}{4} + C_i^o\right)\right]^3} \quad . \quad (G.20)$$

b. <u>Optimum Mass Parameters u_i and t_i are Prescribed by Solution of Optimization Equations</u>

When only u_i and t_i are prescribed by the solution of the optimization equations, only equations (G.1) and (G.2) need be satisfied. They may be rewritten with the help of equations (G.8) and (G.9) as follows:

$$(T_i^{*2} + U_i^{*2})U_i^* = \frac{u_i - \frac{1}{2} B_i^o \alpha_i}{\pi\beta_i\gamma_i D_i^*} \quad (G.21)$$

$$(T_i^{*2} + U_i^{*2})T_i^* = \frac{t_i}{\pi\beta_i\gamma_i D_i^*} , \qquad (G.22)$$

where D_i^* is given. (It has been previously chosen to obtain reasonable dimensions.)

By combining equations (G.21) and (G.22), U_i^* is obtained in terms of T_i^*. Thus

$$U_i^* = \left(\frac{u_i - \frac{1}{2} B_i^o \alpha_i}{t_i}\right) T_i^* . \qquad (G.23)$$

Substitution of equation (G.23) into equation (G.22), and solving for T_i^* yields:

$$T_i^* = t_i \left\{ \frac{1}{\pi\beta_i\gamma_i D_i^* \left[t_i^2 + (u_i - \frac{1}{2} B_i^o \alpha_i)^2 \right]} \right\}^{1/3} . \qquad (G.24)$$

Substituting equation (G.24) into equation (G.23), one obtains

$$U_i^* = (u_i - \frac{1}{2} B_i^o \alpha_i) \left\{ \frac{1}{\pi\beta_i\gamma_i D_i^* \left[t_i^2 + (u_i - \frac{1}{2} B_i^o \alpha_i)^2 \right]} \right\}^{1/3} . \qquad (G.25)$$

The dimensionless counterweight radius can now be found by substituting equations (G.24) and (G.25) into equation (G.7a). Hence

$$R_i^* = (U_i^{*2} + T_i^{*2})^{1/2} = \left\{ \frac{\left[t_i^2 + (u_i - \frac{1}{2} B_i^o \alpha_i)^2 \right]^{1/2}}{\pi \beta_i \gamma_i D_i^*} \right\}^{1/3} . \qquad (G.26)$$

By using equation (G.23) in equation (G.7c), the angular position of the counterweight becomes

$$\theta_i^* = \tan^{-1}\left(\frac{T_i^*}{U_i^*}\right) = \tan^{-1}\left(\frac{t_i}{u_i - \frac{1}{2} B_i^o \alpha_i}\right) . \qquad (G.27)$$

APPENDIX H

SOLUTION OF OPTIMIZATION EQUATIONS FOR TWO COUNTERWEIGHT PROBLEM

1. Outline of Solution Method

The method of solution of the optimization equations (4.43) - (4.48) will now be presented in detail.

First, let these expressions be rewritten for convenience:

$$I_{13} + I_2 t_1^2 + I_2 u_1^2 + 2I_7 u_1 + 2I_5 t_1 = 2\pi q_1^2 f_{41_{RMS_u}}^2 \qquad (H.1)$$

$$I_{14} + I_9 t_3^2 + I_9 u_3^2 + 2I_{12} u_3 + 2I_{10} t_3 = 2\pi q_2^2 f_{43_{RMS_u}}^2 \qquad (H.2)$$

$$I_1 + I_2 t_1 - I_3 u_3 + I_4 t_3 + \lambda_1 (I_5 + I_2 t_1) = 0 \qquad (H.3)$$

$$I_6 + I_2 u_1 + I_4 u_3 + I_3 t_3 + \lambda_1 (I_7 + I_2 u_1) = 0 \qquad (H.4)$$

$$I_8 + I_3 u_1 + I_4 t_1 + I_9 t_3 + \lambda_2 (I_{10} + I_9 t_3) = 0 \qquad (H.5)$$

$$I_{11} + I_4 u_1 - I_3 t_1 + I_9 u_3 + \lambda_2 (I_{12} + I_9 u_3) = 0 \ , \qquad (H.6)$$

where I_1 to I_{14} are given by equations (4.42).

In order to obtain a polynomial in u_3, the following solution steps must be undertaken:

Step 1

Equation (H.3) is solved for λ_1^*, the result is substituted into equation (H.4), and t_1 is obtained from this expression.

---

*λ_1 is given by equation (H.15).

$$t_1(t_3,u_1,u_3) = \frac{1}{I_2(I_6 - I_7 + I_4u_3 + I_3t_3)}\Big[(I_1I_7 - I_5I_6)$$

$$-(I_3I_7 + I_4I_5)u_3 + (I_4I_7 - I_3I_5)t_3 + (I_1I_2 - I_2I_5)u_1$$

$$- I_2I_3u_1u_3 + I_2I_4u_1t_3\Big] . \qquad \text{(H.7)}$$

Step 2

Equation (H.5) is solved for λ_2^*, the result is substituted together with equation (H.7) into equation (H.6), and u_1 is obtained from this expression.

$$u_1(t_3,u_3) = \frac{-(I_{15} + I_{16}t_3 + I_{17}u_3 + I_{18}u_3t_3 + I_{19}u_3^2 + I_{20}t_3^2)}{I_{21} + I_{22}t_3 + I_{23}u_3} , \qquad \text{(H.8)}$$

where I_{15} to I_{23} are listed in Section 2 of the present appendix.

Step 3

Equation (H.7) can be made more compact by introducing certain new constants. Thus

$$t_1(t_3,u_1,u_3) = \frac{I_{24} + I_{25}u_3 + I_{26}t_3 + I_{27}u_1 + I_{28}u_1u_3 + I_{29}u_1t_3}{I_{30} + I_{29}u_3 - I_{28}t_3} . \qquad \text{(H.9)}$$

Again, I_{24} to I_{30} are listed in Section 2.

---

*λ_2 is given by equation (H.16).

Step 4

To express equation (H.9) in terms of t_3 and u_3 only, equation (H.8) is substituted for $u_1(t_3,u_3)$. This results in

$$t_1(t_3,u_3) = \frac{1}{I_{31} + I_{32}u_3 + I_{33}t_3 + I_{34}t_3^2 + I_{35}u_3^2 + I_{36}u_3t_3}\Big[I_{37} + I_{38}u_3 + I_{39}t_3 + I_{40}u_3^2 + I_{41}t_3^2 + I_{42}u_3t_3 + I_{43}u_3^3 + I_{44}t_3^3 + I_{45}t_3u_3^2 + I_{46}t_3^2u_3\Big] . \qquad (H.10)$$

Constants I_{31} to I_{46} in the above are listed in Section 2 of this appendix.

Step 5

In order to rewrite equation (H.1) in terms of u_3 and t_3, equations (H.8) and (H.10) are used. This results in

$$\begin{aligned} &I_{48}t_3^8 + (I_{49} + I_{50}u_3)t_3^7 + (I_{51} + I_{52}u_3 + I_{53}u_3^2)t_3^6 \\ &+ (I_{54} + I_{55}u_3 + I_{56}u_3^2 + I_{57}u_3^3)t_3^5 \\ &+ (I_{58} + I_{59}u_3 + I_{60}u_3^2 + I_{61}u_3^3 + I_{62}u_3^4)t_3^4 \\ &+ (I_{63} + I_{64}u_3 + I_{65}u_3^2 + I_{66}u_3^3 + I_{67}u_3^4 + I_{68}u_3^5)t_3^3 \\ &+ (I_{69} + I_{70}u_3 + I_{71}u_3^2 + I_{72}u_3^3 + I_{73}u_3^4 + I_{74}u_3^5 + I_{75}u_3^6)t_3^2 \\ &+ (I_{76} + I_{77}u_3 + I_{78}u_3^2 + I_{79}u_3^3 + I_{80}u_3^4 + I_{81}u_3^5 + I_{82}u_3^6 + I_{83}u_3^7)t_3 \\ &+ I_{84} + I_{85}u_3 + I_{86}u_3^2 + I_{87}u_3^3 + I_{88}u_3^4 + I_{89}u_3^5 + I_{90}u_3^6 + I_{91}u_3^7 \\ &+ I_{92}u_3^8 = 0 , \qquad (H.11) \end{aligned}$$

where I_{48} to I_{92} are given in Section 2.

Step 6

To obtain a single equation for u_3, equation (H.2) will first be expressed in terms of $t_3(u_3)$, and will then be substituted into equation (H.11). Thus, from (H.2)

$$t_3(u_3) = I_{93} \pm \sqrt{-u_3^2 + I_{94}u_3 + I_{95}}\,, \tag{H.12}$$

where I_{93} to I_{95} are given in Section 2 of the present appendix.

Step 7

Substituting equations (H.12) into equation (H.11), and collecting like powers of u_3 gives:

$$I_{156}u_3^8 + I_{157}u_3^7 + I_{158}u_3^6 + I_{159}u_3^5 + I_{160}u_3^4 + I_{161}u_3^3 + I_{162}u_3^2 + I_{163}u_3 + I_{164} = \mp\left[I_{165}u_3^7 + I_{166}u_3^6 + I_{167}u_3^5 + I_{168}u_3^4 + I_{169}u_3^3 + I_{170}u_3^2 + I_{171}u_3 + I_{172}\right]\sqrt{-u_3^2 + I_{94}u_3 + I_{95}}\,, \tag{H.13}$$

where the constants I_{156} to I_{172} are listed in Section 2.

Step 8

To remove the square root, both sides of equations (H.13) are squared, and the following 16^{th} degree polynomial results:

$$P_1 u_3^{16} + P_2 u_3^{15} + P_3 u_3^{14} + P_4 u_3^{13} + P_5 u_3^{12} + P_6 u_3^{11} + P_7 u_3^{10} + P_8 u_3^{9}$$
$$+ P_9 u_3^{8} + P_{10} u_3^{7} + P_{11} u_3^{6} + P_{12} u_3^{5} + P_{13} u_3^{4} + P_{14} u_3^{3} + P_{15} u_3^{2}$$
$$+ P_{16} u_3 + P_{17} = 0 \ , \qquad \text{(H.14)}$$

where P_1 to P_{17} are listed in Section 2 of this appendix.

For the sake of completeness, the parameters λ_1 and λ_2 are given below:

$$\lambda_1 = \frac{-(I_1 + I_2 t_1 - I_3 u_3 + I_4 t_3)}{I_5 + I_2 t_1} \qquad \text{(H.15)}$$

$$\lambda_2 = \frac{-(I_8 + I_3 u_1 + I_4 t_1 + I_9 t_3)}{I_{10} + I_9 t_3} \ . \qquad \text{(H.16)}$$

2. Expressions for Constants

The following gives a listing of the constants I_{15} to I_{192}, as well as P_1 to P_{17}, of the previous section in the order needed for numerical computation. In addition, the intermediate constants F_1 to F_{62} and G_1 to G_{11} are introduced.

$$I_{15} = -(I_3 I_{10} + I_4 I_{12})(I_1 I_7 - I_5 I_6) + I_2(I_6 - I_7)(I_{10} I_{11} - I_8 I_{12})$$

$$I_{16} = -I_3 I_9 (I_1 I_7 - I_5 I_6) - (I_3 I_{10} + I_4 I_{12})(I_4 I_7 - I_3 I_5)$$
$$+ I_2 I_9 (I_6 - I_7)(I_{11} - I_{12}) + I_2 I_3 (I_{10} I_{11} - I_8 I_{12})$$

$$I_{17} = -I_4 I_9 (I_1 I_7 - I_5 I_6) + (I_3 I_{10} + I_4 I_{12})(I_3 I_7 + I_4 I_5)$$
$$+ I_2 I_9 (I_6 - I_7)(I_{10} - I_8) + I_2 I_4 (I_{10} I_{11} - I_8 I_{12})$$

$$I_{18} = I_3 I_9 (I_3 I_7 + I_4 I_5) - I_4 I_9 (I_4 I_7 - I_3 I_5)$$
$$+ I_2 I_4 I_9 (I_{11} - I_{12}) + I_2 I_3 I_9 (I_{10} - I_8)$$

$$I_{19} = I_4 I_9 (I_3 I_7 + I_4 I_5) + I_2 I_4 I_9 (I_{10} - I_8)$$

$$I_{20} = -I_3 I_9 (I_4 I_7 - I_3 I_5) + I_2 I_3 I_9 (I_{11} - I_{12})$$

$$I_{21} = -I_2 (I_3 I_{10} + I_4 I_{12})(I_1 - I_5) + I_2 (I_6 - I_7)(I_4 I_{10} - I_3 I_{12})$$

$$I_{22} = -I_2 I_3 I_9 (I_1 - I_5) - I_2 I_4 (I_3 I_{10} + I_4 I_{12}) + I_2 I_4 I_9 (I_6 - I_7)$$
$$+ I_2 I_3 (I_4 I_{10} - I_3 I_{12})$$

$$I_{23} = -I_2 I_4 I_9 (I_1 - I_5) + I_2 I_3 (I_3 I_{10} + I_4 I_{12}) - I_2 I_3 I_9 (I_6 - I_7)$$
$$+ I_2 I_4 (I_4 I_{10} - I_3 I_{12})$$

$$I_{24} = I_1 I_7 - I_5 I_6$$

Table H1 Intermediate Constants for Solution of Optimization Equations

$$I_{25} = -(I_4 I_5 + I_3 I_7)$$

$$I_{26} = I_4 I_7 - I_3 I_5$$

$$I_{27} = I_2 (I_1 - I_5)$$

$$I_{28} = -I_2 I_3$$

$$I_{29} = I_2 I_4$$

$$I_{30} = I_2 (I_6 - I_7)$$

$$I_{31} = I_{21} I_{30}$$

$$I_{32} = I_{23} I_{30} + I_{21} I_{29}$$

$$I_{33} = I_{22} I_{30} - I_{21} I_{28}$$

$$I_{34} = -I_{22} I_{28}$$

$$I_{35} = I_{23} I_{29}$$

$$I_{36} = I_{22} I_{29} - I_{23} I_{28}$$

$$I_{37} = I_{21} I_{24} - I_{15} I_{27}$$

$$I_{38} = I_{21} I_{25} + I_{23} I_{24} - I_{17} I_{27} - I_{15} I_{28}$$

$$I_{39} = I_{22} I_{24} + I_{21} I_{26} - I_{15} I_{29} - I_{16} I_{27}$$

$$I_{40} = I_{23} I_{25} - I_{17} I_{28} - I_{19} I_{27}$$

$$I_{41} = I_{22} I_{26} - I_{16} I_{29} - I_{20} I_{27}$$

$$I_{42} = I_{22} I_{25} + I_{23} I_{26} - I_{16} I_{28} - I_{17} I_{29} - I_{18} I_{27}$$

Table H1 continued

$I_{43} = -I_{19}I_{28}$

$I_{44} = -I_{20}I_{29}$

$I_{45} = -I_{19}I_{29} - I_{18}I_{28}$

$I_{46} = -I_{20}I_{28} - I_{18}I_{29}$

$I_{47} = I_{13} - 2\pi q_1^2 f_{41_{RMS_u}}^2$

```
F1 = I41*I41 + 2.*I39*I44
F2 = I16*I16 + 2.*I15*I20
F3 = I33*I33 + 2.*I31*I34
F4 = I16*I22 + I20*I21
F5 = I34*I41 + I33*I44
F6 = I41*I46 + I42*I44
F7 = I21*I46 + I23*I41
F8 = I16*I18 + I17*I20
F9 = I18*I33 + I16*I36
F10 = I33*I36 + I32*I34
F11 = I18*I22 + I20*I23
F12 = I34*I46 + I36*I44
F13 = I46*I46 + 2.*I44*I45
F14 = I18*I18 + 2.*I19*I20
F15 = I36*I36 + 2.*I34*I35
F16 = I37*I44 + I39*I41
F17 = I15*I22 + I16*I21
F18 = I34*I39 + I33*I41 + I31*I44
F19 = I38*I44 + I39*I46 + I41*I42
F20 = I15*I18 + I16*I17
```

Table H1 continued

```
F21 = I31*I36 + I32*I33
F22 = I17*I22 + I18*I21 + I16*I23
F23 = I34*I42 + I33*I46 + I36*I41 + I32*I44
F24 = I42*I46 + I41*I45 + I40*I44
F25 = I17*I18 + I16*I19
F26 = I32*I36 + I33*I35
F27 = I19*I22 + I18*I23
F28 = I34*I45 + I36*I46 + I35*I44
F29 = I43*I44 + I45*I46
F30 = I39*I39 + 2.*I37*I41
F31 = I34*I37 + I33*I39 + I31*I41
F32 = I23*I33 + I21*I36
F33 = I39*I42 + I37*I46 + I38*I41
F34 = I17*I21 + I15*I23
F35 = I34*I38 + I33*I42 + I36*I39 + I31*I46 + I32*I41
F36 = I42*I42 + 2.*I39*I45 + 2.*I38*I46 + 2.*I40*I41
F37 = I17*I17 + 2.*I15*I19
F38 = I32*I32 + 2.*I31*I35
F39 = I19*I21 + I17*I23
F40 = I34*I40 + I33*I45 + I36*I42 + I32*I46 + I35*I41
F41 = I42*I45 + I40*I46 + I41*I43
F42 = I34*I43 + I36*I45 + I35*I46
```

Table H1 continued

```
F43 = I45*I45 + 2.*I43*I46
F44 = I33*I37 + I31*I39
F45 = I37*I42 + I38*I39
F46 = I33*I38 + I36*I37 + I31*I42 + I32*I39
F47 = I37*I45 + I38*I42 + I39*I40
F48 = I33*I40 + I36*I38 + I31*I45 + I32*I42 + I35*I39
F49 = I38*I45 + I40*I42 + I39*I43
F50 = I33*I43 + I36*I40 + I32*I45 + I35*I42
F51 = I42*I43 + I40*I45
F52 = I36*I43 + I35*I45
F53 = I31*I38 + I32*I37
F54 = I38*I38 + 2.*I37*I40
F55 = I31*I40 + I32*I38 + I35*I37
F56 = I31*I43 + I32*I40 + I35*I38
F57 = I40*I40 + 2.*I38*I43
F58 = I32*I43 + I35*I40
F59 = I21*I38 + I23*I37
F60 = I21*I40 + I23*I38
F61 = I37*I43 + I38*I40
F62 = I21*I43 + I23*I40
```

Table H1 continued

```
I48 = I2*(I22*I22*I44*I44 + I20*I20*I34*I34)

I49 =2.*(I2*I22*I22*I41*I44 + I2*I21*I22*I44*I44 + I2*I16*I20*
I34*I34 + I2*I20*I20*I33*I34 - I7*I20*I22*I34*I34 + I5*I22*I22*
I34*I44)

I50 = 2.*(I2*I22*I22*I44*I46 + I2*I22*I23*I44*I44 + I2*I18*I20*
I34*I34 + I2*I20*I20*I34*I36)

I51 = I22*I22*I34*I34*I47 + I2*I22*I22*F1 + 4.*I2*I21*I22*I41*I44
+I2*I21*I21*I44*I44 + I2*I34*I34*F2 + 4.*I2*I16*I20*I33*I34
+I2*I20*I20*F3 - 2.*I7*I34*I34*F4 - 4.*I7*I20*I22*I33*I34
+ 2.*I5*I22*I22*F5 + 4.*I5*I21*I22*I34*I44

I52 = 2.*I2*I22*I22*F6 + 4.*I2*I22*I44*F7 + 2.*I2*I44*I44*I21*I23
+2.*I2*I34*I34*F8 + 4.*I2*I20*I34*F9 + 2.*I2*I20*I20*F10
-2.*I7*I34*I34*F11 - 4.*I7*I20*I22*I34*I36 + 2.*I5*I22*I22*F12
+ 4.*I5*I22*I23*I34*I44

I53 = I2*I22*I22*F13 + 4.*I2*I22*I23*I44*I46 + I2*I23*I23*I44*I44
+ I2*I34*I34*F14 + 4.*I2*I18*I20*I34*I36 + I2*I20*I20*F15

I54 = 2.*I22*I22*I33*I34*I47 + 2.*I21*I22*I34*I34*I47 + 2.*I2*
I22*I22*F16 + 2.*I2*I21*I22*F1 + 2.*I2*I21*I21*I41*I44 + 2.*I2*
I15*I16*I34*I34 + 2.*I2*I33*I34*F2 + 2.*I2*I16*I20*F3 + 2.*I2*
I20*I20*I31*I33 - 2.*I7*I34*I34*F17 - 4.*I7*I33*I34*F4 - 2.*I7*
I20*I22*F3 + 2.*I5*I22*I22*F18 + 4.*I5*I21*I22*F5 + 2.*I5*I21*
I21*I34*I44

I55 = 2.*I22*I22*I34*I36*I47 + 2.*I22*I23*I34*I34*I47 + 2.*I2*
I22*I22*F19 + 4.*I2*I21*I22*F6 + 2.*I2*I22*I23*F1 + 4.*I2*I21*
I23*I41*I44 + 2.*I2*I21*I21*I44*I46 + 2.*I2*I34*I34*F20 + 4.*I2*
I33*I34*F8 + 2.*I2*I34*I36*F2 + 4.*I2*I16*I20*F10 + 2.*I2*I18*
I20*F3 + 2.*I2*I20*I20*F21 - 2.*I7*I34*I34*F22 - 4.*I7*I33*I34*F11
- 4.*I7*I34*I36*F4 - 4.*I7*I20*I22*F10 + 2.*I5*I22*I22*F23 + 4.*
I5*I21*I22*F12 + 4.*I5*I22*I23*F5 + 4.*I5*I21*I23*I34*I44
```

Table H1 continued

```
I56 = 2.*(I2*I22*I22*F24 + I2*I21*I22*F13 + 2.*I2*I22*I23*F6
+ I2*I23*I23*I41*I44 + 2.*I2*I21*I23*I44*I46 + I2*I34*I34*F25
+ I2*I33*I34*F14 + 2.*I2*I34*I36*F8 + I2*I16*I20*F15 + 2.*I2*I18*
I20*F10+ I2*I20*I20*F26 - I7*I34*I34*F27 - 2.*I7*I34*I36*F11
- I7*I20*I22*F15 + I5*I22*I22*F28 + 2.*I5*I22*I23*F12 + I5*I23*
I23*I34*I44)

I57 = 2.*(I2*I22*I22*F29 + I2*I22*I23*F13 + I2*I44*I46*I23*I23
+ I2*I18*I19*I34*I34 + I2*I34*I36*F14 + I2*I18*I20*F15 + I2*I20*
I20*I35*I36)

I58 = I22*I22*I47*F3 + 4.*I22*I34*I47*I21*I33 + I34*I34*I47*I21*
I21 + I2*I22*I22*F30 + 4.*I2*I22*I21*F16 + I2*I21*I21*F1 + I2*
I34*I34*I15*I15 + 4.*I2*I34*I33*I15*I16 + I2*F2*F3 + 4.*I2*I20*
I31*I33*I16 + I2*I20*I20*I31*I31 - 2.*I7*I15*I21*I34*I34
- 4.*I7*I33*I34*F17 - 2.*I7*F4*F3 - 4.*I7*I20*I22*I31*I33
+ 2.*I5*I22*I22*F31 + 4.*I5*I21*I22*F18 + 2.*I5*I21*I21*F5

I591= 2.*(I22*I22*I47*F10 + 2.*I22*I34*I47*F32 + I34*I34*I47*I21*
I23 + I2*I22*I22*F33 + 2.*I2*I22*I21*F19 + 2.*I2*I22*I23*F16
+ I2*I21*I21*F6 + I2*I21*I23*F1 + I2*I34*I34*I15*I17
+ 2.*I2*I34*I33*F20 + 2.*I2*I34*I36*I15*I16 + I2*F2*F10
+ I2*F8*F3 + 2.*I2*I20*I31*F9 + 2.*I2*I20*I32*I33*I16
+ I2*I20*I20*I31*I32 - I7*I34*I34*F34 - 2.*I7*I33*I34*F22
- 2.*I7*I34*I36*F17 - 2.*I7*F4*F10 - I7*F11*F3
- 2.*I7*I20*I22*F21 + I5*I22*I22*F35 + 2.*I5*I22*I21*F23)

I592 = 2.*(2.*I5*I22*I23*F18 + I5*I21*I21*F12 + 2.*I5*I21*I23*F5)

I59 = I591 + I592

I60 = I22*I22*I47*F15 + 4.*I22*I34*I47*I23*I36 + I34*I34*I47*
I23*I23 + I2*I22*I22*F36 + 4.*I2*I22*I21*F24 + 4.*I2*I22*I23*F19 +
I2*I21*I21*F13 + 4.*I2*I21*I23*F6 + I2*I23*I23*F1 + I2*I34*I34*F37
+ 4.*I2*I34*I33*F25 + 4.*I2*I34*I36*F20 + I2*F2*F15
+ 4.*I2*F8*F10 + I2*F14*F3 + 4.*I2*I20*I31*I18*I36
+4.*I2*I20*I32*F9 + 4.*I2*I20*I35*I16*I33 + I2*I20*I20*F38
- 2.*I7*I34*I34*F39 - 4.*I7*I34*I33*F27 - 4.*I7*I34*I36*F22 - 2.*
I7*F4*F15 - 4.*I7*F11*F10 - 4.*I7*I20*I22*F26 + 2.*I5*I22*I22*F40
+ 4.*I5*I22*I21*F28 + 4.*I5*I22*I23*F23 + 4.*I5*I21*I23*F12
+ 2.*I5*I23*I23*F5

I61 = 2.*(I2*I22*I22*F41 + 2.*I2*I22*I21*F29 + 2.*I2*I22*I23*F24
+ I2*I21*I23*F13 + I2*I23*I23*F6 + I2*I34*I34*I17*I19
+ 2.*I2*I34*I33*I18*I19 + 2.*I2*I34*I36*F25 + I2*F8*F15
+ I2*F14*F10 + 2.*I2*I20*I32*I18*I36 + 2.*I2*I20*I35*F9
+ I2*I20*I20*I32*I35 - I7*I34*I34*I23*I19 - 2.*I7*I34*I36*F27
 - I7*F11*F15 - 2.*I7*I20*I22*I35*I36 + I5*I22*I22*F42
+ 2.*I5*I22*I23*F28 + I5*I23*I23*F12)
```

Table H1 continued

```
I62 = I2*I22*I22*F43 + 4.*I2*I22*I23*F29 + I2*I23*I23*F13 + I2*
I19*I19*I34*I34+4.*I2*I18*I19*I34*I36 + I2*F14*F15 + 4.*I2*I18*
I20*I35*I36 + I2*I20*I20*I35*I35

I63 = 2.*(I22*I22*I31*I33*I47 + I21*I22*I47*F3 + I21*I21*I33*I34*
I47 + I2*I22*I22*I37*I39 + I2*I21*I22*F30 + I2*I21*I21*F16
+ I2*I15*I15*I33*I34 + I2*I15*I16*F3 + I2*I31*I33*F2
+ I2*I16*I20*I31*I31 - 2.*I7*I15*I21*I33*I34 - I7*F17*F3
- 2.*I7*I31*I33*F4 - I7*I20*I22*I31*I31 + I5*I22*I22*F44
+ 2.*I5*I21*I22*F31 + I5*I21*I21*F18)

I64 = 2.*I22*I22*I47*F21 + 4.*I21*I22*I47*F10 + 2.*I22*I23*I47*F3
+ 4.*I21*I23*I33*I34*I47 + 2.*I21*I21*I34*I36*I47 + 2.*I2*I22*
I22*F45 + 4.*I2*I21*I22*F33 + 2.*I2*I22*I23*F30 + 2.*I2*I21*I21*
F19 + 4.*I2*I21*I23*F16 + 4.*I2*I15*I17*I33*I34 + 2.*I2*I15*I15*
I34*I36 + 4.*I2*I15*I16*F10 + 2.*I2*F20*F3 + 4.*I2*I31*I33*F8
+ 2.*I2*F21*F2 + 4.*I2*I16*I20*I31*I32 + 2.*I2*I18*I20*I31*I31
- 4.*I7*I33*I34*F34 - 4.*I7*I15*I21*I34*I36 - 4.*I7*F17*F10
- 2.*I7*F22*F3 - 4.*I7*I31*I33*F11 - 4.*I7*F21*F4
- 4.*I7*I20*I22*I31*I32 + 2.*I5*I22*I22*F46 + 4.*I5*I21*I22*F35
+ 2.*I5*I21*I21*F23 + 4.*I5*I22*I23*F31 + 4.*I5*I21*I23*F18

I65 = 2.*(I22*I22*I47*F26 + I21*I22*I47*F15 + 2.*I22*I23*I47*F10
+ I23*I23*I33*I34*I47 + 2.*I21*I23*I34*I36*I47 + I2*I22*I22*F47
+ I2*I21*I22*F36 + 2.*I2*I22*I23*F33 + I2*I21*I21*F24 + 2.*I2*I21*
I23*F19 + I2*I23*I23*F16 + I2*I33*I34*F37 + 2.*I2*I15*I17*I34*I36
+ I2*I15*I16*F15 + 2.*I2*F20*F10 + I2*F25*F3 + I2*I31*I33*F14
+ 2.*I2*F21*F8 + I2*F26*F2 + I2*I16*I20*F38 + 2.*I2*I18*I20*I31*
I32- 2.*I7*I33*I34*F39 - 2.*I7*I34*I36*F34 - I7*F17*F15 - 2.*I7*
F22*F10 - I7*F27*F3 - 2.*I7*F21*F11 - 2.*I7*F26*F4 - I7*I20*I22*
F38 + I5*I22*I22*F48 + 2.*I5*I21*I22*F40 + 2.*I5*I22*I23*F35 + I5*
I21*I21*F28 + 2.*I5*I21*I23*F23 + I5*I23*I23*F18)

I66 = 2.*(I22*I22*I35*I36*I47 + I22*I23*I47*F15 + I23*I23*I34*
I36*I47+I2*I22*I22*F49+2.*I2*I21*I22*F41+I2*I22*I23*F36 + I2*
I21*I21*F29 + 2.*I2*I21*I23*F24 + I2*I23*I23*F19 + 2.*I2*I17*
I19*I33*I34 + I2*I34*I36*F37 + I2*F20*F15 + 2.*I2*F25*F10 + I2*
I18*I19*F3 + I2*F21*F14 + 2.*I2*F26*F8 + I2*I35*I36*F2 + 2.*I2*
I16*I20*I32*I35 + I2*I18*I20*F38 - 2.*I7*I19*I23*I33*I34 - 2.*I7*
I34*I36*F39 - I7*F22*F15 - 2.*I7*F27*F10 - 2.*I7*F26*F11 - 2.*
I7*I35*I36*F4 - 2.*I7*I20*I22*I32*I35 + I5*I22*I22*F50 + 2.*I5*
I21*I22*F42 + 2.*I5*I22*I23*F40 + 2.*I5*I21*I23*F28 + I5*I23*
I23*F23)

I67 = 2.*(I2*I22*I22*F51 + I2*I21*I22*F43 + 2.*I2*I22*I23*F41
+ 2.*I2*I21*I23*F29 + I2*I23*I23*F24 + I2*I19*I19*I33*I34
+ 2.*I2*I17*I19*I34*I36 + I2*F25*F15 + 2.*I2*I18*I19*F10
+ I2*F26*F14 + 2.*I2*I35*I36*F8 + I2*I16*I20*I35*I35
+ 2.*I2*I18*I20*I32*I35 - 2.*I7*I19*I23*I34*I36 - I7*F27*F15
- 2.*I7*I35*I36*F11 - I7*I20*I22*I35*I35 + I5*I22*I22*F52
+ 2.*I5*I22*I23*F42 + I5*I23*I23*F28)

I68 = 2.*(I2*I22*I22*I43*I45 +I2*I22*I23*F43 + I2*I23*I23*F29
+ I2*I19*I19*I34*I36 + I2*I18*I19*F15 + I2*I35*I36*F14
+ I2*I18*I20*I35*I35)
```

Table H1 continued

```
I69 = I22*I22*I31*I31*I47 + 4.*I21*I22*I31*I33*I47 + I21*I21*I47*
F3 + I2*I22*I22*I37*I37 + 4.*I2*I21*I22*I37*I39 + I2*I21*I21*F30
+ I2*I15*I15*F3 + 4.*I2*I15*I16*I31*I33 + I2*I31*I31*F2 - 2.*I7*
I15*I21*F3 - 4.*I7*I31*I33*F17 - 2.*I7*I31*I31*F4
+ 2.*I5*I22*I22*I31*I37 + 4.*I5*I21*I22*F44 + 2.*I5*I21*I21*F31

I70 = 2.*(I22*I22*I31*I32*I47 + 2.*I22*I31*I47*F32 + 2.*I21*I22*
I32*I33*I47 + I21*I21*I47*F10 + I21*I23*I47*F3 + I2*I22*I22*I37*
I38 + 2.*I2*I21*I22*F45 + 2.*I2*I22*I23*I37*I39 + I2*I21*I21*F33
+ I2*I21*I23*F30 + I2*I15*I15*F10 + I2*I15*I17*F3 + 2.*I2*I31*I33*
F20 + 2.*I2*I15*I16*F21 + I2*I31*I31*F8 + I2*I31*I32*F2 - 2.*I7*
I15*I21*F10 - I7*F34*F3 - 2.*I7*I31*I33*F22- 2.*I7*F21*F17
- I7*I31*I31*F11 - 2.*I7*I31*I32*F4 + I5*I22*I22*F53 + 2.*I5*
I21*I22*F46 + 2.*I5*I22*I23*F44 + I5*I21*I21*F35 + 2.*I5*I21*
I23*F31)

I711= I22*I22*I47*F38 + 4.*I22*I31*I23*I36*I47 + 4.*I22*I32*
I47*F32 + 4.*I21*I22*I33*I35*I47 + I21*I21*I47*F15 + 4.*I21*
I23*I47*F10 + I23*I23*I47*F3 + I2*I22*I22*F54 + 4.*I2*I21*I22*
F47 + 4.*I2*I22*I23*F45 + I2*I21*I21*F36 + 4.*I2*I21*I23*F33 + I2*
I23*I23*F30 + I2*I15*I15*F15 + 4.*I2*I15*I17*F10 + I2*F37*F3
+ 4.*I2*I31*I33*F25 + 4.*I2*F21*F20 + 4.*I2*I15*I16*F26 + I2*
I31*I31*F14 + 4.*I2*I31*I32*F8 + I2*F38*F2 - 2.*I7*I15*I21*F15
- 4.*I7*F34*F10 - 2.*I7*F39*F3 - 4.*I7*I31*I33*F27
- 4.*I7*F21*F22 - 4.*I7*F26*F17 - 4.*I7*I31*I32*F11 - 2.*I7*
F38*F4 + 2.*I5*I22*I22*F55 + 4.*I5*I21*I22*F48 + 4.*I5*I22*I23*F46

I712 = 2.*I5*I21*I21*F40 + 4.*I5*I21*I23*F35 + 2.*I5*I23*I23*F31

I71 = I711 + I712

I721= 2.*(I22*I22*I32*I35*I47 + 2.*I22*I23*I32*I36*I47 + 2.*I22*
I35*I47*F32 + I21*I23*I47*F15 + I23*I23*I47*F10 + I2*I22*I22*F61
+ 2.*I2*I21*I22*F49 + 2.*I2*I22*I23*F47 + I2*I21*I21*F41
+ I2*I21*I23*F36 + I2*I23*I23*F33 + I2*I15*I17*F15
+I2*F37*F10 + I2*I17*I19*F3 + 2.*I2*I18*I19*I31*I33
+ 2.*I2*F21*F25 + 2.*I2*F26*F20 + 2.*I2*I15*I16*I35*I36
+ I2*I31*I32*F14 + I2*F38*F8 + I2*I32*I35*F2 - I7*F34*F15
- 2.*I7*F39*F10 - I7*I19*I23*F3 - 2.*I7*F21*F27 - 2.*F26*F22*I7
- 2.*I7*I35*I36*F17 - I7*F38*F11 - 2.*I7*I32*I35*F4 + I5*I22*I22*
F56 + 2.*I5*I21*I22*F50 + 2.*I5*I22*I23*F48 + I5*I21*I21*F42)

I722 = 2.*(2.*I5*I21*I23*F40 + I5*I23*I23*F35)

I72 = I721 + I722

I73 = I22*I22*I35*I35*I47 + 4.*I22*I23*I35*I36*I47 + I23*I23*
I47*F15 + I2*I22*I22*F57 + 4.*I2*I21*I22*F51 + 4.*I2*I22*I23*F49
+ I2*I21*I21*F43 + 4.*I2*I21*I23*F41 + I2*I23*I23*F36
+ I2*F37*F15 + 4.*I2*I17*I19*F10 + I2*I19*I19*F3 + 4.*I2*I18*
I19*F21+4.*I2*F26*F25+4.*I2*I35*I36*F20 + I2*F38*F14 + 4.*I2*
I32*I35*F8 + I2*I35*I35*F2 - 2.*I7*F39*F15 - 4.*I7*I19*I23*F10
- 4.*I7*F26*F27 - 4.*I7*I35*I36*F22 - 4.*I7*I32*I35*F11 - 2.*I7*
I35*I35*F4 + 2.*I5*I22*I22*F58 + 4.*I5*I21*I22*F52 + 4.*I5*I22*
I23*F50 + 4.*I5*I21*I23*F42 + 2.*I5*I23*I23*F40
```

Table H1 continued

```
I74 = 2.*(I2*I22*I22*I40*I43 + 2.*I2*I21*I22*I43*I45 + 2.*I2*I22*
I23*F51 + I2*I21*I23*F43 + I2*I23*I23*F41 + I2*I17*I19*F15
+ I2*I19*I19*F10 + 2.*I2*I18*I19*F26 + 2.*I2*I35*I36*F25 + I2*
I32*I35*F14 + I2*I35*I35*F8 - I7*I19*I23*F15 - 2.*I7*I35*I36*F27
- I7*I35*I35*F11 + I5*I22*I22*I35*I43 + 2.*I5*I22*I23*F52 + I5*
I23*I23*F42)

I75 = I2*I22*I22*I43*I43 + 4.*I2*I22*I23*I43*I45 + I2*I23*I23*F43
+ I2*I19*I19*F15 + 4.*I2*I18*I19*I35*I36 + I2*I35*I35*F14

I76 = 2.*(I21*I22*I31*I31*I47+I21*I21*I31*I33*I47+I2*I21*I22*I37*
I37 + I2*I21*I21*I37*I39 + I2*I15*I15*I31*I33 + I2*I15*I16*I31*I31
- 2.*I7*I15*I21*I31*I33 - I7*I31*I31*F17 + 2.*I5*I21*I22*I31*I37
+ I5*I21*I21*F44)

I77 = 2.*(I22*I23*I31*I31*I47 + 2.*I21*I22*I31*I32*I47 + 2.*I21*
I23*I31*I33*I47 + I21*I21*I47*F21 + 2.*I2*I21*I22*I37*I38 + I2*
I22*I23*I37*I37 + I2*I21*I21*F45 + 2.*I2*I21*I23*I37*I39 + 2.*
I2*I15*I17*I31*I33 + I2*I15*I15*F21 + I2*I31*I31*F20 + 2.*I2*
I15*I16*I31*I32 - 2.*I7*I31*I33*F34 - 2.*I7*I15*I21*F21 - I7*
I31*I31*F22 - 2.*I7*I31*I32*F17 + 2.*I5*I22*I31*F59 + 2.*I5*I21*
I22*I32*I37 + I5*I21*I21*F46 + 2.*I5*I21*I23*F44)

I78 = 2.*(I21*I22*I47*F38 + 2.*I22*I23*I31*I32*I47 + I23*I23*
I31*I33*I47 + 2.*I21*I23*I47*F21 + I21*I21*I47*F26 + I2*I21*
I22*F54 + 2.*I2*I22*I23*I37*I38 + I2*I21*I21*F47 + 2.*I2*I21*
I23*F45 + I2*I23*I23*I37*I39 + I2*I31*I33*F37 + 2.*I2*I15*I17*
F21 + I2*I15*I15*F26 + I2*I31*I31*F25 + 2.*I2*I31*I32*F20
+ I2*I15*I16*F38 - 2.*I7*I31*I33*F39 - 2.*I7*F21*F34 - 2.*I7*
I15*I21*F26 - I7*I31*I31*F27 - 2.*I7*I31*I32*F22 - I7*F38*F17
+ 2.*I5*I22*I31*F60 + 2.*I5*I22*I32*F59 + 2.*I5*I21*I22*I35*I37
+ I5*I21*I21*F48 + 2.*I5*I21*I23*F46 + I5*I23*I23*F44)

I791= 2.*(2.*I21*I22*I32*I35*I47 +I22*I23*I47*F38 + I23*I23*
I47*F21 + 2.*I21*I23*I47*F26 + I21*I21*I35*I36*I47 + 2.*I2*I21*
I22*F61 + I2*I22*I23*F54 + I2*I21*I21*F49 + 2.*I2*I21*I23*F47
+ I2*I23*I23*F45 + 2.*I2*I17*I19*I31*I33 + I2*F21*F37
+ 2.*I2*I15*I17*F26 + I2*I15*I15*I35*I36 + I2*I18*I19*I31*I31
+ 2.*I2*I31*I32*F25 + I2*F38*F20 + 2.*I2*I15*I16*I32*I35
- 2.*I7*I19*I23*I31*I33 - 2.*I7*F21*F39 - 2.*I7*F26*F34
- 2.*I7*I15*I21*I35*I36 - 2.*I7*I31*I32*F27 - I7*F38*F22
- 2.*I7*I32*I35*F17 + 2.*I5*I22*I31*F62 + 2.*I5*I22*I32*F60
+ 2.*I5*I22*I35*F59 + I5*I21*I21*F50 + 2.*I5*I21*I23*F48)

I792 = 2.*(I5*I23*I23*F46)

I79 = I791 + I792
```

Table H1 continued

```
I80 = 2.*(I21*I22*I35*I35*I47 + 2.*I22*I23*I32*I35*I47 + I23*
I23*I47*F26 + 2.*I21*I23*I35*I36*I47 + I2*I21*I22*F57 + 2.*I2*I22*
I23*F61 + I2*I21*I21*F51 + 2.*I2*I21*I23*F49 + I2*I23*I23*F47
+ I2*I19*I19*I31*I33 + 2.*I2*I17*I19*F21 + I2*F26*F37 + 2.*I2*
I15*I17*I35*I36 + 2.*I2*I18*I19*I31*I32 + I2*F38*F25 + 2.*I2*
I32*I35*F20 + I2*I35*I35*I15*I16 - 2.*I7*I19*I23*F21 - 2.*I7*
F26*F39 - 2.*I7*I35*I36*F34 - I7*F38*F27- 2.*I7*I32*I35*F22
- I7*I35*I35*F17 + 2.*I5*I22*I23*I31*I43 + 2.*I5*I22*I32*F62
+ 2.*I5*I22*I35*F60 + I5*I21*I21*F52 + 2.*I5*I21*I23*F50 + I5*
I23*I23*F48)

I81 = 2.*(I22*I23*I35*I35*I47 + I23*I23*I35*I36*I47 + 2.*I2*I21*
I22*I40*I43 + I2*I22*I23*F57 + I2*I21*I21*I43*I45 + 2.*I2*I21*
I23*F51 + I2*I23*I23*F49 + I2*I19*I19*F21 + 2.*I2*I17*I19*F26
+ I2*I35*I36*F37 + I2*I18*I19*F38 + 2.*I2*I32*I35*F25 + I2*I35*
I35*F20 - 2.*I7*F26*I19*I23 - 2.*I7*I35*I36*F39 - 2.*I7*I32*I35*
F27 - I7*I35*I35*F22 + 2.*I5*I22*I23*I32*I43 + 2.*I5*I22*I35*F62
+ 2.*I5*I21*I23*F52 + I5*I23*I23*F50)

I82 = 2.*(I2*I21*I22*I43*I43 + 2.*I2*I22*I23*I40*I43 + 2.*I2*
I21*I23*I43*I45 + I2*I23*I23*F51 + I2*I19*I19*F26 + 2.*I2*I17*
I19*I35*I36 + 2.*I2*I18*I19*I32*I35 + I2*I35*I35*F25 - 2.*I7*
I19*I23*I35*I36 - I7*I35*I35*F27 + 2.*I5*I22*I23*I35*I43 + I5*
I23*I23*F52)

I83 = 2.*(I2*I22*I23*I43*I43 + I2*I23*I23*I43*I45 + I2*I19*I19*
I35*I36 + I2*I18*I19*I35*I35)

I84 = I21*I21*I31*I31*I47 + I2*I21*I21*I37*I37 + I2*I15*I15*I31*
I31 - 2.*I7*I15*I21*I31*I31 + 2.*I5*I21*I21*I31*I37

I85 = 2.*(I21*I23*I31*I31*I47 + I21*I21*I31*I32*I47 + I2*I21*I21*
I37*I38 + I2*I21*I23*I37*I37 + I2*I15*I17*I31*I31 + I2*I15*I15*
I31*I32 - I7*I31*I31*F34 - 2.*I7*I15*I21*I31*I32 + I5*I21*I21*F53
+ 2.*I5*I21*I23*I31*I37)

I86 = I23*I23*I31*I31*I47 + 4.*I21*I23*I31*I32*I47 + I21*I21*I47*
F38 + I2*I21*I21*F54 + 4.*I2*I21*I23*I37*I38 + I2*I23*I23*I37*I37
+ I2*I31*I31*F37 + 4.*I2*I15*I17*I31*I32 + I2*I15*I15*F38
- 2.*I7*I31*I31*F39 - 4.*I7*I31*I32*F34 - 2.*I7*I15*I21*F38
+ 2.*I5*I21*I21*F55 + 4.*I5*I21*I23*F53 + 2.*I5*I23*I23*I31*I37

I87 = 2.*(I23*I23*I31*I32*I47 + I21*I23*I47*F38 + I21*I21*I32*
I35*I47 + I2*I21*I21*F61 + I2*I21*I23*F54 + I2*I23*I23*I37*I38
+ I2*I17*I19*I31*I31 + I2*I31*I32*F37 + I2*I15*I17*F38
+ I2*I15*I15*I32*I35 - I7*I19*I23*I31*I31 - 2.*I7*I31*I32*F39
- I7*F38*F34   - 2.*I7*I15*I21*I32*I35 + I5*I21*I21*F56 + 2.*
I5*I21*I23*F55 + I5*I23*I23*F53)

I88 = I23*I23*I47*F38 + 4.*I21*I23*I32*I35*I47 + I21*I21*I35*
I35*I47 + I2*I21*I21*F57 + 4.*I2*I21*I23*F61 + I2*I23*I23*F54
+ I2*I19*I19*I31*I31 + 4.*I2*I17*I19*I31*I32 + I2*F38*F37 + 4.*I2*
I15*I17*I32*I35 + I2*I15*I15*I35*I35 - 4.*I7*I19*I23*I31*I32 - 2.*
I7*F38*F39 - 4.*I7*I32*I35*F34 - 2.*I7*I15*I21*I35*I35 + 2.*I5*
I21*I21*F58 + 4.*I5*I21*I23*F56 + 2.*I5*I23*I23*F55
```

Table H1 continued

```
I89 = 2.*(I23*I23*I32*I35*I47 + I21*I23*I35*I35*I47 + I2*I21*I21*
I40*I43 + I2*I21*I23*F57 + I2*I23*I23*F61 + I2*I19*I19*I31*I32
+ I2*I17*I19*F38 + I2*I32*I35*F37 + I2*I15*I17*I35*I35 - I7*
I19*I23*F38 - 2.*I7*I32*I35*F39 - I7*I35*I35*F34 + I5*I21*I21*
I35*I43 + 2.*I5*I21*I23*F58 + I5*I23*I23*F56)

I90 = I23*I23*I35*I35*I47 + I2*I21*I21*I43*I43 + 4.*I2*I21*I23*
I40*I43 + I2*I23*I23*F57 + I2*I19*I19*F38 + 4.*I2*I17*I19*I32*I35
+ I2*I35*I35*F37 - 4.*I7*I19*I23*I32*I35 - 2.*I7*I35*I35*F39
 + 4.*I5*I21*I23*I35*I43 + 2.*I5*I23*I23*F58

I91 = 2.*(I2*I21*I23*I43*I43 + I2*I23*I23*I40*I43 + I2*I19*I19*
I32*I35 + I2*I17*I19*I35*I35 - I7*I19*I23*I35*I35 + I5*I23*I23*
I35*I43)

I92 = I2*(I23*I23*I43*I43 + I19*I19*I35*I35)
```

$$I_{93} = -I_{10}/I_9$$

$$I_{94} = -2I_{12}/I_9$$

$$I_{95} = (I_{10}^2 - I_9(I_{14} - 2\pi q_2^2 f_{43_{RMS_u}}^2))/I_9^2$$

```
I96 = -1.

I97 = I95 + I93*I93

I98 = 2.*I93

I99 = -3.*I93

I100 = 3.*I93*I94

I101 = 3.*I93*I95 + I93*I93*I93

I102 = I95 + 3.*I93*I93

I103 =-2.*I94

I104 = I94*I94 - 2.*I95 - 6.*I93*I93

I105 = 2.*I94*(I95 + 3.*I93*I93)

I106 = 6.*I93*I93*I95 +    I93*I93*I93*I93 + I95*I95
```

Table H1 continued

```
I107 = -4.*I93

I108 = 4.*I93*I94

I109 = 4.*I93*(I95 + I93*I93)

I110 = 5.*I93

I111 = -10.*I93*I94

I112 = 5.*I93*(I94*I94 - 2.*I95 - 2.*I93*I93)

I113 = 10.*I93*I94*(I95 + I93*I93)

I114 = 10.*I93*I93*I93*I95 + I93*I93*I93*I93*I93 + 5.*I93*I95*I95

I115 = I94*I94 - 2.*I95 - 10.*I93*I93

I116 = 2.*I94*(I95 + 5.*I93*I93)

I117 = 10.*I93*I93*I95 + 5.*I93*I93*I93*I93 + I95*I95

I118 = 3.*I94

I119 = -3.*(I94*I94 - I95 - 5.*I93*I93)

I120 = -I94*(6.*I95 - I94*I94 + 30.*I93*I93)

I121 = 3.*(I94*I94*I95 - I95*I95 - 10.*I93*I93*I95 + 5.*I93*I93*
I94*I94 - 5.*I93*I93*I93*I93)

I122 = 3.*I94*(I95*I95 + 10.*I93*I93*I95 + 5.*I93*I93*I93*I93)

I123 = 15.*I93*I93*I95*I95 + 15.*I93*I93*I93*I93*I95 + I93*I93*
I93*I93*I93*I93 + I95*I95*I95

I124 = 6.*I93

I125 = -12.*I93*I94

I126 = 2.*I93*(3.*I94*I94 - 6.*I95 - 10.*I93*I93)

I127 = 4.*I93*I94*(3.*I95 + 5.*I93*I93)

I128 = 2.*I93*(10.*I93*I93*I95 + 3.*I93*I93*I93*I93 + 3.*I95*I95)

I129 = -7.*I93

I130 = 21.*I93*I94
```

Table H1 continued

```
I131 = 7.*I93*(3.*I95 - 3.*I94*I94 + 5.*I93*I93)

I132 = -7.*I93*I94*(6.*I95 - I94*I94 + 10.*I93*I93)

I133 = 7.*I93*(3.*I94*I94*I95 - 3.*I95*I95 - 10.*I93*I93*I95
+ 5.*I93*I93*I94*I94 - 3.*I93*I93*I93*I93)

I134 = 7.*I93*I94*(3.*I95*I95 + 10.*I93*I93*I95 + 3.*I93*I93*
I93*I93)

I135 = I93*(35.*I93*I93*I95*I95 + 21.*I93*I93*I93*I93*I95
+ 7.*I95*I95*I95 + I93*I93*I93*I93*I93*I93)

I136 = -3.*(I94*I94 - I95 - 7.*I93*I93)

I137 = -I94*(6.*I95 - I94*I94 + 42.*I93*I93)

I138 = 3.*I94*I94*I95 - 3.*I95*I95 - 42.*I93*I93*I95 + 21.*I93*
I93*I94*I94 - 35.*I93*I93*I93*I93

I139 = I94*(3.*I95*I95 + 42.*I93*I93*I95 + 35.*I93*I93*I93*I93)

I140 = 21.*I93*I93*I95*I95 + 35.*I93*I93*I93*I93*I95 + 7.*I93*
I93*I93*I93*I93*I93 + I95*I95*I95

I141 = -4.*I94

I142 = -2.*(2.*I95 - 3.*I94*I94  + 14.*I93*I93)

I143 = 4.*(3.* I95 - I94*I94 + 21.*I93*I93)*I94

I144 = -12.*I94*I94*I95 + 6.*I95*I95 + 84.*I93*I93*I95 + I94*I94
- 84.*I93*I93*I94*I94 + 70.*I93*I93*I93*I93

I145 =-4.*I94*(3.*I95*I95 - I94*I94*I95 + 42.*I93*I93*I95 - 7.*
I93*I93*I94*I94 + 35.*I93*I93*I93*I93)

I146 = 2.*(3.*I94*I94*I95*I95 - 2.*I95*I95*I95 - 42.*I93*I93*
I95*I95 + 42.*I93*I93*I94*I94*I95 - 70.*I93*I93*I93*I93*I95
+ 35.*I93*I93*I93*I93*I94*I94 - 14.*I93**6)

I147 = 4.*I94*(I95*I95*I95 + 21.*I93*I93*I95*I95 + 35.*I93*I93*
I93*I93*I95 + 7.*I93*I93*I93*I93*I93*I93)

I148 = 28.*I93*I93*I95*I95*I95 + 70.*I93*I93*I93*I93*I95*I95
+ 28.*I93*I93*I93*I93*I93*I93*I95 + I95*I95*I95*I95 + I93**8

I149 = -8.*I93

I150 = 24.*I93*I94
```

Table H1 continued

```
I151 = -8.*I93*(3.*I94*I94 - 3.*I95 - 7.*I93*I93)

I152 = -8.*I93*I94*(6.*I95 - I94*I94 + 14.*I93*I93)

I153 = 8.*I93*(3.*I94*I94*I95 - 3.*I95*I95 - 14.*I93*I93*I95 +7.*
I93*I93*I94*I94 - 7.*I93*I93*I93*I93)

I154 = 8.*I93*(3.*I94*I95*I95 + 14.*I93*I93*I94*I95 + 7.*I93*I93*
I93*I93*I94)

I155 = 8*I93*(7.*I93*I93*I95*I95 + 7.*I93*I93*I93*I93*I95
+ I95*I95*I95 + I93*I93*I93*I93*I93*I93)

I156 = I48 + I53*I96 + I62 + I75*I96 + I92

I157 = I48*I141 + I50*I129 + I52*I96 + I53*I118 + I57*I110 + I61
+ I62*I103 + I68*I99 + I74*I96 + I75*I94 + I83*I93 + I91

I158 = I48*I142 + I49*I129 + I50*I130 + I51*I96 + I52*I118
+ I53*I119 + I56*I110 + I57*I111 + I60 + I61*I103 + I62*I104
+ I67*I99 + I68*I100 + I73*I96 + I74*I94 + I75*I97 + I82*I93 + I90

I159 = I48*I143 + I49*I130 + I50*I131 + I51*I118 + I52*I119
+ I53*I120 + I55*I110 + I56*I111 + I57*I112 + I59 + I60*I103
+ I61*I104 + I62*I105 + I66*I99 + I67*I100 + I68*I101 + I72*I96
+ I73*I94 + I74*I97 + I81*I93 + I89

I160 = I48*I144 + I49*I131 + I50*I132 + I51*I119 + I52*I120
+ I53*I121 + I54*I110 + I55*I111 + I56*I112 + I57*I113 + I58
+ I59*I103 + I60*I104 + I61*I105 + I62*I106 + I65*I99 + I66*I100
+ I67*I101 + I71*I96 + I72*I94 + I73*I97 + I80*I93 + I88

I161 = I48*I145 + I49*I132 + I50*I133 + I51*I120 + I52*I121
+ I53*I122 + I54*I111 + I55*I112 + I56*I113 + I57*I114
+ I58*I103 + I59*I104 + I60*I105 + I61*I106 + I64*I99 + I65*I100
+ I66*I101 + I70*I96 + I71*I94 + I72*I97 + I79*I93 + I87

I162 = I48*I146 + I49*I133 + I50*I134 + I51*I121 + I52*I122
+ I53*I123 + I54*I112 + I55*I113 + I56*I114 + I58*I104 + I59*I105
+ I60*I106 + I63*I99 + I64*I100 + I65*I101 + I69*I96 + I70*I94
+ I71*I97 + I78*I93 + I86

I163 = I48*I147 + I49*I134 + I50*I135 + I51*I122 + I52*I123
+ I54*I113 + I55*I114 + I58*I105 + I59*I106 + I63*I100 + I64*I101
+ I69*I94 + I70*I97 + I77*I93 + I85

I164 = I48*I148 + I49*I135 + I51*I123 + I54*I114 + I58*I106
+ I63*I101 + I69*I97 + I76*I93 + I84

I165 = I50*I96 + I57 + I68*I96 + I83
```

Table H1 continued

```
I166 = I48*I149 + I49*I96 + I50*I118 + I53*I124 + I56
+ I57*I103 + I62*I107 + I67*I96 + I68*I94 + I75*I98 + I82

I167 = I48*I150 + I49*I118 + I50*I136 + I52*I124 + I53*I125
+ I55 + I56*I103 + I57*I115 + I61*I107 + I62*I108 + I66*I96
+ I67*I94 + I68*I102 + I74*I98 + I81

I168 = I48*I151 + I49*I136 + I50*I137 + I51*I124 + I52*I125
+ I53*I126 + I54 + I55*I103 + I56*I115 + I57*I116 + I60*I107
+ I61*I108 + I62*I109 + I65*I96 + I66*I94 + I67*I102 + I73*I98
+ I80

I169 = I48*I152 + I49*I137 + I50*I138 + I51*I125 + I52*I126
+ I53*I127 + I54*I103 + I55*I115 + I56*I116 + I57*I117 + I59*I107
+ I60*I108 + I61*I109 + I64*I96 + I65*I94 + I66*I102 + I72*I98
+ I79

I170 = I48*I153 + I49*I138 + I50*I139 + I51*I126 + I52*I127
+ I53*I128 + I54*I115 + I55*I116 + I56*I117 + I58*I107 + I59*I108
+ I60*I109 + I63*I96 + I64*I94 + I65*I102 + I71*I98 + I78

I171 = I48*I154+ I49*I139 + I50*I140 + I51*I127 + I52*I128
+ I54*I116 +I55*I117 + I58*I108 + I59*I109 + I63*I94 + I64*I102
+ I70*I98 + I77

I172 = I48*I155 + I49*I140 + I51*I128 + I54*I117 + I58*I109
+ I63*I102 + I69*I98 + I76
```

$$G_1 = I_{166}^2 + 2I_{165}I_{167}$$

$$G_2 = 2(I_{165}I_{168} + I_{166}I_{167})$$

$$G_3 = I_{167}^2 + 2(I_{165}I_{169} + I_{166}I_{168})$$

$$G_4 = 2(I_{165}I_{170} + I_{166}I_{169} + I_{167}I_{168})$$

$$G_5 = I_{168}^2 + 2(I_{165}I_{171} + I_{166}I_{170} + I_{167}I_{169})$$

$$G_6 = 2(I_{165}I_{172} + I_{166}I_{171} + I_{167}I_{170} + I_{168}I_{169})$$

$$G_7 = I_{169}^2 + 2(I_{166}I_{172} + I_{167}I_{171} + I_{168}I_{170})$$

$$G_8 = 2(I_{167}I_{172} + I_{168}I_{171} + I_{169}I_{170})$$

Table H1 continued

$$G_9 = I_{170}^2 + 2(I_{168}I_{172} + I_{169}I_{171})$$

$$G_{10} = 2(I_{169}I_{172} + I_{170}I_{171})$$

$$G_{11} = I_{171}^2 + 2I_{170}I_{172}$$

Table H1 continued

$$P_1 = I_{156}^2 + I_{165}^2$$

$$P_2 = 2(I_{156}I_{157} + I_{165}I_{166}) - I_{94}I_{165}^2$$

$$P_3 = I_{157}^2 + 2(I_{156}I_{158} - I_{94}I_{165}I_{166}) - I_{95}I_{165}^2 + G_1$$

$$P_4 = 2(I_{156}I_{159} + I_{157}I_{158} - I_{95}I_{165}I_{166}) - G_1I_{94} + G_2$$

$$P_5 = I_{158}^2 + 2(I_{156}I_{160} + I_{157}I_{159}) - G_1I_{95} - G_2I_{94} + G_3$$

$$P_6 = 2(I_{156}I_{161} + I_{157}I_{160} + I_{158}I_{159}) - G_2I_{95} - G_3I_{94} + G_4$$

$$P_7 = I_{159} + 2(I_{156}I_{162} + I_{157}I_{161} + I_{158}I_{160}) - G_3I_{95} - G_4I_{94} + G_5$$

$$P_8 = 2(I_{156}I_{163} + I_{157}I_{162} + I_{158}I_{161} + I_{159}I_{160}) - G_4I_{95} - G_5I_{94} + G_5$$

$$P_9 = I_{160}^2 + 2(I_{156}I_{164} + I_{157}I_{163} + I_{158}I_{162} + I_{159}I_{161}) - G_5I_{95} - G_6I_{94} + G_7$$

$$P_{10} = 2(I_{157}I_{164} + I_{158}I_{163} + I_{159}I_{162} + I_{160}I_{161}) - G_6I_{95} - G_7I_{94} + G_8$$

$$P_{11} = I_{161}^2 + 2(I_{158}I_{164} + I_{159}I_{163} + I_{160}I_{162}) - G_7I_{95} - G_8I_{94} + G_9$$

$$P_{12} = 2(I_{159}I_{164} + I_{160}I_{163} + I_{161}I_{162}) - G_8I_{95} - G_9I_{94} + G_{10}$$

Table H2 Coefficients of 16^{th} Degree Solution Polynomial

$$P_{13} = I_{162}^2 + 2(I_{160}I_{164} + I_{161}I_{163}) - G_9I_{95} - G_{10}I_{94} + G_{11}$$

$$P_{14} = 2(I_{161}I_{164} + I_{162}I_{163}) - G_{10}I_{95} - G_{11}I_{94} + 2I_{171}I_{172}$$

$$P_{15} = I_{163}^2 + 2I_{162}I_{164} - G_{11}I_{95} - 2I_{94}I_{171}I_{172} + I_{172}^2$$

$$P_{16} = 2(I_{163}I_{164} - I_{95}I_{171}I_{172}) - I_{94}I_{172}^2$$

$$P_{17} = I_{164}^2 - I_{95}I_{172}^2$$

Table H2 continued

APPENDIX I

PROOF OF THE EXISTENCE OF A MINIMUM FOR THE TWO COUNTERWEIGHT OPTIMIZATION PROBLEM

It will now be shown that one of the extrema found in Section IVC is a global minimum. This will be accomplished, similar to the manner of Appendix F, by using the theorem concerning continuous functions of closed and bounded sets.

The function under consideration is the RMS shaking force, which must be minimized while limiting the RMS ground bearing forces by constraint equations, and using a prescribed value of the moment of inertia of the output link. The aforementioned sets are represented by those points which satisfy the constraint equations. Since the expression for the RMS shaking force is continuous everywhere, the theorem is applicable if one can show that all points which satisfy the constraint equations represent a closed and bounded set.

To prove this point, consider first that any set of points which satisfy an equation represents a closed set. Thus, the set of points satisfying each of the constraint equations is a closed set. Furthermore, since the intersection of closed sets is a closed set [4], the set of points satisfying the constraint equations simultaneously, represents a closed set. In addition, the set is bounded as can be seen by rewriting the constraint equations (4.43) and (4.44) by applying the method of completing the square. Thus, these equations become:

$$\left(t_1 + \frac{I_5}{I_2}\right)^2 + \left(u_1 + \frac{I_7}{I_2}\right)^2 = \frac{2\pi q_1^2 f_{41_{RMS_u}}^2 - I_{13}}{I_2} + \frac{I_5^2 + I_7^2}{I_2^2} \tag{I.1}$$

$$\left(t_3 + \frac{I_{10}}{I_9}\right)^2 + \left(u_3 + \frac{I_{12}}{I_9}\right)^2 = \frac{2\pi q_2^2 f_{43_{RMS_u}}^2 - I_{14}}{I_9} + \frac{I_{10}^2 + I_{12}^2}{I_9^2} . \tag{I.2}$$

The above expressions represent equations of circles in the u_1,t_1 and u_3,t_3 planes, respectively, and thus the magnitudes of u_1, t_1, u_3 and t_3 are bounded.

From the above, it can be concluded that the points satisfying the constraint equations represent a closed and bounded set.

APPENDIX J

DETERMINATION OF DIMENSIONLESS LINK MASS PARAMETERS OF FULLY FORCE BALANCED FOUR-BAR LINKAGE OF STANDARD CONFIGURATION

The present appendix shows how the masses, mass moments of inertia, as well as the positions of the centers of mass of the links of a fully force balanced four-bar linkage of standard configuration may be obtained in dimensionless form.

The counterweight design equations for a link are given by [2] in the following dimensional form:

$$m_{i_b}^* r_{i_b}^* = \sqrt{(m_i r_i)^2 + (m_i^o r_i^o)^2 - 2m_i m_i^o r_i r_i^o \cos(\theta_i - \theta_i^o)} \qquad (J.1)$$

$$\tan\theta_{i_b}^* = \frac{m_i r_i \sin\theta_i - m_i^o r_i^o \sin\theta_i^o}{m_i r_i \cos\theta_i - m_i^o r_i^o \cos\theta_i^o} . \qquad (J.2)$$

In the above, $m_{i_b}^*$, m_i^o, m_i represent the masses of the counterweight, the original link and the total link, respectively; $r_{i_b}^*$, r_i^o, r_i represent the positions of the centers of mass of the counterweight, the original link and the total link, respectively; $\theta_{i_b}^*$, θ_i^o, θ_i represent the angular positions of the centers of mass of the counterweight, the original link and the total link, respectively.

It is now desirable to obtain the above expressions in dimensionless form:

The $m_i^o r_i^o$ terms may be evaluated by recalling that

$$m_i^o = \rho^o a_1^3 B_i^o \quad \text{(see equations (A.119a) and (A.119c), which deal with standard configuration four-bar linkages),} \tag{J.3}$$

and since the links are symmetric

$$r_1^o = \frac{a_1}{2}, \qquad r_3^o = \alpha_3 \frac{a_1}{2} \quad \text{(for } \alpha_3\text{, see equations (A.115)).} \tag{J.4}$$

Furthermore, the $m_i r_i$ terms can be obtained by using equations (12) and (13) of [2] in the following form:

$$m_1 r_1 = \rho^o a_1^4 B_2^o \left(1 - \frac{r_2^o}{a_2}\right) \tag{J.5}$$

$$m_3 r_3 = \rho^o a_1^4 B_2^o \frac{r_2^o}{a_2} \alpha_3 . \tag{J.6}$$

Again, because the links are symmetric

$$\theta_1^o = \theta_3^o = 0 . \tag{J.7}$$

Finally, the θ_i terms can be found from equations (12) and (13) of [2]. Thus

$$\theta_1 = \theta_3 = 180^o. \tag{J.8}$$

Substituting equations (J.3) - (J.8) into equations (J.1) and (J.2), one obtains

$$m_{i_b}^* r_{i_b}^* = \rho^o a_1^4 \Gamma_{i_b}^* \tag{J.9}$$

$$\theta_{i_b}^* = 180^o , \tag{J.10}$$

where

$$\Gamma^*_{1_b} = B_2^o\left(1 - \frac{r_2^o}{a_2}\right) + \frac{B_1^o}{2} \tag{J.11}$$

$$\Gamma^*_{3_b} = \alpha_3\left(\frac{B_2^o r_2^o}{a_2} + \frac{B_3^o}{2}\right) . \tag{J.12}$$

For the circular, tangent counterweights under consideration

$$m^*_{i_b} = \rho^*_{i_b}\,\pi\, r^{*2}_{i_b}\, h^*_{i_b} , \tag{J.13}$$

where $\rho^*_{i_b}$ and $h^*_{i_b}$ represent the counterweight mass density and thickness, respectively.

Substituting equation (J.13) into equation (J.9), and using the following definitions:

$$\delta_{i_b} = \frac{h^*_{i_b}}{h_i} , \quad D^*_{i_b} = \delta_{i_b}\left(\frac{\rho^*_{i_b}}{\rho^o}\right), \quad R^*_{i_b} = \frac{r^*_{i_b}}{a_1} \tag{J.14}$$

(for β_i and γ_i, see equations (A.115)), one may solve for the dimensionless counterweight radius $R^*_{i_b}$. Thus

$$R^*_{i_b} = \left[\frac{\Gamma^*_{i_b}}{\pi D^*_{i_b}\beta_i\gamma_i}\right]^{1/3} . \tag{J.15}$$

This expression together with equations (J.14) may now be substituted into equation (J.13) to find the dimensionless counterweight mass $B^*_{i_b}$. This yields

$$m^*_{i_b} = \rho^o a_1 B^*_{i_b} , \tag{J.16}$$

where

$$B^*_{i_b} = (\pi D^*_{i_b} \beta_i \gamma_i \Gamma^{*2}_{i_b})^{1/3} \quad . \tag{J.17}$$

To obtain the dimensionless total link mass parameters B_i, U_i, T_i and W_i, where B_i represents the mass, U_i, T_i represent the coordinates of the position of the center of mass, and W_i represents the radius of gyration, one adds the parameters referring to the original link to those of the counterweight. Thus, for the counterweight center of mass

$$U^*_{i_b} = R^*_{i_b} \cos\theta^*_{i_b} = -\left[\frac{\Gamma^*_{i_b}}{\pi D^*_{i_b} \beta_i \gamma_i}\right]^{1/3} \tag{J.18}$$

$$T^*_{i_b} = R^*_{i_b} \sin\theta^*_{i_b} = 0 \tag{J.19}$$

$$W^*_{i_b} = \frac{1}{\sqrt{2}} \left[\frac{\Gamma^*_{i_b}}{\pi D^*_{i_b} \beta_i \gamma_i}\right]^{1/3} \quad , \tag{J.20}$$

while the dimensionless mass of the counterweight is given by equation (J.17). The parameters of the original link are given by:

$$U^o_i = \frac{1}{2} \alpha_i \tag{J.21}$$

$$T^o_i = 0 \tag{J.22}$$

$$W^o_i = \sqrt{C^o_i / B^o_i} \quad , \tag{J.23}$$

where B^o_i represents the dimensionless mass of the original link (see equations (A.119a) and (A.119c)), and C^o_i represents the dimensionless moment of inertia of the original link

(see equation (A.119e)).

With the above, the mass parameters of the total link may be expressed as follows:

$$B_i = B_i^o + B_{i_b}^* = B_i^o + (\pi D_{i_b}^* \beta_i \gamma_i \Gamma_{i_b}^{*2})^{1/3} \tag{J.24}$$

$$U_i = \frac{B_i^o U_i^o + B_{i_b}^* U_{i_b}^*}{B_i} = \frac{\frac{B_i^o \alpha_i}{2} - \Gamma_{i_b}^*}{B_i^o + (\pi D_{i_b}^* \beta_i \gamma_i \Gamma_{i_b}^{*2})^{1/3}} \tag{J.25}$$

$$T_i = \frac{B_i^o T_i^o + B_{i_b}^* T_{i_b}^*}{B_i} = 0 \tag{J.26}$$

$$W_i = \left[\frac{B_i^o (U_i^{o2} + T_i^{o2} + W_i^{o2}) + B_{i_b}^* (U_{i_b}^{*2} + T_{i_b}^{*2} + W_{i_b}^{*2})}{B_i} - (U_i^2 + T_i^2) \right]^{1/2}$$

$$= \left[\frac{\frac{B_i^o \alpha_i^2}{4} + C_i^o + \frac{3}{2} \left(\frac{\Gamma_{i_b}^{*4}}{\pi D_{i_b}^* \beta_i \gamma_i} \right)^{1/3}}{B_i^o + (\pi D_{i_b}^* \beta_i \gamma_i \Gamma_{i_b}^{*2})^{1/3}} - \left(\frac{\frac{B_i^o \alpha_i}{2} - \Gamma_{i_b}^*}{B_i^o + (\pi D_{i_b}^* \beta_i \gamma_i \Gamma_{i_b}^{*2})^{1/3}} \right)^2 \right]^{1/2} . \tag{J.27}$$

VI. REFERENCES

1. R. S. Berkof, "On the Optimization of Mass Distribution in Mechanisms," PhD Dissertation, City University of New York, University Microfilms, Ann Arbor, Michigan, 1969 (no. 69-19052).

2. R. S. Berkof & G. G. Lowen, "A New Method for Complete Force Balancing of Simple Linkages," Journal of Engineering for Industry, Trans. ASME, Series B, vol. 91, no. 1, 1969, pp. 21-26.

3. R. S. Berkof & G. G. Lowen, "Theory of Shaking Moment Optimization of Force-Balanced Four-Bar Linkages," Journal of Engineering for Industry, Trans. ASME, Series B, vol. 93, no. 1, 1971, pp. 53-60.

4. R. C. Buck, Advanced Calculus, 2nd Ed., McGraw-Hill Book Co., New York, 1965.

5. W. L. Carson & J. Tinsley, "Reduction of Shaking Forces in a Slider-Crank Mechanism," ASME Paper No. 70-Mech-8.

6. T. H. Davies, "The Kinematics and Design of Linkages, Balancing Mechanisms and Machines," Machine Design Engineering, March 1968, pp. 40-51.

7. Ya. L. Geronimus, On the Application of Chebyshev's Methods to the Problem of the Balancing of Mechanisms (Russian), OGIZ, Gostekhizdat, Moscow-Leningrad, 1948, 148 pp.

8. B. A. Hockey, "The Method of Dynamically Similar Systems Applied to the Distribution of Mass in Spatial Mechanisms," Journal of Mechanisms, vol. 5, 1970, pp. 169-180.

9. P. Jacobi, "Vollständiger Tragheitskraftausgleich bei mehrgliedrigen Koppelgetrieben," Maschinenbautechnik, vol. 18, no. 11, 1969, pp. 605-606.

10. V. A. Kamenskii, "On the Question of the Balancing of Plane Linkages," Journal of Mechanisms, vol. 3, 1968, pp. 303-322.

11. W. Kaplan, Advanced Calculus, Addison-Wesley Publishing Co., Cambridge, Mass., 1953.

12. R. E. Kaufman & G. N. Sandor, "Complete Force Balancing of Spatial Linkages," Journal of Engineering for Industry, Trans. ASME, Series B, vol. 93, no. 2, 1971, pp. 620-626.

13. G. G. Lowen & R. S. Berkof, "Survey of Investigations into the Balancing of Linkages," Journal of Mechanisms, vol. 3, 1968, pp. 221-231.

14. G. G. Lowen & R. S. Berkof, "Determination of Force-Balanced Four-Bar Linkages With Optimum Shaking Moment Characteristics," Journal of Engineering for Industry, Trans. ASME, Series B, vol. 93, no. 1, 1971, pp. 39-46.

15. G. G. Lowen, R. S. Berkof & F. R. Tepper, "The Effect of Full Force Balancing on the Bearing Forces, Input Moment and Shaking Moment of 40 Families of Four-Bar Linkages," Article in preparation.

16. B. Paul, "A Unified Criterion for the Degree of Constraint of Plane Kinematic Chains," Journal of Applied Mechanics, vol. 27, Trans. ASME, vol. 82, Series E, no. 1, 1960, pp. 196-200.

17. G. Salmon, "Conic Sections, 6th Ed., Chelsea Publishing Co., New York, 1954.

18. A. A. Sherwood & B. A. Hockey, "The Optimisation of Mass Distribution in Mechanisms Using Dynamically Similar Systems," Journal of Mechanisms, vol. 4, 1969, pp. 234-260.

19. Ye. A. Shorokh, "Design of Counterweights for Unloading the Main Supports of a Crankshaft," (Russian), Izv. Vyssh. Ucheb. Zaved. - Mashinostroenie, no. 3, 1969, pp. 74-77.

20. D. Tesar & C. E. Benedict, "Optimal Torque Balance for a Complex Stamping and Indexing Machine," ASME Paper No. 70-Mech-82.

VII. AUTOBIOGRAPHICAL STATEMENT

Frederick R. Tepper was born on July 16, 1941 in Brooklyn, New York. He attended Brooklyn Public School No. 137, Queens Public School No. 147, and Andrew Jackson High School, graduating from the latter with an academic diploma in June 1959. He attended the City College of New York, from which he received a Bachelor of Mechanical Engineering degree in June 1964.

Subsequently, he joined the Vertol Division of the Boeing Co. as a stress analyst, where he worked on various helicopter design problems.

In September 1966, he entered the doctoral program at the City University of New York. During the Summer of 1966 he was employed by the Harry Diamond Laboratories in Washington, D.C., working on several problems involving the analysis of mechanisms. In June 1967 he received a Master of Engineering (Mechanical) degree.

On May 11, 1972, he successfully defended his dissertation, thus completing the requirements for the degree of Doctor of Philosophy.

In 1971 and 1972 he published two papers on the balancing of linkages together with Dr. Gerard G. Lowen.

He presently resides in Kew Gardens, New York, with his wife and his son.